MONASH University

Understanding the molecular mechanism of male infertility using flies, mice, and humans

Lachlan Mark Cauchi

Doctor of Philosophy

A thesis submitted as part of the joint award Ph.D. program between Monash University and Justus Liebig University Giessen

Inaugural Dissertation

submitted to the

Faculty of Veterinary Medicine

in partial fulfillment of the requirements

for the PhD-Degree

of the Faculties of Veterinary Medicine and Medicine

of the Justus Liebig University Giessen

by

Cauchi, Lachlan

of

Australia

Giessen, 2021

From the Institute of Veterinary Biology and Anatomy

Director / Chairman: Prof. Dr. Dr. Stefan Arnhold

of the Faculty of Veterinary Medicine of the Justus Liebig University Giessen

First Supervisor and Committee Member: Dr Richard Burke

Second Supervisor and Committee Member: Prof Moira O'Bryan

Committee Members: PD Dr Daniela Fietz

Date of Doctoral Defence: 20/06/2022

Copyright notice

I certify that I have made all reasonable efforts to secure copyright permissions for third-party content included in this thesis and have not knowingly added copyright content to my work without the owner's permission.

“I declare that I have completed this dissertation single-handedly without the unauthorized help of a second party and only with the assistance acknowledged therein. I have appropriately acknowledged and referenced all text passages that are derived literally from or are based on the content of published or unpublished work of others, and all information that relates to verbal communications. I have abided by the principles of good scientific conduct laid down in the charter of the Justus Liebig University of Giessen in carrying out the investigations described in the dissertation.”

Abstract - English

Male infertility is an extremely complex disorder that is contributed to by genetics, the environment, or a combination of both. Infertility variants are large in number, but low in incidence, meaning there are a large number of variants which can cause infertility, but the number of each is relatively low. Therefore, studying these mutations in large cohorts is difficult. For this reason, model organisms are required to screen large numbers of genes to determine their role in male reproduction.

This study used the *Drosophila melanogaster* and mouse model organisms in order to screen a large number of genes to determine if they play a role in male fertility. While previous research had significantly outlined and compared spermatogenesis between organisms at many points in the process, there has yet to be a review which broke down the individual steps of spermatogenesis. This is important to determine whether genes expressed at specific points during spermatogenesis can be studied using *Drosophila.* For this reason, the first step was to write a literature review specifically outlining the steps of spermatogenesis where *Drosophila* could be used to study male infertility.

In collaboration with the International Male Infertility Genomics Consortium, a list of gene variants discovered through exome analysis of infertile men was designed. From this list, 10 genes with *Drosophila* orthologues were further analysed. *Zn72D* with the patient orthologue *ZFR2* and *DCAF12* with the patient orthologue *DCAF12L1* were found to cause infertility when knocked down in the testis. Analysis in human testicular tissue confirmed that both *ZFR2* and *DCAF12L1* were expressed in the testis. As *ZFR2* was a promising candidate, a $Zfr2^{-/-}$ knockout mouse was generated. These knockout mice were healthy and able to produce litter of a size comparable to the control. There were no noticeable defects in the testicular or epididymal histology, nor in their sperm motility or morphology. For this reason, it was determined that *Zfr2* is not an absolute requirement for male fertility in the mouse.

The effect of zinc and zinc transport on fertility was also analysed. Previous research has determined that zinc is important in fertility, as decreased zinc in the seminal plasma was associated with subfertility. Zinc transport, through the Zrt-, Irt-like protein (ZIP) and Zinc Transporter (ZnT) protein families, which are responsible for zinc influx and efflux

respectively, was manipulated to determine its effect on fertility. In particular, *Zip42C.1, Zip42C.2, Zip89B* and *Zip71B* were found to cause a significant reduction in fertility when mis-expressed in the testis. The expression of the human orthologues of these were then analysed in human tissue. It was found that *ZIP1* was expressed primarily in germ cells, and *ZIP5* and *ZnT9* were expressed primarily in Sertoli cells.

In order to determine the environmental role of zinc, by omitting it from the *Drosophila* diet, a chemically defined diet was used. Removing neither zinc nor copper caused a noticeable reduction in fertility compared to the control.

In conclusion, this research has demonstrated how *Drosophila* and mice can be used to evaluate infertility candidate genes.

Abstract – German

Männliche Unfruchtbarkeit ist eine äußerst komplexe Störung, zu deren Entstehung genetische Mutationen, Umweltfaktoren oder eine Kombination aus beidem beitragen können. Bekannte genetische Varianten, die zu Unfruchtbarkeit führen, sind häufig, kommen aber in relativ kleinen Fallzahlen vor; d. h. es gibt eine große Anzahl von Varianten, die Infertilität verursachen können, aber die Anzahl betroffener Männer ist relativ gering. Daher ist es schwierig, diese Mutationen in großen Kohorten zu untersuchen. Aus diesem Grund werden Modellorganismen benötigt, um die bereits bekannte große Anzahl von Genen zu untersuchen und ihre Rolle bei der männlichen Fortpflanzung zu bestimmen.

In dieser Arbeit wurden als Modellorganismen die Fruchtfliege *Drosophila melanogaster* und die Maus verwendet. Auch wenn frühere Forschungsarbeiten die Spermatogenese im Gesamten bei Fliege, Maus und Mensch verglichen haben, gibt es bisher keine Übersichtsarbeiten, die die einzelnen Schritte der Spermato- und Spermiogenese gegenübergestellt haben. Dies ist aber essentiell um einen Vergleich der Genexpression von „Infertilitätsgenen“ bei Fliege und Maus vorzunehmen. Das erste Kapitel der vorliegenden Arbeit ist deswegen eine Literaturübersicht, in der speziell die einzelnen Schritte der Spermatogenese, in denen Drosophila als Modell zur Untersuchung der männlichen Unfruchtbarkeit eingesetzt werden könnte, beschrieben werden.

In Zusammenarbeit mit dem International Male Infertiltiy Genomics Consortium wurde eine Liste von Genvarianten erstellt, die durch Exomanalysen bei infertilen Männern entdeckt wurden. Von dieser Liste wurden 10 Gene mit bekannten Drosophila-Orthologen weiter analysiert. Es wurde festgestellt, dass Zn72D mit dem humanen Ortholog ZFR2 und DCAF12

mit dem humanen Ortholog DCAF12L1 bei der Fliege Unfruchtbarkeit verursachen, wenn sie im Hoden ausgeschaltet werden. Analysen von menschlichem Hodengewebe bestätigten, dass sowohl ZFR2 als auch DCAF12L1 exprimiert werden. Da ZFR2 ein besonders vielversprechender Kandidat war, wurde eine Zfr2-/- Knockout-Maus erzeugt. Diese Knockout-Mäuse waren gesund und in der Lage, Würfe von vergleichbarer Größe wie die Kontrollmäuse zu produzieren. Es gab weder auffälligen Defekte in der Hoden- oder Nebenhodenhistologie, noch in der Spermienmotilität oder -morphologie. Aus diesem Grund wurde festgestellt, dass Zfr2 keine absolute Voraussetzung für die männliche Fruchtbarkeit bei der Maus ist.

Die Auswirkungen von Zink und seiner Transportproteine auf die Fruchtbarkeit wurden ebenfalls untersucht. Frühere Untersuchungen haben ergeben, dass ein verminderter Zinkgehalt im Samenplasma mit Subfertilität in Verbindung gebracht werden kann und somit Zink wichtig für die Fertilität ist. Um diese Hypothese weiter zu untersuchen, wurden Mitglieder der Zinktransporterfamilien Zrt, Irt-like protein (ZIP) und Zinc Transporter (ZnT), die für den Zinkin- bzw. efflux verantwortlich sind, ausgeschaltet. Insbesondere wurde festgestellt, dass Zip42C.1, Zip42C.2, Zip89B und Zip71B eine signifikante Verringerung der Fruchtbarkeit verursachen, wenn sie im Hoden falsch exprimiert werden. Anschließend wurde die Expression der menschlichen Orthologe dieser Gene in menschlichem Gewebe analysiert. Es zeigte sich, dass ZIP1 vor allem in Keimzellen und ZIP5 vor allem in Sertoli-Zellen exprimiert wird.

Die Rolle von Zink selbst für die Fruchtbarkeit wurde untersucht, indem es aus der Ernährung von Fliegen entfernt wurde. Der Entzug von Zink oder Kupfer führte hier zu einer spürbaren Verringerung der Fruchtbarkeit im Vergleich zur Kontrollgruppe.

Zusammenfassend lässt sich sagen, dass die Untersuchungen, die im Rahmen dieser Doktorarbeit durchgeführt wurden, gezeigt haben, dass und in welchem Ausmaß Drosophila und Mäuse zur Untersuchung von Kandidatengenen für die männliche Infertilität verwendet werden können.

Thesis including published works declaration

I hereby declare that this thesis contains no material which has been accepted for the award of any other degree or diploma at any university or equivalent institution and that, to the best of my knowledge and belief, this thesis contains no material previously published or written by another person, except where due reference is made in the text of the thesis.

This thesis includes 1 original submitted publication. The core theme of the thesis is the genetics of male infertility. The ideas, development and writing up of all the papers in the thesis were the principal responsibility of myself, the student, working within the School of Biological Science under the supervision of Richard Burke. The inclusion of co-authors reflects the fact that the work came from active collaboration between researchers and acknowledges input into team-based research.

This thesis also includes 3 chapters which have not been submitted for publication. In the case of my 4 chapters, my contribution to the work involved the following:

Thesis Chapter	**Publication Title**	**Status** *(published, in press, accepted or returned for revision, submitted)*	**Nature and % of student contribution**	**Co-author name(s) Nature and % of Co-author's contribution***	**Co-author(s), Monash student Y/N***
Chapter 1	Comparing fly and mammalian spermatogenesis – A Literature Review	Not submitted	100%. Conceptualization, Investigation, methodology, data collection, writing		

Chapter 2	The discovery of novel fertility genes from infertile patients using Drosophila	Not submitted	100%. Conceptualization, Investigation, methodology, data collection, writing		
Chapter 3	Zinc finger RNA-binding protein 2 (Zfr2) is not required for male fertility in the mouse	Submitted	50%. Conceptualization, Investigation, methodology, data collection, writing of initial draft	1) Brendan Houston, 15%, conceptualisation, input into manuscript, supervision 2) Liina Nagirnaja, 3%, patient data collection 3) Anne O'Connor, 4% mouse data collection 4) D Jo Merriner, 4%, mouse data collection 5) Kenneth Aston, 1%, Patient data collection and manuscript review 6) Peter Schlegel, 1%, Patient data collection and manuscript review	1) No 2) No 3) No 4) No 5) No 6) No 7) No 8) No

				7) Don Conrad, 2%, Patient data collection and manuscript review 8) Richard Burke, 7%, supervision, conceptualisation, input into manuscript 9) Moira O'Bryan, 13%, Conceptualization, funding acquisition, project administration, input into manuscript	9) No
Chapter 4	The role of zinc and zinc transport in male fertility	Not submitted	100%. Conceptualization, Investigation, methodology, data collection, writing		

I have renumbered sections of submitted or published papers in order to generate a consistent presentation within the thesis.

Student name: Lachlan Cauchi

Student signature: Date: 20/12/2021

I hereby certify that the above declaration correctly reflects the nature and extent of the student's and co-authors' contributions to this work. In instances where I am not the responsible author I have consulted with the responsible author to agree on the respective contributions of the authors.

Main Supervisor name: Dr Richard Burke

Main Supervisor signature: **Date:** 20/12/21

Acknowledgements

I can barely begin to describe the adventure that has been the past 4 years. With all its ups and downs, I have no doubt that the support around me has, in no small part, made me the scientist and person I am today. First and foremost, I would like to thank my supervisory panel, Dr Richard Burke, Prof Moira O'Bryan, and Dr Daniela Fietz.

To my fly supervisor Rich…thank you for your constant support, supervision, and enthusiasm during my PhD. You were always present when I came knocking at your door in a panic because of one or another "major" disasters in the lab (which weren't at all major in the end) and were simply remedied with your guidance. You constantly encouraged me to think for myself which is a skill I have proudly developed over the last few years. Your time was invaluable, especially when I just needed someone to blurt ideas out to, so that I can hear them for myself. It has been a pleasure to be a part of the Burke lab and to work with you over the last few years. Most importantly, thank you for believing in me.

To my mouse supervisor Moira…thankyou for your mentorship, leadership and guidance. You have taught me how to become a better researcher. I could always rely on you to support and put me back on track when it felt like the wheels were falling off. Your leadership and motivation were invaluable and have made me into the scientist I am today. Thankyou for the amazing opportunities this PhD has provided, especially introducing me to the IRTG and IMIGC. You have given me opportunities that I never thought possible, which have inspired me to grow as a researcher and as a person. Most importantly, thank you for believing in me.

To my human supervisor Dani…thankyou for your mentorship, friendship and support. Without your support I would not have been able to thrive as a researcher and a person in Germany. Moving to a new country was a massive step for me, and you made it infinitely easier by being my mentor and friend. Thankyou for the opportunities you provided to present at international conferences, and for teaching me lab skills which I will undoubtedly use for the rest of my career. Most importantly, thank you for believing in me.

To my colleague and mentor Dr Brendan Houston…thankyou for your guidance over the last 4 years. I definitely could not have completed this without you. Your support and experience has not only taught me numerous techniques which I will take with me into my future, but also how to be a better researcher. Most importantly, thank you for believing in me.

I would also like to thank the numerous members of the labs which I have been fortunate enough to be a part. From the Burke Lab: Thankyou to the research assistants, Sebastian Judd-Mole and Pontus LeBlanc, for your support and hard-work, which made my PhD so much less stressful. To the past and present members of the Burke Lab, Bichao Zhang, Lauren Kirn, and Kyle Lyon, thankyou for the support and friendship in the lab. A special mention also to Grace Jefferies and the Johnson lab. Thankyou also to Matt Piper and the Piper lab for their expertise and support in my dietary metal assay. Most importantly, thank you for believing in me.

From the O'Bryan Lab: Special thanks to Anne O'Connor and Jo Merriner for their patience, knowledge and expertise, in teaching me pretty much everything there is to know about mouse fertility. Your guidance and support were invaluable, and I cannot describe how much I appreciated your support and guidance. Thanks also to the rest of the O'Bryan lab who were

gave me their support, especially Jess Dunleavy, Christiane Pleuger, Amy Luan, Sam Cheers, Avinash Gaikwad, and Gemma Stathatos. Most importantly, thank you for believing in me.

From the Fietz Lab: Special thanks to Katja Hartmann for her guidance and expertise during my time in Germany, and for tying off some loose ends after I had left. Thanks also to Alexandra Hax for her support and knowledge. Thanks also to the rest of the Fietz Lab for their friendship and support, especially Anna Freitag, Rashidul Islam and Shashika Kothalawala. Most importantly, thank you for believing in me.

Thankyou also to the members of my panel, Dr Christen Mirth, A/Prof Craig Smith and especially panel chair A/Prof Matt Piper. I have greatly appreciated your support and expertise during the last four years. Thankyou you for your passion in guiding my PhD on the right track. Most importantly, thank you for believing in me.

Thanks also to my IRTG colleagues, especially Rama Ravinthran, Siv Indumathy, Julia Bender and Bea Stadler. It has been a fantastic experience working with you over the last 4 years. Massive thankyou also to the coordinators of the IRTG program, Kate Loveland, Andreas Meinhardt, Pia Jurgens and Liza O'Donnell, for giving me the opportunity to undertake the bi-national PhD, and training me to be a better scientist. A very special thanks to my mentor Sarah Meachem. I am extremely thankful for your guidance, especially over the last few months. I have always felt like you truly believed in me, and you have always inspired me to aim high. Most importantly, thank you for believing in me.

Thankyou to the many friends and colleagues I have made along the way, especially my A-Team. André Nogueira Alves, thankyou for your support, being there to geek out with, and

reminding me of my love of reading. Avishikta Chakraborty, thankyou for being my spirit guide, and for helping me to grow as a person. Amy Luan, thankyou for your friendship and support, and all the help in the lab, especially in the final hours. I love you all and would not have been able to make it without your love and support. Thankyou to all the other friends and colleagues that have supported me throughout my PhD journey, especially Lukas, Vanessa, Billy, Jade, Daniel, Tahlia, Sarah, Arani and Zahra.

Last but certainly not least, thankyou to my family.To my brother Cameron…thankyou for the laughter, the support and the friendship, not only for the last 4 years, but throughout our lives. It has been a pleasure to watch you grow into the man you are, and I look forward to many more years ahead. And to my parents, Mark and Julie. I absolutely would not be here without your love and support. Thankyou for being proud of your son who "plays with flies all day." Thankyou for giving me every single opportunity to follow my dreams, and become the person that I want to become. I cannot even begin to describe how much I appreciate everything you have done for me. This thesis is for you and because of you. Most importantly, thank you for believing in me.

I would like to end with a quote from, Doctor Who. "*We all change, when you think about it. We are different people, all throughout our lives. But that's okay, that's great! You've got to keep moving; so long as you remember who you used to be*" I am a different person than the 22-year-old who started his PhD 4 years ago. I have grown and developed into a person and researcher that I am very proud of. I was able to do this, through all the love and support of everyone listed here, and countless others. Thank you for believing in me.

This research was supported by an Australian Government Research Training Program (RTP) Scholarship

Abbreviations

A-to-I	Adenosine-to-inosine
A_{al}	$A_{aligned}$ spermatogonia
A_d	A_{dark} spermatogonia
A_p	A_{pale} spermatogonia
A_{pr}	A_{paired} spermatogonia
A_s	A_{single} spermatogonia
ADAR	Adenosine deaminase acting on RNA
AEC	3-Amino-9-Ethylcarbazole
ART	Assisted Reproductive Technologies
bb	Basal body
BTB	Blood-testis barrier
Cu	Copper
CySC	Cyst stem cell
DAPI	4′,6-diamidino-2-phenylindole
DIOPT	DRSC interactive orthologue prediction tool
DRSC	*Drosophila* RNAi screening center
ESC	Ectoplasmic specialisation complex
GB	Gonialblast
GEMINI	Genetics of male infertility initiative
GFP	Green fluorescence protein
GSC	Germline stem cell
HGNC	HUGO Genome Nomenclature Committee
IC	Individualisation complex
ICSI	Intracytoplasmic sperm injection
IFT	Intra-flagellar transport
IMT	Intra-manchette transport
IVF	In-vitro fertilisation
KD	RNAi knockdown
MSL	Male Sex Lethal
NOA	Non-obstructive azoospermia
NSP	Normal spermatogenesis

ODF	Outer dense fibre
OE	Over-expression
OA	Obstructive azoospermia
PFA	Paraformaldehyde
PBS	Phosphate buffer saline
qPCR	Quantitative PCR
RNA-seq	RNA sequencing
RNAi	RNA interference
SC	Single cell
SCO	Sertoli-cell only
SLC	Solute carrier family
SNV	Single nucleotide variant
SSC	Spermaotogonial stem cell
SV	Seminal vesicle
SY	Sugar-yeast media
TBCs	Tubulobulbar complex
Te	Testis
TNPs	Transition proteins
TPEN	N,N,N′,N′-tetrakis(2-pyridinylmethyl)-1,2-ethanediamine
TZ	Transition zone
UAS	Upstream activation sequence
ZIP	Zrt-, Irt-like protein family
Zn	Zinc
ZnT	Zinc Transporter family

Table of contents

Chapter 1: Comparing mammalian and fly spermatogenesis – A literature review

1.1 Introduction

Male infertility is a complex disorder that affects approximately 7% of men, and in the majority of cases the exact aetiology is unknown (Tournaye et al., 2017). Estimates indicate that at least 50% of cases are caused by genetic variants. The reality is that such estimates are guesses and usually only consider recessive forms of infertility. However, models indicate that male infertility, can also be caused by dominant de novo mutations within the paternal germline, indicating that up to 90% of cases may, in fact, be genetic in origin (Xavier et al., 2021). Yet another complexity of male infertility is the fact that it is often multifactorial i.e. involving an interaction between multiple genetic variants, or between genetic variants and environmental factors. Male infertility presents itself in many forms, ranging from a complete absence of spermatozoa in the ejaculate (azoospermia), through to reduced sperm count (oligozoospermia) abnormal sperm motility (asthenozoospermia), defects to sperm structure (teratozoospermia), or a combination of multiple defects (asthenoteratozoospermia) and changes to the quality of seminal fluid (Krausz and Riera-Escamilla, 2018).

Male infertility has been associated with increased mortality. A cohort study of over 40,000 men demonstrated a clear link between mortality and semen quality (Jensen et al., 2009), highlighting that men with a decrease in semen quality were likely to die younger than men with normal semen parameters, and that the degree of life shortening scaled with the degree of semen compromise. This decrease in longevity was also consistent between childless and fertile men who had not had children, suggesting that these changes could not be solely attributed to differences in lifestyle or environmental factors. The authors proposed the use of semen quality as a biomarker for overall health in men (Jensen et al., 2009). Broadly consistent findings have been replicated in subsequent studies (Eisenberg et al., 2014, Glazer et al., 2017).

Therefore, determining the genetic causes of infertility is clinically significant and crucial in ensuring the reproductive health and general well-being of a father and children conceived through the use of reproductive technologies (Krausz and Riera-Escamilla, 2018).

Conservative estimates suggest that approximately 20,000 genes are expressed in spermatogenesis (Soumillon et al., 2013) with thousands enriched in the testis (Djureinovic et al., 2014, Fagerberg et al., 2014, Uhlen et al., 2015). However, efforts to elucidate mutations causing infertility have been hamstrung by the fact that these men cannot generate the large families required for traditional linkage studies. Notably, any infertility causing *de novo* mutations will not be passed on to future generations naturally, as they cause infertility. In fact, the advent of assisted reproductive technologies (ARTs), such as *in vitro* fertilisation (IVF) and intracytoplasmic sperm injection (ICSI), has accentuated the need for more research into the aetiology of male infertility. If the cause of infertility is genetic, the natural barriers preventing infertile men from having children are often bypassed when ARTs are used, and thus these mutations can be passed on to future generations. This emphasises the need to generate a comprehensive catalogue of fertility-required genetic variants for screening purposes, to break the cycle of infertility and provide better genetic counselling.

While male infertility is common at a population scale, the incidence of each individual infertility-causing mutation is relatively low and as indicated above is predicted to span thousands of gene targets. Hence, model organisms are likely to be needed to validate to test causality. *Drosophila melanogaster* (fruit flies), as well as mice, are commonly used as models for studying human spermatogenesis, as the process of sperm production is highly conserved (reviewed in Bonilla and Xu (2008) and White-Cooper and Bausek (2010)).

The mouse is the gold standard model organism for studying male infertility (reviewed in Jamsai and O'Bryan (2011) and Borg et al. (2010)). Thus far, mouse models have been used to discover over 500 genes involved in male fertility (Xavier et al., 2021). The process of spermatogenesis is well conserved amongst mammals (Jamsai and O'Bryan, 2011). However, the mouse model does have some drawbacks compared to other model organisms. For instance, male mice do not become fertile until 7 weeks of age. Furthermore, the maintenance of mouse colonies is expensive, and the workload required to study even one gene knockout model is often high.

Drosophila, on the other hand, are undoubtedly useful in studying human genetics, as over 75% of human disease genes have *Drosophila* orthologues (Pandey and Nichols, 2011). There are notable similarities between spermatogenesis in mammals and invertebrates. Flies are also cheaper, have a faster generation time than mouse models, and have a wide variety of well-defined genetic tools (reviewed in Siddall and Hime (2017)). For example, a study by Yu et al. (2015) demonstrated the utility of *Drosophila* in screening for infertility genes. Using a non-obstructive azoospermia GWAS in a Han Chinese population (Hu et al., 2011b), Yu et al. were able to discover candidate single nucleotide variants (SNVs) and screen the fly orthologues of affected genes for roles in male fertility using RNA interference (RNAi). Through this approach, seven genes essential for spermatogenesis were discovered (Yu et al., 2015). While functional validation in higher organisms such as mice is ultimately needed, *Drosophila* provides the opportunity to pre-screen multiple potential genes rapidly and efficiently. Furthermore, sophisticated molecular genetic tools allow the 'humanising' of the *Drosophila* genome, whereby a *Drosophila* gene is replaced by its human orthologue, and then the human genetic variant *in vivo*. Comparing *in vivo* function of the wildtype human gene with that of a

candidate infertility causing variant is the most direct approach to determine if the variant is the actual cause of the infertility in the original patient(s).

While *Drosophila* are undoubtedly useful in studying many aspects of infertility, there are some distinct differences between fly and mammalian reproduction, which must be considered. This review aims to directly compare and contrast the cell biology of *Drosophila* and human spermatogenesis in at each developmental stage. This will not only highlight the benefits of using *Drosophila*, but also outline the potential caveats and limitations of using this invertebrate model.

1.2 Sperm morphology across species

The sperm is a highly specialised cell designed to transport and transfer DNA, the centrioles and a package of RNA from the male, into the egg. Overall, sperm structure is conserved from flies to humans, with all Bilateria sperm having a head, a midpiece and a tail (Bonilla and Xu, 2008). However, within these structures there is significant diversity between species, in the size and shape of the head, the length and size of the midpiece and tail, the entire sperm length, and the number of sperm produced. Each of these differences in sperm morphology assist the sperm in surviving in each organism's particular testicular environment and functioning optimally during their fertilisation journey in the female reproductive tract.

1.3 The structure of the reproductive system

Before comparing spermatogenesis between species, it is important to clarify the similarities and disparities in nomenclature between tissue and cellular structures.

1.3.1 Human

The process of mammalian spermatogenesis is initiated in the seminiferous tubules of the testis. The seminiferous epithelium is comprised of somatic Sertoli cells, which sit on the basement membrane, as well as the germ cells at various phases of development, which are distributed throughout the depth of the epithelium (Figure 1, adapted from Houston et al. (2021)) (Sharma et al., 2018). Sertoli cells are essential for male fertility, as they provide nutritional and structural support, to the developing germ cells throughout spermatogenesis (Rato et al., 2012). Sertoli cells are also responsible for the maintenance of the blood-testis barrier (BTB), a series of junctions between Sertoli cells, that allows the development of spermatocytes and spermatids in an immune privileged location (Cheng and Mruk, 2009). The Sertoli cells are also responsible for the movement of germ cells through the seminiferous epithelium via specialised actin-based adhesion junctions known as ectoplasmic specialisation complexes (ESCs) (Lee and Cheng, 2004). Comparison of the somatic cells in the fly and human testes will be discussed later.

Post-testicular sperm modification and the location of sperm storage differs between humans and flies. Mammalian post-testicular maturation occur primarily in the epididymis, a highly coiled tube attached to the testis via efferent ducts. Spermatozoa travel sequentially through the three major regions of the epididymis: the initial section/caput (or head), the corpus (or body) and the cauda (or tail). Each region has its own specialised functions. While the caput and corpus are primarily responsible for the maturation of the spermatozoa, the cauda acts as a storage vessel for functionally mature spermatozoa prior to ejaculation (Cornwall, 2009). Epididymal modifications include the acquisition of the ability for progressive motility, changes in internal sperm protein and RNA content, changes to the plasma membrane and the

acquisition capacitation potential, which are essential for sperm to bind and fertilise an oocyte (Gervasi and Visconti, 2017).

Once mammalian sperm are ejaculated, they are mixed with the seminal fluid secreted from the seminal vesicles and the prostate, and fluids within the female reproductive tract. The seminal fluid provides metabolites, immune and functional support to sperm as they travel through the female reproductive tract (Drabovich et al., 2014). Within the female reproductive tract, sperm undergo capacitation, then ultimately hyperactivated motility and enables the sperm to bind to an oocyte, and undergo the acrosome reaction.

1.3.2 *Drosophila*

The *Drosophila* testis is a small blunt ended, coiled tube, with spermatogenesis beginning at the apical tip and progressing along the apical-basolateral axis (Figure 2). All phases of spermatogenesis can be viewed concurrently in a single fly testis. Cyst cells (analogous to mammalian Sertoli cells) and germ cells originate from their respective stem cell populations that sit at the apical tip. Each germ stem cell is surrounded by two cyst stem cells, which develop concurrently with the germ cell. Upon commitment to spermatogenesis, two cyst cells surround a developing germline cell, protecting the developing spermatogonia, spermatocytes and spermatids, and providing signals to stimulate differentiation (Hardy et al., 1979, Cheng et al., 2011).

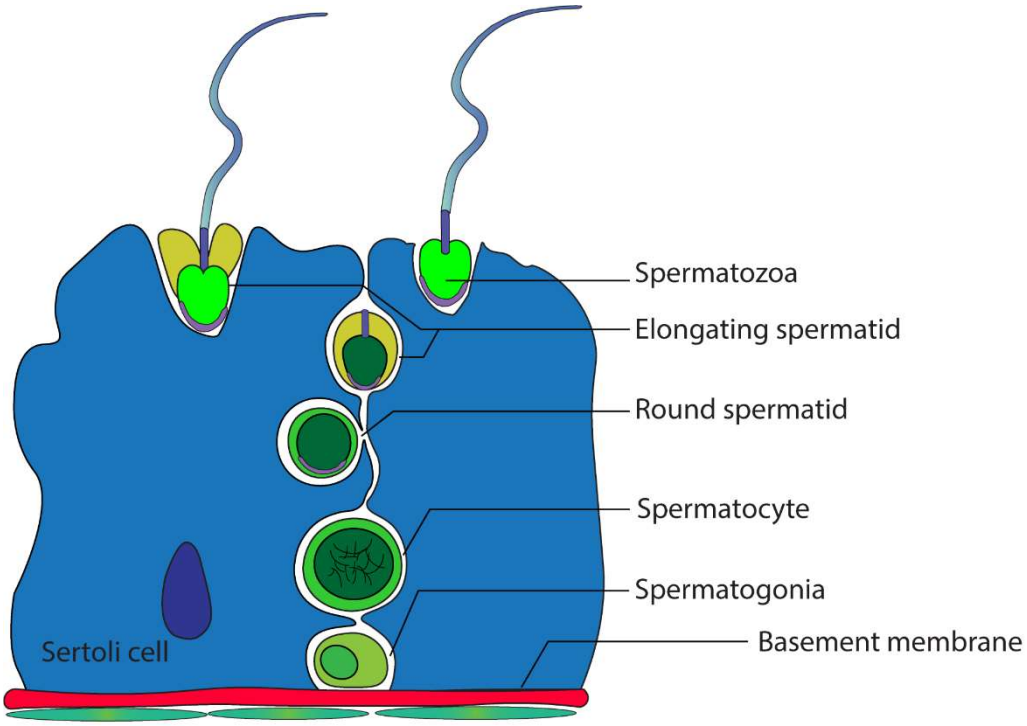

Figure 1: Spermatogenesis in the human testis. Spermatogenesis begins on the basement membrane of the testis. The seminiferous epithelium is made up of developing germ cells and somatic Sertoli cells. Spermatogenesis begins with A_{dark} spermatogonia which replicate to form another A_{dark} spermatogonium, and an A_{pale} spermatogonia. These A_{pale} spermatogonia then divide to develop into type B spermatogonia. When B spermatogonia begin to undergo meiosis, they are named primary spermatocytes, which undergo meiosis I. The secondary spermatocytes undergo meiosis II to form four round spermatids. The round spermatids undergo spermiogenesis to gain the properties required for a developed spermatozoa such as elongation and sperm tail formation. The elongated spermatids are released into the lumen of the seminiferous tubule. Figure adapted from Houston et al. (2020)

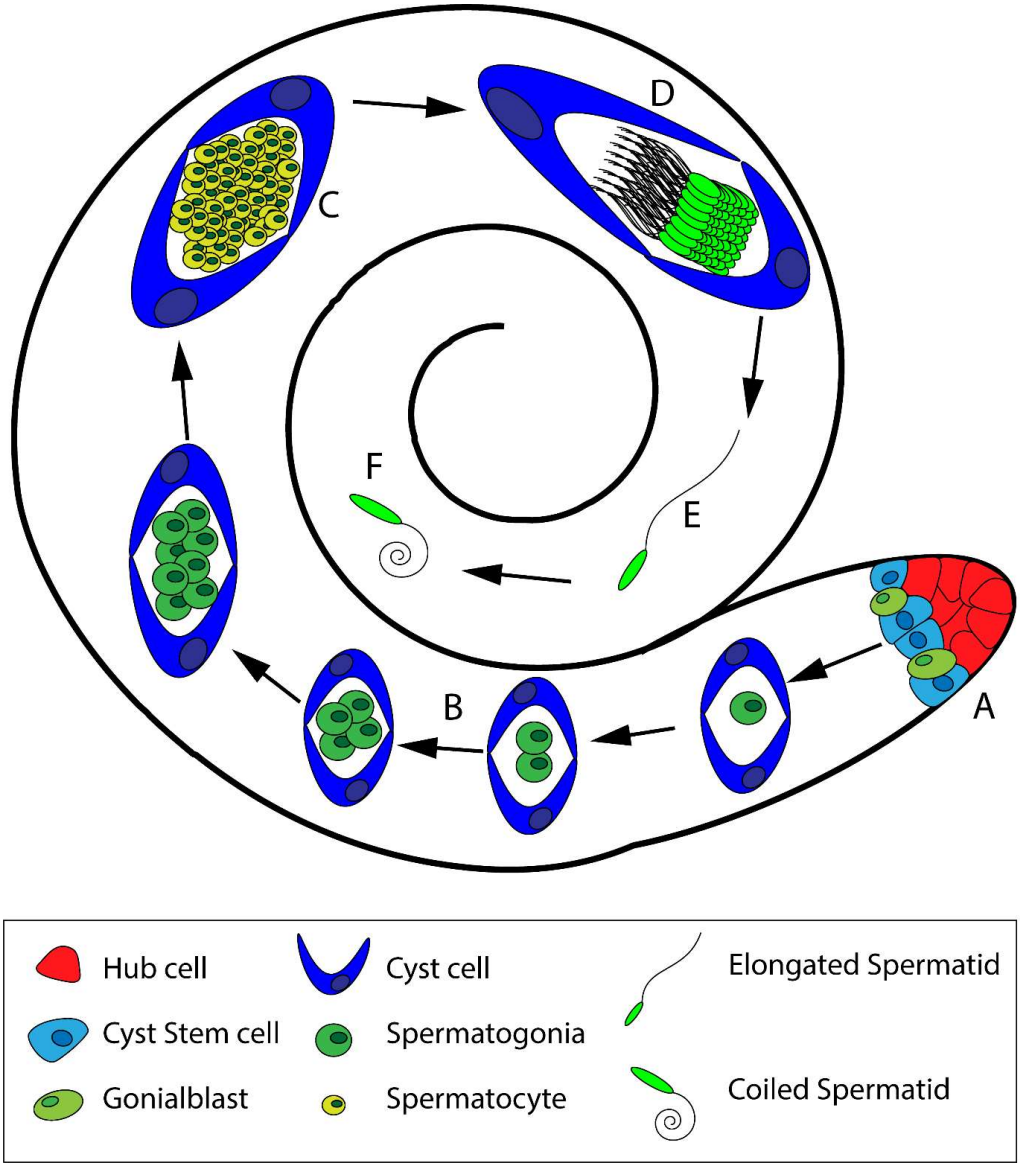

Figure 2: Spermatogenesis in the *Drosophila melanogaster* testis. The *Drosophila* testis is a spiral-shaped blunt ended tube. Spermatogenesis begins at the blunt end of the tube (A) where the hub cells (red) provide a niche supporting the stem cells. The cyst stem cells (light blue) surround the germline stem cells (light green). These differentiate into a single gonialblast, the *Drosophila* equivalent of the mammalian spermatogonium (dark green) surrounded by two cyst cells (dark blue). These undergo multiple rounds of transit-amplifying divisions (B) to produce 64 spermatocytes (yellow) (C). Spermatids undergo spermiogenesis, where the acrosome and tail begin to form, and the chromatin condenses within the sperm head (D). At this point, the cyst cells also differentiate into the head and tail cyst cells. The spermatids then undergo individualisation, which breaks the bonds connecting the sperm in the bundle (E). Finally, the spermatids coil at the open end of the tube (F).

Drosophila sperm are also not completely mature upon exiting the testis. Flies do not, however, have an epididymis. Instead, sperm enter a structure, rather confusingly known as the seminal vesicle, where they are stored. As the sperm travel from the seminal vesicles to the ejaculatory duct, they come in contact with seminal fluid proteins that are released from the accessory glands and the ejaculatory bulb (Avila et al., 2011), tissues analogous to the mammalian seminal vesicles and prostate, respectively.

While the complete composition of the *Drosophila* seminal plasma is yet to be determined (Majewska et al., 2014), there are thought to be over 100 proteins released from the accessory glands, ejaculatory duct and ejaculatory bulb, which assist in cellular metabolism, proteolysis and cell signalling, among other functions (Takemori and Yamamoto, 2009).

In summary, while the processes of spermatogenesis are highly conserved between species, there are some distinct differences between the male reproductive systems.

1.4 Somatic cells

In both human and *Drosophila* spermatogenesis, the somatic cells provide an optimal environment for the germline cells to develop. However, while the Sertoli cells in mammals and the cyst cells in *Drosophila* may play a similar role, there are some significant differences in their function which must be understood to accurately compare spermatogenesis.

1.4.1 Human

The Sertoli cell, or ‘nurse’ cell, plays numerous roles in spermatogenesis, including nutritional and physical support, as well as paracrine signalling. They have a large surface area, and many cellular extensions which allow them to remain in contact with a large number of germ cells at

numerous stages of development, as well as other Sertoli cells The junctions between Sertoli cells form the blood-testis barrier (BTB) which has many roles (reviewed in (Cheng and Mruk, 2012)), including providing a physical barrier to regulate the entry of nutrients, endocrine molecules and harmful toxins, into the area surrounding the developing germ cells. The BTB also provides a barrier to sequester the highly immunogenic spermatocytes and spermatids from immune-mediated attack (Fijak et al., 2011).

The Sertoli cells also secrete substances which are crucial in spermatogenesis such as energy sources for the developing germ cells. One example of this is the production of lactate for pachytene spermatocytes and round spermatids which require a high amount of energy production (Jutte et al., 1981). Other critical energy sources such as glucose and pyruvate are also secreted by the Sertoli cell (reviewed in (Alves et al., 2013)).

The Sertoli cell begins to function in its 'nurse' role in the testis in the embryo, protecting the embryonic germ cells, called gonocytes, and initiates the formation of the early seminiferous tubules (Griswold, 1998). In order for Sertoli cells to mature and begin to form the required junctions for the BTB, their proliferation must terminate, which occurs during puberty (Griswold, 1998, Meroni et al., 2019). Therefore, the number of Sertoli cells present in a testis does not increase significantly after this time. Furthermore, Sertoli cell number is directly correlated with an increase in sperm production (Orth et al., 1988, Meroni et al., 2019). Conversely, in impaired spermatogenesis or Sertoli-cell only syndrome, where germ cells are impaired or completely absent, Sertoli cell development is also disrupted. Steger et al. (1996) found that patients with impaired spermatogenesis had Sertoli cells which effectively de-differentiated, as they continued to express markers which are usually only expressed during puberty.

1.4.2 *Drosophila*

Much like the germline stem cells (GSCs) in *Drosophila* (discussed later), the somatic cyst cells originate from a stem cell lineage, the cyst stem cells (CySCs). This is different from mammalian spermatogenesis, where the somatic (Sertoli) cell number is mostly determined during puberty (Orth et al., 1988). Differentiating CySCs are flat and irregularly shaped, which allows them to encapsulate the GSC, both protecting it as well as ensuring constant GSC/CySC signalling (Cheng et al., 2011). The signalling between the CySCs and GSCs is important, especially regarding the proliferation of the cells. Like the GSCs, when the CySC divides, one daughter cell continues as a CySC while the other becomes a cyst cell (Hardy et al., 1979). Importantly however, Gönczy and DiNardo (1996) demonstrated that in the absence of germ cells, daughter cyst cells continue to proliferate, instead of differentiating into the cyst cell, suggesting again that reciprocal signalling and cross talk between the GSCs and the CySCs assists in the regulation of the stem cell proliferation.

After differentiation, two cyst cells surround one gonialblast, which is this *Drosophila* equivalent of the mammalian spermatogonium. This forms one group of developing cells, called a cyst. Much like the mammalian Sertoli cells, the cyst cells isolate the developing germline cells, preventing the germ cells from contact with other cells. This continues through gonialblast differentiation into spermatogonia and eventually into spermatocytes. At this point, both cyst cells and germ cells grow in size in order to accommodate the increase in size and number of the germ cells (Zoller and Schulz, 2012). As spermatids begin to undergo spermiogenesis and form the head and tail of the elongating spermatid, the cyst cells also differentiate. The caudal cyst cell lengthens to accommodate the sperm tail, becoming the tail cyst cell, while the rostral cell is called the head cyst cell (Zoller and Schulz, 2012). By the late

elongating spermatid stage, the spermatid nuclei are oriented to place them at the head cyst cell end of the cyst (Fabian and Brill, 2012)

There are many key differences between the function of the Sertoli cells in human spermatogenesis and cyst cells in fly spermatogenesis. In humans, the number of Sertoli cells is relatively fixed and does not change significantly throughout life, nor can they be renewed. Comparatively, *Drosophila* cyst cells are constantly generated from cyst stem cells and develop alongside the germ cell they are enclosing. As the germ cells in mammalian spermatogenesis are moving through the seminiferous tubules, they have contact with 5-6 Sertoli cells. In flies, the germ cells are only in contact with the two cyst cells which encase them.

1.5 Stem cells and spermatogonia

1.5.1 Human

Mammalian spermatogenesis begins with a population of cells called spermatogonial stem cells (SSCs), which reside in a stem cell niche. The SSCs can either renew themselves or commit to developing into spermatogonia. There are multiple hypotheses, reviewed in de Rooij (2017), to explain how the balance between differentiation and self-renewal might occur. However, it is important to first clarify the nomenclature surrounding the types of spermatogonia, as they differ between mice and humans (Guo et al., 2014b)

The model for categorising human spermatogonia was first defined by Clermont (1966), who separated the spermatogonia based on their chromatin structure and nuclear intensity when stained with haematoxylin. A_{dark} (A_d) spermatogonia are small, spherical cells that reside on the basement membrane of the seminiferous tubules. They have a uniformly stained nucleus and dense chromatin which is most easily viewed by a uniform haematoxylin stain, and a bright "halo" surrounding the nucleus. A_{pale} (A_p) spermatogonia, have much less haematoxylin

staining, and are lighter in colour (hence the name, pale). Type B spermatogonia, also have pale haematoxylin-stained chromatin but can be differentiated from A_p spermatogonia, as type B spermatogonia contain heterochromatin (De Rooij and Russell, 2000).

Both A_d and A_p spermatogonia can be defined as stem cells however they perform very different functions in maintaining the human germline. A_d spermatogonia serve as the more traditional stem cells, which very rarely divide, while A_p are the transit-amplifying equivalent, and divide regularly to both self-replicate and produce B spermatogonia, which then commit to sperm production and through their subsequent mitotic division, form spermatocytes (Figure 3A) (Waheeb and Hofmann, 2011).

The nomenclature for mouse spermatogonia (Figure 3B) was outlined over 40 years ago, and, while the model is somewhat out dated, the nomenclature is still used today (Huckins, 1971). A_{single} (A_s) spermatogonia were proposed to be the only SSCs. The daughter cells from one A_s division either remain SSCs, or pair off to become A_{paired} (A_{pr}) spermatogonia. The A_{pr} spermatogonia then proliferate to form long chains (4-16 cells in length) of spermatogonia called $A_{aligned}$ (A_{al}) spermatogonia. These A_{al} spermatogonia then undergo many rounds of mitosis to form the eventual spermatozoa (Huckins, 1971), thus this is called the A_s model.

While many variations have been proposed since the publication of the original A_s model (Hara et al., 2014), the most widely accepted model for spermatogenesis in rodents is the hierarchical model. This model is based on work by Kubota et al. (2004), which found that glial cell line-derived neurotrophic factor (GDNF) is an essential growth factor for mammalian SSCs. Further work determined that Inhibitor of DNA-binding 4 (ID4, Inhibitor of Differentiation 4) is expressed in a small population of A_s spermatogonia, and is regulated by GDNF signalling

(Oatley et al., 2011). Most importantly however, the same group found that ID4 levels are heterogeneous among A_s spermatogonia. Some A_s cells, named $SSC_{ultimate}$ show high levels of ID4, while also exhibiting high self-renewal capacity. These $SSC_{ultimate}$ then undergo numerous rounds of division and eventually begin showing lower levels of ID4 signalling.

These cells then become more likely to undergo differentiation into A_{pr} spermatogonia and become $SSC_{transitory}$ cells. Thus, as ID4 levels in the SSCs decrease, the cells become more likely to differentiate into A_{pr} spermatogonia, than to self-renew, and eventually differentiate into spermatocytes (Helsel et al., 2017). While ID4 levels do seem to provide an indication of self-renewal potential, they are far from the only factor which must be taken into consideration. Proteins such as paired box 7 (PAX7) and B cell-specific Moloney murine leukaemia virus integration site 1 (BMI1) also play a role (reviewed in de Rooij (2017)), and there are undoubtedly others. It is important to understand that this is a rodent model and may not be identical to the human model.

After the proliferation of A_{pr} spermatogonia, the cells form chains of cells called A_{al} spermatogonia. After the A_{al} period, the cells cease mitosis, and form A_1 spermatogonia, which undergo multiple divisions (forming A_2, A_3 and A_4 spermatogonia), at which point the A_4 spermatogonia undergo one further round of division to form Intermediate spermatogonia. One further round of division forms the type B spermatogonia, which following one final division forms the preleptotene spermatocytes (De Rooij and Russell, 2000). The distinguishing feature between type A and type B spermatogonia, is that type Bs have dispersed clumps of heterochromatin, whereas type A spermatogonia have “dusty” heterochromatin. Intermediate spermatogonia have an intermediate between the two. Fortunately, despite the differences between the human and mouse spermatogonia, comparison is still possible (Figure 3).

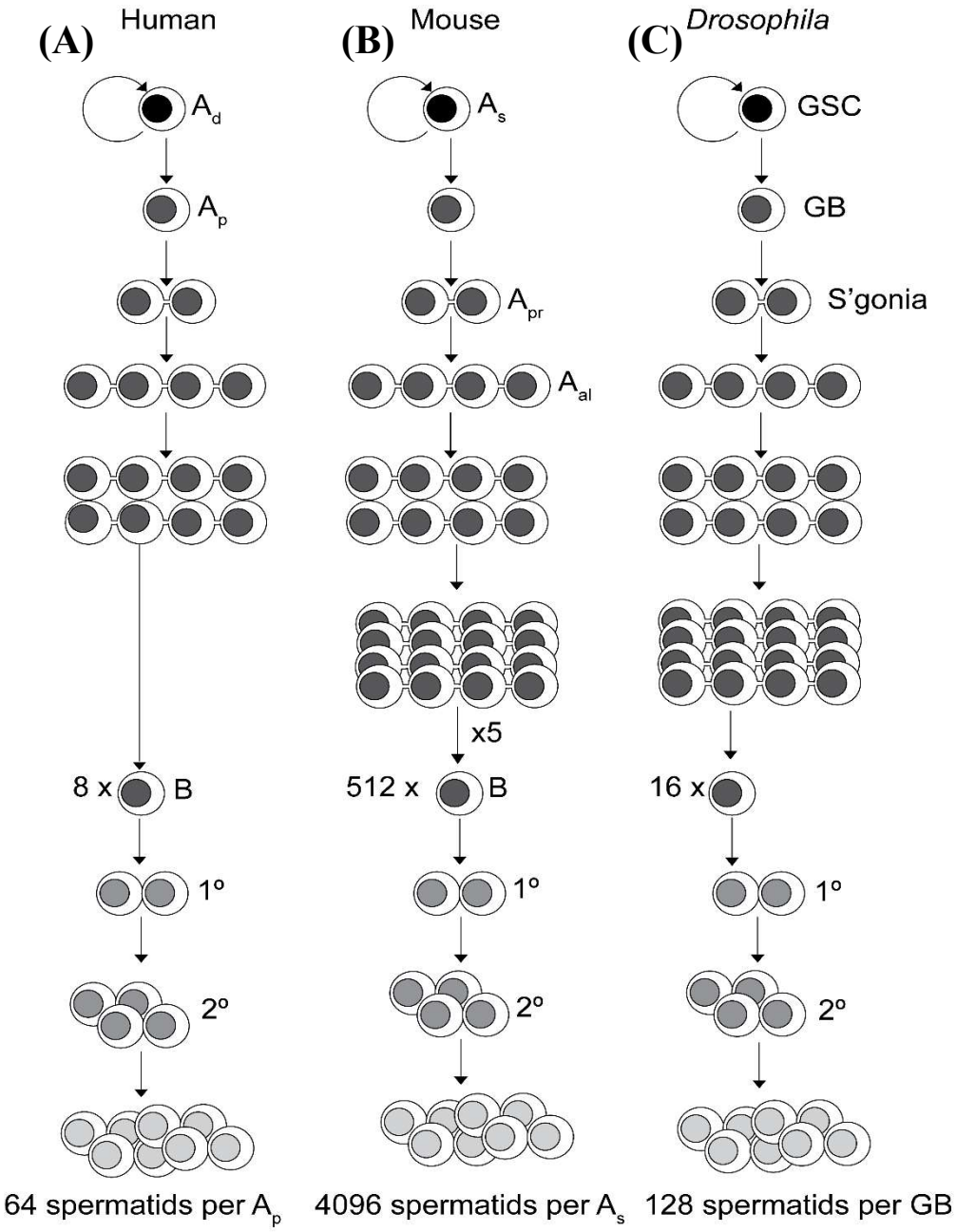
(A)
Human
A_d
A_p
8 x B
1º
2º
64 spermatids per A_p
(B)
Mouse
A_s
A_{pr}
A_{al}
x5
512 x B
1º
2º
4096 spermatids per A_s
(C)
Drosophila
GSC
GB
S'gonia
16 x
1º
2º
128 spermatids per GB

Figure 3: Germ cell expansion from spermatogenic stem cells in humans, mice and flies. (A) The human germ cell begins with a single A_d spermatogonia, which renews itself, as well as giving rise to a daughter A_p spermatogonia. The A_p cells undergo two transit amplifying replications to produce eight B spermatogonia. A singular B spermatogonia then produces two primary spermatocytes. The two primary spermatocytes undergo meiosis I to produce four secondary spermatocytes, which undergo meiosis II to produce 8 spermatids. 64 spermatids are produced from a single A_p spermatogonia. (B) Mouse germ cell development begins with an A_s spermatogonia, which renews itself and produces a differentiated A_{pr} spermatogonia. These divide to produce multiple A_{al} spermatogonia, which undergo seven rounds of transit-amplifying replications to produce 512 B spermatogonia. A singular B spermatogonia forms two primary spermatocytes. The two primary spermatocytes undergo meiosis I to produce four secondary spermatocytes. The four secondary spermatocytes undergo meiosis II to produce eight spermatids. From a single A_{pr} spermatogonia, 4096 spermatids are produced. (C) In *Drosophila*, the germline stem cells (GSCs) self-renew and produce a gonialblast (GB). The GB replicates to form a spermatogonia, which in turn undergoes three TA replications to form 16 spermatogonia. A single spermatogonia produces two 1° spermatocytes, which undergoes meiosis I to produce four 2° spermatocytes. The 2° spermatocytes then undergo meiosis II to produce eight spermatids. In total, 128 spermatids are produced from a single GB.

Legend: 1°- Primary spermatocytes, 2°- Secondary spermatocytes, A_{al}- $A_{aligned}$ spermatogonia, A_d- A_{dark} spermatogonia, A_p- A_{pale} spermatogonia, A_{pr}- A_{paired} spermatogonia, B- B spermatogonia, GB- Gonialblast, S'gonia- Spermatogonia, GSC- Germline stem cell

1.5.2 *Drosophila*

In *Drosophila*, the male germline is an excellent model for examining stem cell self-renewal and differentiation (Davies and Fuller, 2008). Like in mammals, *Drosophila* GSCs reside within a "stem cell niche", a microenvironment that assists the stem cells to either commit to spermatogenesis, or undergo self-renewal. These processes are tightly controlled by the niche, as excessive differentiation or commitment leads to a depletion of the GSCs, while too much self-renewal can lead to an over population of replicating cells, and eventually tumorigenesis, much like in mammals (Yamashita et al., 2005). This niche resides at the apical tip of the *Drosophila* testis (de Cuevas and Matunis, 2011)

Once the GSCs divide, one remains attached to the hub in order to remain a GSC and the other, the gonialblast, divides away from the niche and will eventually differentiate into a developed sperm cell (de Cuevas and Matunis, 2011). The gonialblast itself is surrounded by two somatic cyst cells. After four rounds of transit-amplifying divisions, a group of 16 spermatogonial cells generated from a singular gonialblast remain encased within the original two cyst cells.

In summary, the pre-meiotic phase of spermatogenesis is highly conserved between flies and mammals. Flies have long been used to further understand the role of the testicular stem cell niche, and of transit amplification, which contributes to our understanding of the mammalian processes. While conserved, the number of transit amplifications are slightly different between species, as a single spermatogonium/gonialblast results in 64 spermatids in the human, 4096 in the mouse and 128 in the fly (Figure 3).

1.6 Meiosis

Meiosis is an essential process in gametogenesis that involves the ultimate production of four haploid daughter cells from a diploid (but 4N) spermatocyte. Appropriate chromosomal segregation is critical to ensure that each germ cell receives only one copy of each chromatid. As meiosis is an extremely complex process, this review will focus on a few key mechanisms, including cohesion and synapsis of homologous chromosomes, recombination and chromosome segregation. Recombination (‘crossing over’) is especially important to discuss, as this represents a distinct difference between flies and humans during male meiosis. Male meiosis in both humans and flies begins with a single round of DNA replication in primary spermatocytes (Figure 4Ai and Bi). Once replication is complete, meiosis diverges between flies and humans.

1.6.1 Human

In humans, homologous chromosomes pair and undergo synapsis during prophase. This involves the formation of the synaptonemal complex (Figure 4Aii), a ladder-like structure that holds homologous chromosomes together. Synapsis allows the physical exchange of double-stranded DNA between two non-sister chromatids, known as crossing over or recombination, at a structure called the chiasma (Figure 4Aiii). Recombination contributes to a further increase in the genetic diversity that results from sexual reproduction (Zickler and Kleckner, 2015). The generation of chiasmata during meiosis I is thought to be essential for the correct segregation of homologous chromosomes into separate daughter cells, as chromosome pairs lacking chiasmata often undergo non-disjunction, resulting in aneuploid gametes (Carpenter, 1994). Next, the chromosomes align along the equator of the cell at metaphase I.

Chromosomal segregation begins with the initial attachment of microtubule spindle bundles, originating from each of the nuclear poles to the centromere of each chromosome (McKee et al., 2012). At anaphase I, the highly conserved (including in flies) enzyme Separase is activated. Active Separase cleaves REC8, which aligns sister chromatids. However, during meiosis I, the highly conserved protein Shugoshin maintains sister chromatid cohesion by recruiting protein phosphatase 2A (PP2A) (Figure 4Aiv) which phosphorylates some of the REC8, protecting it from cleavage by Separase (Kitajima et al., 2006, Clift and Marston, 2011).

The synaptonemal complex, which holds homologous chromosomes together, then disassembles through the breakdown of the individual sub-complexes (reviewed in Cahoon and Hawley (2016)). After disassembly, the homologous chromosomes are weakly held

together by the chiasmata. The spindle bundles at separate poles then pull apart the chiasmata, separating the homologous chromosomes into two sets of sister chromatids (Figure 4Av). The cell divides through incomplete cytokinesis to form two diploid spermatocytes, each containing one set of sister chromatids and connected by intercellular bridges (Figure 4Avi). These bridges, which have also been formed between spermatogonia (Haglund et al., 2011) persist throughout germ cell development, and allow the sharing of protein and RNA across cells, maintaining the synchronised development of connected germ cells.

At the beginning of meiosis II, the sister chromatids are still held together by the centromere, as well as by REC8. Much like the separation of homologous chromosomes during meiosis I, microtubule spindle bundles attach to the centromeres of the sister chromatids from the nuclear poles (Figure 4Avii). The pulling strength of these spindles is so great that Shugoshin is inactivated, REC8 is cleaved by Separase, and the sister chromatids separate to opposite poles of the dividing cell (Clift and Marston, 2011, McKee et al., 2012) (Figure 4Aviii). This results in the final product of meiosis; four haploid spermatids connected by intercellular bridges (4Aix).

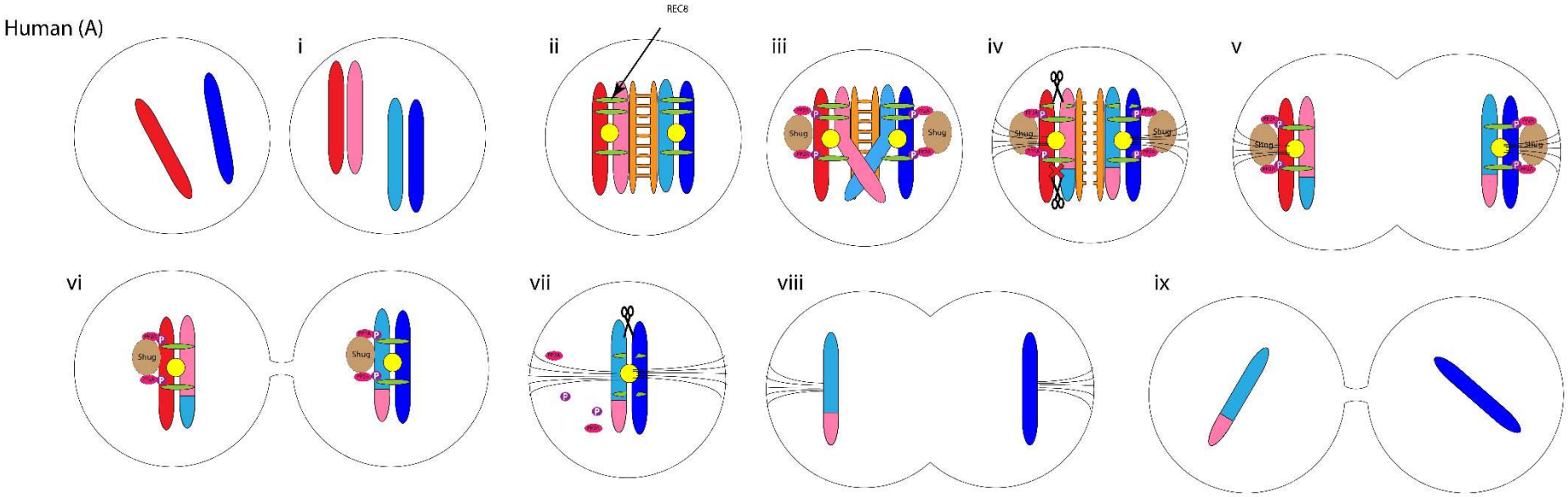
Human (A)
i
ii
REC8
iii
iv
v
vi
vii
viii
ix
Shug
Sgo1
PP2A
P
Drosophila (B)
i
ii
solo
ord
mnm
snm
iii
iv
v
vi
vii
viii
ix
Mei-S332
uno

Figure 4: Comparison of meiosis between humans (A) and flies (B). Meiosis in both humans and flies begins with a single round of DNA replication (Ai and Bi). In the human spermatocytes, REC8 (green) aligns sister chromatids and the synaptonemal complex (orange ladder) holds homologous chromosomes together (Aii). Shugoshin recruits PP2A, which phosphorylates REC8. Crossing-over occurs, assisted by the synaptonemal complex (Aiii). Separase breaks down the synaptonemal complex and cleaves the unphosphorylated REC8. Spindle fibres attach to homologous chromosomes (Aiv). Spindle fibres separate the homologous chromosomes (Av). The cell splits through incomplete diakinesis, forming two cells with a single pair of sister chromatids (Avi). Shugoshin is removed, REC8 is dephosphorylated and cleaved by Separase, and the spindle fibres attach to the sister chromatids (Avii). The spindle fibres pull the sister chromatids to opposite ends of the cell (Aviii). The cell splits via incomplete diakinesis, forming two cells with a single chromatid. In the *Drosophila* spermatocyte, sister chromatids are aligned by solo and ord, while the homologous chromosomes are aligned via mnm and snm (Bii). Uno is a cohesion which holds the homologous chromosomes together (Biii). Separase cleaves uno, while Mei-S332 prevents Separase from cleaving ord and solo. The spindle fibres attach to the homologous chromosomes (Biv). The spindle fibres pull each pair of sister chromatids to opposite ends of the cell (Bv). The cell splits through incomplete diakinesis, forming two connected cells, each with a pair of sister chromatids (Bvi). Mei-S332 is removed and Separase cleaves ord and solo. The spindle fibres attach to the sister chromatids (Bvii). The spindle fibres separate the sister chromatids (Bviii) and the cell splits via incomplete diakinesis to form two cells each with a single chromatid (Bix)

1.6.2 *Drosophila*

Much like meiosis in human spermatocytes, meiosis I in *Drosophila* testes takes place immediately following the 16-cell stage of spermatogenesis. At this point, the germ cells are still located near the blunt-ended apical tip of the testis, within the testis somatic cell cyst.

A critical difference in chromosomal synapsis between human and *Drosophila* males is that a synaptonemal complex does not form in *Drosophila* spermatogenesis. This means that homologous chromosomes in *Drosophila* males neither form chiasmata nor undergo recombination (Orr-Weaver, 1995).

Instead, meiotic pairing of chromosomal homologues in *Drosophila* spermatocytes occurs via two proteins named modifier of mdg4 (mnm) and stromalin in meiosis (Stromalin-2/snm) (Figure 4Bii). These form a conjunction complex, analogous to the synaptonemal complex in humans which, when absent, leads to aberrant segregation of chromosomes (Sun et al., 2019, Thomas et al., 2005)

While mnm and snm play a role in the conjunction of homologous chromosomes, they do not seem to have a role in the cohesion (Sun et al., 2019). In short, these conjunction complexes bring homologous chromosomes close, and cohesins are the "glue" that holds them together. Rather than the synaptonemal complex, chromosome cohesion in *Drosophila* male meiosis involves meiotic cohesins. A recent study by Weber et al. (2020) reported a protein, univalent only (uno), that requires cleavage by Separase in male meiosis I, which suggests that uno could be performing a role analogous to that of chiasmata human homologous chromosome cohesion (Figure 3Biii). In summary, during human meiosis, the synaptonemal complex is responsible for both conjunction and cohesion (through the chiasmata). During fly meiosis, snm and mnm purportedly function in the conjunction of homologous chromosomes, while uno plays a role in their actual cohesion.

Much like in the human, *Drosophila* meiosis involves mei-S332, a member of the Shugoshin family, which protects sister chromatid cohesion from being broken in meiosis I (Kerrebrock

et al., 1995) Figure 4Biii and iv). Given that the separation of sister chromatids requires members of the Shugoshin family in both fly and human germ cells, these mechanisms are relatively similar (Figure Bv-Bix). The mechanisms underlying cohesion of sister chromatids in *Drosophila* is yet to be determined, however, it is suggested that two genes, *sisters on the loose (solo)* (Yan et al., 2010) and *orientation disruptor (ord)* (Bickel et al., 1997) have functional similarities to human REC8 (McKee et al., 2012).

1.7 Spermiogenesis

Spermiogenesis, which begins immediately after the second meiotic division, is the process by which the round spermatid (named such due to the shape of both the cell and the nucleus), develop into a spermatozoon. In developing from round to elongated spermatids, germ cells in both humans and flies undergo four major changes: i) the formation of the acrosome; ii) the condensation and shaping of the nucleus; iii) the development of the flagellum; and iv) the removal of most of the cytoplasm.

Before comparing spermiogenesis, it is important to outline the unique process in insect spermiogenesis called mitochondrial morphogenesis, which involves a number of complex changes to the mitochondria, including aggregation, fusion, fission and elongation (Phillips, 1970). This results in a single large mitochondrial derivative that encircles the flagellum at the midpiece, rather than several helically arranged mitochondria seen in mammalian sperm.

The first step of mitochondrial morphogenesis occurs during the polarisation of the cell, whereby the mitochondria aggregate on the posterior end of the nucleus, near the basal body. The mitochondria fuse to form a major and a minor derivative, which wrap around each other, forming an onion-like structure called the nebenkern (Tokuyasu, 1975). This fusion is mediated

by a protein called fuzzy onions (fzo) the mutation of which causes sterility, as rather than forming a singular onion-shaped nebenkern, multiple smaller onion-shaped mitochondrial derivatives are formed. This mutation results in elongating spermatids containing individual elongating mitochondria, rather than the two elongating derivatives which normally form from the nebenkern (Hales and Fuller, 1997).

Mitochondrial fission, the breakdown of a singular mitochondrial tubule into multiple structures, also occurs in *Drosophila* spermatogenesis, mediated in part by *dynamin-related protein 1* (*drp1*) (Okamoto and Shaw, 2005). This initially occurs in the spermatocyte during meiosis, where *drp1* is responsible for the fragmentation of the nebenkern, which enables appropriate mitochondrial segregation (Aldridge et al., 2007). Mutation in *drp1* causes a large mass of interconnected mitochondria, resulting in aberrant mitochondrial separation during each meiotic division. Furthermore, *drp1*-mediated fission is also required in the later stages of mitochondrial morphogenesis, in order to appropriately counterbalance mitochondrial fusion, as a balance is required to allow for the elongation of the mitochondrial derivative. This involves the unfurling of the mitochondrial derivatives to allow elongation of the spermatid, and formation of the tail (Aldridge et al., 2007). The elongation and formation of the sperm tail will be discussed in greater depth later in this review.

1.8 Acrosome and acroplaxome formation

1.8.1 Human

The first phase of human spermiogenesis involves coordination between the surrounding Sertoli cells and three key structures within the developing sperm cell. The acrosome, the acroplaxome, and the manchette, ensure the sperm has a functional and species-specific head shape (Kierszenbaum and Tres, 2004). The function of the sperm's acrosome is to: i) transport

specific enzymes required to achieve the acrosome reaction and digest the zona pellucida of the egg in the female reproductive tract; and ii) streamline the shape of the head to optimise the hydrodynamics of sperm movement. Acrosome formation is complex, as it involves the production of a large number of proteins produced by the Golgi and endocytic pathways, some of which are produced as early as the pachytene spermatocyte stage (Escalier et al., 1991). Acrosomal biogenesis can be split into four phases, the Golgi phase, the cap phase, the acrosome elongation phase and the maturation phase (Clermont and Leblond, 1955, Khawar et al., 2019, Pleuger et al., 2020).

During the initial Golgi phase of acrosome development, acrosomal vesicles produced from both the Golgi apparatus and the endocytic pathways attach and indent into the apical pole of the spermatid nucleus (Berruti et al., 2010). This proceeds with the continued recruitment of acrosomal vesicles and creates the acrosomal granule. During the cap phase, the acrosomal granule is localised to the acrosomal pole and begins to enlarge and flatten over the nucleus forming the acrosomal cap. The acrosome is surrounded by a double membrane, consisting of the outer acrosomal membrane which sits adjacent to the plasma membrane, and the inner acrosomal membrane which attaches to the nucleus (Buffone et al., 2008). The increase in size of the acrosomal granule is due to the addition of glycoproteins produced by the Golgi apparatus and endoplasmic reticulum. During the cap phase, the acroplaxome, a plate-like structure, is formed between the inner acrosomal membrane and the nucleus.

When fully formed, the acroplaxome sits between the acrosome and the nucleus, and consists of F-actin microfilament proteins, and a ‘marginal ring’ which contains keratin 5 filaments (Kierszenbaum et al., 2003). During acrosome development, the acroplaxome has two main functions; to anchor the acrosome to the nucleus and to provide a structure for the shaping of

the sperm head (Kierszenbaum et al., 2003). The latter will be discussed in the following section. In the elongating/acrosome phase, the acrosome starts to migrate along the sperm head, and attach to the inner acrosomal membrane. The final (maturation) phase is characterised by the spread of the acrosome across the entire acrosomal membrane, aided structurally by the acroplaxome, covering almost the entire sperm head.

1.8.2 *Drosophila*

While there has not been research to indicate that the four distinct phases outlined in Clermont and Leblond (1955) also occur in flies, similar language will be used here, as many of the acrosome biogenesis processes appear similar. In the fly, the formation of the acrosome begins at what would be the Golgi phase, which is concurrent with the formation of the mitochondrial structure, the nebenkern. The Golgi generates a structure called the acroblast, which is made up of a combination of Golgi-derived components and assembles at the opposite side of the nucleus to the basal body (a modified centriole structure) (Fuller, 1993). This highlights that both human (in part) and fly acrosomes are derived from the Golgi. Interestingly, the acroblast in *Drosophila* is unique from other Golgi-derived structures in the fly, as it forms a Golgi ribbon, which is a large organelle of multiple connected Golgi. While this differs from the usual Golgi stacks found in other cells of the fly (Kondylis and Rabouille, 2009), it is similar to the Golgi ribbons found in mammalian cells, and in mammalian acrosome formation. This may suggest that while Golgi formation in general is different between humans (ribbons) and flies (stacks), the acrosome formation in both organisms, via Golgi ribbons, is conserved.

In *Drosophila,* the acrosome appears to be made solely from Golgi-derived material, without the addition of endocytic material, seen in the human acrosome. In *Drosophila,* the *trans*-side

of the Golgi binds to the acroblast, much like the binding of the *trans*-side of the Golgi to the acroplaxome in humans (Moreno et al., 2000, Fári et al., 2016). This suggests the fly acroblast plays an analogous role to the human acroplaxome in acrosome shaping. In round spermatids, the fly acrosome is horseshoe-shaped, covering the tip of the elongating nucleus (Fári et al., 2016), similar to the corresponding human acrosome shape. As the spermatid develops, the acrosomic granule is generated from the side of the acroblast adhering to the nucleus (Fuller, 1993, Yasuno et al., 2013). The acroblast is then broken down, and scattered at the posterior side of the nucleus, and discarded as a part of the "waste bag" (Yasuno et al., 2013), which will be discussed later in this review.

One particularly interesting difference between fly and human spermiogenesis is the lack of acrosome reaction in *Drosophila* fertilisation. *Drosophila* sperm enter the oocyte with their membrane (including the acrosome) completely intact, and it is only when inside the oocyte, that the acrosome and cellular membrane breaks down (Perotti, 1975). However, this does not mean that the acrosome is not essential in fly oocyte fertilisation, as mutation of acrosome-specific proteins results in a failure to fertilise (Wilson et al., 2006). The latter is perhaps evidence of the acrosomes' essential role in entering the oocyte.

In summary, there are some distinct similarities between the fly and the human acrosome. Importantly the acrosome is exclusively derived from Golgi materials in flies, while endocytic material also contributes to acrosome formation in human spermatozoa. In both organisms, the acrosome plays a similar role in head shaping, however the shape of the sperm heads is different (needle shaped in the fly, oval-shaped in the human). Importantly in flies, the acrosome remains intact when entering the oocyte, and unlike human sperm does not undergo the acrosome reaction, meaning *Drosophila* is not suitable to study the acrosome reaction. However, major

similarities in acrosome biogenesis, make the fly a suitable model for studying the role of Golgi derived vesicles in the process of acrosome formation.

1.9 Nuclear condensation and sperm head shaping

1.9.1 Human

Another important process in mammalian spermiogenesis involves the significant condensation and subsequent shaping of the nucleus, as highlighted by the dense aggregation of chromatin in the sperm. In spermatogonia and spermatocytes, the genome is packaged by histones, similar to the packaging of DNA in somatic cells (Balhorn, 2018). In elongating spermatids, these histones are replaced by transition proteins (TNPs), which in turn are replaced by protamines. This ensures extremely tight packaging of DNA to minimise the space required for its transport (Oliva, 2006). Chromatin remodelling and the proper condensation of DNA is a crucial part of spermatogenesis, as aberrant expression of TNPs or protamines leads to male infertility (Sharma and Agarwal, 2018). TNPs are first expressed in elongating spermatids (Zhao et al., 2004). The two main nuclear transition proteins are TNP1 and TNP2, and knockout of either causes subfertility, while knockout of both causes sterility, suggesting that while the function of each TNP may be partially redundant, TNPs in general are fundamental for efficient sperm production (Meistrich et al., 2003). While the functional properties of TNP1 and TNP2 individually have not yet been explained, it has been suggested that TNPs cause changes to the structure of the DNA to make it more accessible for the eventual binding of the protamines (Rathke et al., 2014).

In elongated spermatids, the TNPs are replaced by protamines, resulting in approximately 85% of sperm DNA being packaged around protamines. In mammals, there are two types of protamine. Protamine 1 (P1) is the more evolutionarily conserved, shown to be present in all

vertebrates studied (Oliva, 2006). Less conserved is the protamine P2 family, which consists of P2, P3 and P4 components, and has been found to be expressed in fewer mammalian species, but it expressed in mice and humans (Oliva, 2006). Protamines account for several potential functions (outlined in Oliva and Dixon (1991)), including the condensation of the nuclear DNA to ensure optimal sperm head shape as well as the protection of the DNA from both nucleases and transcription factors as the sperm passes through the male and female reproductive tract. The binding of protamines to DNA results in uncharged chromatin, which allows DNA molecules to be highly condensed into toroid structures (Ward, 2009). This nuclear condensation is crucial in ensuring that the sperm has a small, hydrodynamic head, as it has been shown that inappropriately condensed DNA results in abnormal head shape (Belokopytova et al., 1993), DNA damage (Yassine et al., 2015) and often abnormal acrosome formation, which often leads to infertility.

However, the nucleus within the sperm head also needs to elongate to appropriately form the sperm head. F-actin rings from the surrounding Sertoli cells work in conjunction with the manchette to ensure optimal head shaping, as reviewed by Pleuger et al. (2020). The manchette is formed through the assembly of many short microtubules, which accumulate around the sperm nucleus at a peri-nuclear ring, forming a skirt-like structure (Rattner and Brinkley, 1972). As spermiogenesis progresses, the manchette migrates to the base of the sperm head. The constriction of both the perinuclear ring from the manchette, and the F-actin rings from Sertoli cells combine to promote the elongation of the spermatid nucleus.

1.9.2 *Drosophila*

Similar to spermiogenesis in the human, there are two distinct mechanisms that are involved in nuclear remodelling in the *Drosophila*: i) the remodelling of the chromatin to facilitate a highly condensed state; and ii) the change in shape from spherical to long and needle-shaped (Tokuyasu, 1974).

The reorganisation of chromatin within *Drosophila* spermatids is remarkably similar to human spermatids and begins on the inner side of the canoe-shaped nucleus after head shaping is complete. There is only a single transition protein in *Drosophila* spermiogenesis, Tpl94D, which, like its human orthologues, facilitates the replacement of histones with protamine (Fabian and Brill, 2012). While human sperm have two major types of protamine (P1 and P2), the mature *Drosophila* sperm contains protamine A (Mst35Ba), protamine B (Mst35Bb), and Mst77F. Interestingly, Mst77F has another function aside from its protamine component, as it plays a role in the nuclear microtubules to assist in sperm head shaping (Rathke et al., 2010).

In the round spermatid, the nucleus flattens itself on the basal body side of the cell. Perinuclear microtubules then form and arrange into parallel bundles, developing a structure known as the dense body. This actin-rich structure provides structural support to the nucleus, playing a role akin to that of the manchette in human nuclear reshaping (Fabian and Brill, 2012). It is expected that the dense body is responsible for the early shaping of the nucleus (Tokuyasu, 1974). The fly sperm head elongates much more significantly than the human sperm, becoming canoe- or needle-shaped (Tokuyasu, 1974), rather than oval-shaped.

In summary, the histone to protamine transition is well conserved between *Drosophila* and mammals. In addition, it seems that the acroblast and dense body in fly sperm development play similar roles to the acroplaxome and manchette respectively, in human spermatogenesis.

1.10 Axoneme formation

The formation of the axoneme is critical in spermiogenesis, providing the central, conserved structure of the sperm tail, which is required for motility. The beginning of the axonemal implantation onto the nucleus occurs early in spermiogenesis, i.e. in the round spermatid. Initially, the proximal centriole, which aggregates at the base of the cell opposite to the acrosomal pole, and a distal centriole, which attaches to the axoneme (Avidor-Reiss et al., 2019, Fawcett and Phillips, 1969). The proximal centriole plays a role in generating a centriolar adjunct to form the sperm neck, while microtubules extend from the distal centriole, which will eventually lengthen to form the microtubular section of the sperm tail (Fawcett and Phillips, 1969). At this point, the cell nucleus is ovoid and there are two nuclear poles, the acrosomal pole and the flagellar pole (Holstein and Roosen-Runge, 1981)

In understanding axoneme formation it is important to discuss the fundamental differences between the two types of ciliogenesis (reviewed in Avidor-Reiss and Leroux (2018)), as it highlights a significant difference between mammalian and *Drosophila* processes. In the sperm of many organisms, including mammals and flies, the compartmentalised cilium is the distal portion of the axoneme and is contained within a pocket of cytoplasm, separate from the rest of the sperm cell. Conversely, the cytosolic cilium shares cytosol with rest of the sperm cell. The transition zone (TZ), or the annulus in mammals, sits between the compartmentalised and cytosolic cilia, and functions as a diffusion barrier between the cytosolic and compartmentalised sections of the axoneme. It is important to note that in human sperm, there is a short cytosolic axoneme, and a longer compartmentalised axoneme, whereas flies have a long cytosolic axoneme and a shorter compartmentalised axoneme (Avidor-Reiss and Leroux, 2018).

1.10.1 Human

Axoneme formation begins early in human spermiogenesis, when the centriole (which matures into the basal body) attaches into the implantation fossa, on the posterior side of the nucleus. Once the basal body has bound to the nucleus and plasma membrane, the axoneme begins to extend through a process called intra-flagellar transport (IFT), forming a compartmentalised cilia (Avidor-Reiss and Leroux, 2018). IFT is highly conserved in all eukaryotic cilia and flagella, and uses IFT motor proteins to transport vesicles and protein complexes along the axonemal microtubules, resulting in the extension of the axoneme itself reviewed by Pleuger et al. (2020). At the interface between cytoplasm and the compartmentalised cilia, the TZ forms. The TZ acts as a barrier at the base of the ciliary compartment, preventing the diffusion of signalling molecules from the cytosolic section of the axoneme into the compartmentalised cilia (Avidor-Reiss and Leroux, 2018). Towards the end of sperm tail development, the TZ migrates along the axoneme, away from the basal body, creating a short segment of cytosolic cilia (Kwitny et al., 2010), while also defining the junction between the mid-piece and the principal piece of the sperm tail (Toure et al., 2011). The final position of the migrated TZ is at the base of the midpiece, where it is made up of an electron-dense ring that contains septin proteins, referred to as the annulus (Toure et al., 2011).

This newly exposed cytosolic section of the axoneme shares cytoplasm with the cell, and allows the loading of the mitochondria into the sperm tail, to form the mitochondrial sheath, which plays a role in energy production. In summary, the principal piece of the sperm tail is produced using IFT, while the mitochondria are loaded onto the proximal region of the axoneme, after the compartmentalised axoneme has been formed.

The mammalian axoneme is made up of α- and β- tubulins, which polymerise into a single filament, forming what are known as microtubule doublets (Gunes et al., 2018). The microtubules in the mammalian sperm tail axoneme are arranged in a "9+2" structure, which refers to a ring of 9 microtubule doublets surrounding a central pair of singlet microtubules. Each doublet is linked to adjacent doublets by a structure called the nexin link, while radial spokes connect each doublet to the central pair. The function of the radial spokes and nexin links are to regulate motility (Kobayashi and Takeda, 2012). The final component of the axoneme, which are critical for their motility, is the dynein arms, which attach to the outer microtubule doublets. Outer dynein arms are located on the cilial membrane, while the inner dynein arms are proximal to the central radial spokes, and play a role in increasing the frequency of ciliary beating, for both motility and the penetration of the zona pellucida (Inaba and Mizuno, 2016).

The human sperm tail also contains accessory structures, which include the fibrous sheath, the outer dense fibres (ODFs) and the mitochondrial sheath. The fibrous sheath is the first accessory structure to be formed, aided by a mechanism called intra-manchette transport (IMT). IMT utilises the microtubules of the manchette, which project into the cytoplasmic lobes of the spermatid, and allow the transport of required proteins close to the entry of the ciliary compartment. Many of the proteins required for fibrous sheath formation are initially found in the manchette, hence the belief is that IMT is involved in this process (Pleuger et al., 2020). The fibrous sheath itself is composed of numerous proteins required for structural support during cilial beating, glycolysis, and in signal transduction (Eddy et al., 2003). Fibrous sheath components begin to appear at the distal end of the axoneme, and as the axoneme lengthens distally, the components extend proximally, opposite to axoneme formation.

The ODFs are another essential accessory structure, which elongate adjacent to the axoneme as the sperm tail develops, contributing to the elasticity and structural support of the beating sperm tail (Baltz et al., 1990). The ODFs are thought to protect against any shearing forces the sperm may be subjected to during and after development, and in the female reproductive tract (Zhao et al., 2018). The last accessory structure to be loaded is the mitochondrial sheath, which provides some of the energy required for sperm motility. The mitochondrial sheath contains a large number of mitochondria (studies in rodents have found between 50 and 75 (Otani et al., 1988)), which accumulate end-to-end in a helix are attached directly to the ODFs (Otani et al., 1988). The mechanisms recruiting the mitochondria are poorly understood, but it is thought that they may also be transported primarily via manchette microtubules (Pleuger et al., 2020).

1.10.2 *Drosophila*

Much like the human sperm axoneme, the *Drosophila* sperm axoneme microtubules are also arranged in the "9+2" structure. However, in *Drosophila*, there is an additional set of "accessory microtubules" surrounding the 9+2 structure, like a crown, giving a 9+9+2 structure (Mencarelli et al., 2008). The *Drosophila* axoneme also includes nexin links; which join the microtubule doublets, radial spokes; which join the outer doublets to the central doublets, as well as the dynein arms (Mencarelli et al., 2008). A notable difference in *Drosophila* sperm is that they do not contain two of the three accessory structures present in mammalian sperm, the ODFs and the fibrous sheath.

The attachment of the basal body to the cellular membrane is the first step in the formation of the *Drosophila* axoneme. Much like in human sperm, a compartmentalised cilium is formed

first. However, this compartmentalised cilium is generated solely though TZ proteins rather than through IFT that occurs in human sperm (Basiri et al., 2014).

The initiation of axoneme formation in *Drosophila* occurs during the spermatocyte stage. The centriole, which eventually becomes the basal body, begins to assemble the required ciliary structures during the primary spermatocyte period (Riparbelli et al., 2012). The four centrioles present in primary spermatocytes persist through two rounds of meiosis, and segregate into four round spermatids each with a singular centriole/basal body (Riparbelli et al., 2012). This is the point at which the basal body docks onto the nucleus, and forms what will ultimately become the implantation fossa.

The Drosophila sperm flagellum is initiated when the basal body imbeds into the posterior side of the nucleus at the nuclear envelope (Kim and Dynlacht, 2013, Fabian and Brill, 2012). The microtubules extend out of the TZ, distally from the basal body dock, to form the compartmentalised region of the cilia. The TZ itself then extends distally along the developing axoneme, forming the long, cytosolic section of the axoneme (Avidor-Reiss and Leroux, 2018).

Mitochondrial elongation has been shown to be one of the primary drivers of fly sperm tail lengthening, with studies (Noguchi et al., 2011) demonstrating that the lengthening mitochondrial derivative plays a structural role, which is highly dependent on the protein, Milton. Milton has been found to facilitate the anchoring of the nebenkern to the nucleus, as well as the elongation of the mitochondria along the sperm tail (Aldridge et al., 2007). In *Milton* mutants, the mitochondrial fusion structure is impaired, which resulted in spermatids with bent tails. This suggests that the axoneme alone is not structurally strong enough to facilitate tail elongation (Noguchi et al., 2011), and that mitochondrial elongation is a main driver of sperm

tail length and structure. It is has also been shown that microtubules assemble mitochondria independently of the classical microtubule-organising centres (Noguchi et al., 2011).

In sperm tail elongation, new microtubules are formed on the surface of the elongating mitochondria. These microtubules are crosslinked with the mitochondria, and are then able to generate a sliding force, which lengthens the mitochondria. As extension progresses, more microtubules are crosslinked to the microtubules attached to the mitochondria, which slows the lengthening process. This crosslinked microtubule network is then strong enough to hold the extended mitochondria in place, allowing for continued extension (Noguchi et al., 2011). This suggests that the mitochondria at the tip of the tail are essential for sperm tail elongation.

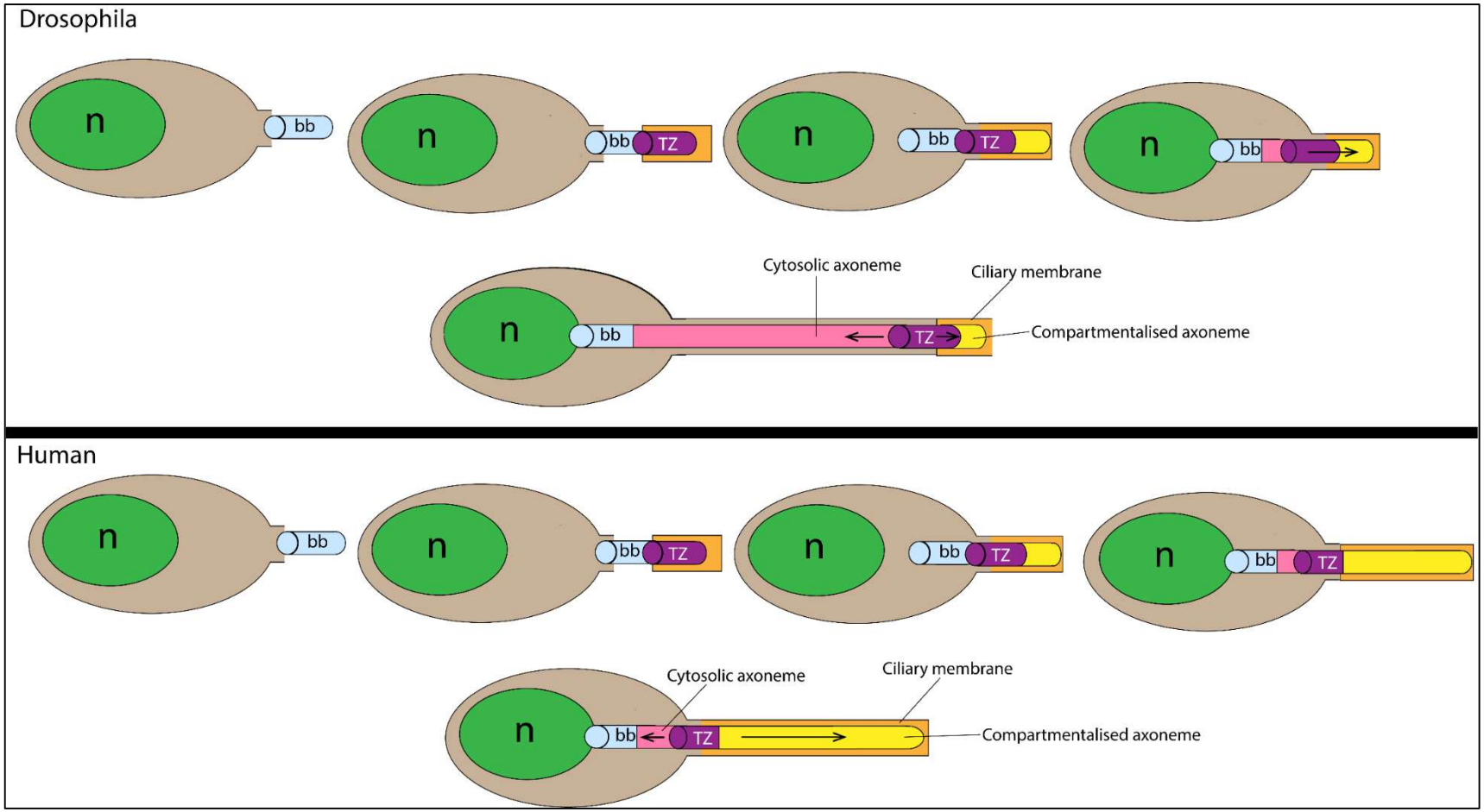

Figure 5: Comparing sperm ciliogenesis between *Drosophila* and Humans. In both organisms, ciliogenesis begins when the basal body (bb, blue) attaches to the plasma membrane (brown), which in turn forms the Transition Zone (TZ, purple). The TZ generates a compartmentalised axoneme (yellow) encased within an independent ciliary membrane (orange). Once the basal body binds to the nucleus (n, green), the TZ travels away from the basal body to form the cytosolic axoneme (pink). The key difference is that humans have a short cytosolic axoneme, and a long compartmentalised axoneme, whereas *Drosophila* have a shorter compartmentalised axoneme, and a longer cytosolic axoneme.

In summary, both the structure and the formation of the axoneme are significantly different when comparing human and fly spermiogenesis. While both species have the microtubules arranged in a "9+2" structure, the fly has an additional ring of microtubules, showing a "9+9+2" structure. The human sperm tail also contains accessory structures such as the ODFs, fibrous sheath and mitochondrial sheath, while flies do not have ODFs or a fibrous sheath. While sperm from both species have both a compartmentalized and a cytosolic portion of the cilia, the formation of these, as well as the size of each section differs greatly. In human sperm, the axoneme extends via IFT, and forms a long, compartmentalised cilium while a short, cytosolic cilium is formed by the annulus using TZ machinery. Conversely, the fly sperm has a short, compartmentalised cilium generated from TZ machinery, and a much longer cytosolic cilium.

1.11 Intercellular bridges, individualisation and spermiation

A final element of spermatogenesis in need of comparison is the role of the intercellular bridges between the developing germ cells, which has previously been reviewed in (Greenbaum et al., 2011).

1.11.1 Human

The final phases of spermiogenesis in the human are the removal of the excess cytoplasm and spermiation. Spermiation is a complex process, by which the sperm are released from the Sertoli cells into the lumen of the seminiferous epithelium. This step begins as the developing elongated spermatids line up along the edge of the lumen (O'Donnell et al., 2011). Tubulobulbar complexes (TBCs) are present on the head of the elongated spermatid, between the spermatid and the Sertoli cell, as it begins to move towards the lumen of the seminiferous tubule (Russell and Malone, 1980). They are cytoplasmic outgrowths that penetrate into the surrounding Sertoli cells. As the TBCs develop, they facilitate cleavage of the ectoplasmic

specialization complexes (ESCs) (O'Donnell et al., 2011). The ESCs are junctions between the Sertoli cell and developing spermatids, which help them move through the seminiferous epithelium and must be broken down in order for the sperm to be released (Wong et al., 2008). From the point of ESC cleavage, until release into the lumen, it is proposed that the shear stress placed on the spermatids by the Sertoli cells holds them in place (O'Donnell et al., 2011).

Another potential function of TBCs is in the excision of excess cytoplasm from the spermatid (Russell, 1979). This reduces the size of the sperm head, ensuring it has the optimal shape for motility. Interestingly, the location of TBC protein expression has been found to vary between species. In rodents, which have sickle-shaped sperm heads, TBCs were found in the curve of the "sickle". In other species, like humans which have spatulate-shaped heads, they were found at the apical tip of the heads (Russell and Malone, 1980, O'Donnell et al., 2011).

The final step of spermiation in human spermiogenesis is disengagement, where the spermatid completely detaches from the seminiferous epithelium, and is released into the lumen. From this stage, the sperm travels to the epididymis, where it undergoes post-testicular modifications and is stored prior to ejaculation (O'Donnell et al., 2011).

1.11.2 *Drosophila*

In flies, the final phase of spermiogenesis involves the breaking of the intercellular bridges, and the individualisation of each spermatid with its own membrane. This process involves the removal of the excess cytoplasm and organelles from the sperm membrane (Tokuyasu, 1972). To facilitate individualization, the individualization complex (IC) is formed, which travels from the head to the tail of the cyst. The IC is made up of a number of investment cones

containing F-actin, forming an arrow shape that travels distally from the nucleus to the tip of the tail, in the opposite direction to which the arrow points (Fabrizio et al., 1998). As the IC travels along the spermatid, excess cytoplasm is removed from between the individualising sperm. When the IC reaches the tail, it detaches and can be referred to as a "waste bag" as is contains a large amount of cytoplasm and organelles, including the broken down acroblast, which are no longer needed by the individualised spermatid (Fabrizio et al., 1998, Tokuyasu, 1972)

Drosophila spermatids undergo an additional step, called coiling. This is required primarily due to the immense length of the *Drosophila* sperm tail (~1.8mm) compared to human sperm (50um). Coiling involves the twisting of the 64 sperm tails, previously contained within the same cyst, and the retraction of the spermatids at the distal (open) end of the testis, until they are released into the seminal vesicles for storage (Fabian and Brill, 2012). The coiling process is initiated in the head region of the spermatid bundle, which at this point, appears to be at the distal side of the testis, away from the hub. The head is trapped by the terminal epithelium, and the tail begins to retract towards the open end of the testis tube. As the sperm bundle coils, it also rotates to form a helix, where the tails are packed into a hexagonal lattice. The complexity of this process also allows any defective sperm to be removed from the bundle (Tokuyasu et al., 1972).

1.12 Summary

The *Drosophila* is undoubtedly a suitable model organism for studying a wide range of human genetic diseases, male infertility included. However, as there are some notable differences between the spermatogenic processes between these very diverse organisms, it is important for budding fertility biologists to understand these. The purpose of this review was to summarise

and breakdown spermatogenesis in each organism to clearly define which parts of human spermatogenesis can be confidently studied using *Drosophila*, and which parts must be approached with caution.

Both organisms have a testis which has the primary role of generating sperm cells. One distinct structural difference is that a human testis contains multiple tubules, each with its own ability to generate sperm, independent of the others. This is quite different from the *Drosophila* testis, where a testis is like a single tubule. While both organisms have a method of sperm storage, these mechanisms differ. After spermatogenesis, the human sperm undergoes post-testicular modifications and is then stored in the epididymis. In *Drosophila*, the sperm are stored in the organ termed the seminal vesicle, and do not undergo any post-testicular modifications. This can lead to confusion, as in the human, the organ termed the "seminal vesicle" is responsible for the production of seminal fluid.

In both organisms, the testis contains somatic cells which protect the developing germ cells. There are however two major differences between the Sertoli cell (human) and the cyst cell (*Drosophila*). The number of Sertoli cells is mostly fixed after puberty, and each cell has contact with 3-4 other Sertoli cells and 4-5 developing germ cells. In comparison, in *Drosophila* the cyst cell develops synchronously with the developing germ cell from the 'stem cell' stage. Two cyst cells develop in parallel with a single gonialblast. This means that early on in spermatogenesis, the cyst cell is in contact with only the gonialblast, but later these same cyst cells surround the 64 spermatids. This creates a single independent cyst within the two cyst cells, and synchronises the development of the sperm bundle. The cyst cells are degraded at the end of spermatogenesis.

Germ cells in both organisms develop from a stem cell niche. In the human, the spermatogonia can be differentiated into A_{dark} (divide rarely), A_{pale} (divide frequently) and B spermatogonia (which initiate meiosis, and become primary spermatocytes). In *Drosophila*, a gonialblast develops from the germline stem cell, and undergoes four rounds of transit-amplifying divisions to form sixteen spermatogonia. The cyst stem cells also reside within this stem cell niche. There are also some minor differences in the meiosis processes, the most notable being the lack of recombination in *Drosophila* spermatogenesis. This is because no chiasmata are formed to join homologous chromosomes

The mitochondrial rearrangement is quite different between these organisms. The formation of the nebenkern is quite specific to insect spermatogenesis. This spherical accumulation of mitochondria aggregates occurs at the basal body, at the base of the nucleus around the sperm tail. As the nebenkern unfurls, the mitochondrial derivative extends along the tip of the sperm tail and provides structural support to the developing axoneme. This does not occur in human spermiogenesis; instead, the mitochondria assemble at the periphery of the spermatid. As the spermatid elongates, the annulus migrates down the developing sperm tail, exposing the mitochondria to the cytoplasmic axoneme. The final destination of the mitochondria is the midpiece, where they form a tight helix around the axoneme.

The formation of the acrosome and sperm head are relatively similar between the organisms as acrosomes from both species are derived from the Golgi. The human acrosome is also derived from endocytic vesicles. The human manchette the *Drosophila* dense body are both structures made of microtubule bundles which function in nuclear head shaping. While humans have a spatula-shaped sperm head, the *Drosophila* sperm head is canoe, or needle shaped.

The condensation of chromatin is an essential step in spermiogenesis, so it is unsurprising that this process is highly conserved. Both organisms replace the histones with protamine, through transition proteins. Humans use TNP1 and TNP2 whereas *Drosophila* uses Tpl94D. and while analogous in function they have no structural similarities.

In axoneme formation, while both species contain α- and β-tubulins, the arrangement of the microtubules is slightly different. While the human axoneme microtubules are arranged in a 9+2 structure, *Drosophila* microtubules have a 9+9+2 structure, which involves an extra set of accessory microtubules around the 9+2 structure in the human. Another difference is the addition of axoneme accessory structures in the human, such as the outer dense fibres and the fibrous sheath, neither of which are present in the *Drosophila* sperm. Both species do however contain dynein arms.

Two types of axoneme, compartmentalised and cytosolic, are present in both species, with length being a major differentiating factor. The *Drosophila* sperm tail is approximately 1.8mm long, where the average human sperm is 50 μm. This is due to a difference in the size of the axonemes. The human sperm contains a short cytosolic axoneme, and a longer compartmentalised axoneme, whereas *Drosophila* have a longer cytosolic axoneme and a shorter compartmentalised axoneme. There are also some differences in the formation of the axonemes (outlined in Figure 5).

The final step of spermiogenesis is spermiation, where the elongated spermatids are released. In humans, TBCs move from the head to the tail, removing the ectoplasmic specialisations which were responsible for keeping the spermatids attached to the Sertoli cells. In *Drosophila*, individualisation occurs via investment cones which contain F-actin, and travel from head to

tail within the bundles, breaking the intracellular bridges between the sperm. One similarity in spermiation is the removal of excess cytoplasm from the elongated spermatid. In the human, this is removed by the TBCs. In *Drosophila*, this excess cytoplasm is removed via a "waste bag" which also contains some now redundant organelles.

This review has highlighted some significant differences, and many similarities between *Drosophila* and human spermatogenesis. The benefit of using *Drosophila* is that it provides a fast, cheap, and quick method to screen a large number of genes. Hence, screening these genes is important and *Drosophila* provides a solid model for screening these genes efficiently. However, due to these differences in human it is important to stress that further analysis of the genes found by screens, are also studied in other model organisms, such as mice, as well as in human patients to further identify the function of these mutations.

1.13 References

ALDRIDGE, A. C., BENSON, L. P., SIEGENTHALER, M. M., WHIGHAM, B. T., STOWERS, R. S. & HALES, K. G. 2007. Roles for Drp1, a dynamin-related protein, and milton, a kinesin-associated protein, in mitochondrial segregation, unfurling and elongation during Drosophila spermatogenesis. *Fly (Austin),* 1**,** 38-46.

ALVES, M. G., RATO, L., CARVALHO, R. A., MOREIRA, P. I., SOCORRO, S. & OLIVEIRA, P. F. 2013. Hormonal control of Sertoli cell metabolism regulates spermatogenesis. *Cell Mol Life Sci,* 70**,** 777-93.

AVIDOR-REISS, T. & LEROUX, M. R. 2018. Shared and distinct mechanisms of compartmentalized and cytosolic ciliogenesis. *Curr Biol,* 25**,** R1145-50.

AVIDOR-REISS, T., MAZUR, M., FISHMAN, E. L. & SINDHWANI, P. 2019. The Role of Sperm Centrioles in Human Reproduction – The Known and the Unknown. *Front. Cell Dev. Biol,* 7**,** 188.

AVILA, F. W., SIROT, L. K., LAFLAMME, B. A., RUBINSTEIN, C. D. & WOLFNER, M. F. 2011. Insect seminal fluid proteins: identification and function. *Annu Rev Entomol,* 56**,** 21-40.

BALHORN, R. 2018. Chapter 1 - Sperm Chromatin: An Overview. *In:* ZINI, A. & AGARWAL, A. (eds.) *A Clinician's Guide to Sperm DNA and Chromatin Damage.* Cham: Springer.

BALTZ, J. M., WILLIAMS, P. O. & CONE, R. A. 1990. Dense fibers protect mammalian sperm against damage. *Biol Reprod,* 43**,** 485-91.

BASIRI, M. L., HA, A., CHADHA, A., CLARK, N. M., POLYANOVSKY, A., COOK, B. & AVIDOR-REISS, T. 2014. A Migrating Ciliary Gate Compartmentalizes the Site of Axoneme Assembly in Drosophila Spermatids. *Curr Biol,* 24**,** 2622-31.

BELOKOPYTOVA, I. A., KOSTYLEVA, E. I., TOMILIN, A. N. & VOROB'EV, V. I. 1993. Human male infertility may be due to a decrease of the protamine P2 content in sperm chromatin. *Mol Reprod Dev,* 34**,** 53-7.

BERRUTI, G., RIPOLONE, M. & CERIANI, M. 2010. USP8, a regulator of endosomal sorting, is involved in mouse acrosome biogenesis through interaction with the spermatid ESCRT-0 complex and microtubules. *Biol Reprod,* 82**,** 930-9.

BICKEL, S. E., WYMAN, D. W. & ORR-WEAVER, T. L. 1997. Mutational Analysis of the Drosophila Sister-Chromatid Cohesion Protein ORD and its role in the maintenance if centromeric cohesion. *Genetics,* 146**,** 1319-31.

BONILLA, E. & XU, E. Y. 2008. Identification and characterization of novel mammalian spermatogenic genes conserved from fly to human. *Mol Hum Reprod,* 14**,** 137-42.

BORG, C. L., WOLSKI, K. M., GIBBS, G. M. & O'BRYAN, M. K. 2010. Phenotyping male infertility in the mouse: how to get the most out of a 'non-performer'. *Hum Reprod Update,* 16**,** 205-24.

BUFFONE, M. G., FOSTER, J. A. & GERTON, G. L. 2008. The role of the acrosomal matrix in fertilization. *Int J Dev Biol,* 52**,** 511-22.

CAHOON, C. K. & HAWLEY, R. S. 2016. Regulating the construction and demolition of the synaptonemal complex. *Nat Struct Mol Biol,* 23**,** 369-77.

CARPENTER, A. T. 1994. Chiasma Function. *Cell,* 77**,** 959-62.

CHENG, C. Y. & MRUK, D. D. 2009. An intracellular trafficking pathway in the seminiferous epithelium regulating spermatogenesis: a biochemical and molecular perspective. *Crit Rev Biochem Mol Biol,* 44**,** 245-63.

CHENG, C. Y. & MRUK, D. D. 2012. The Blood-Testis Barrier and Its Implications for Male Contraception. *Pharmacol Rev,* 64**,** 16-64.

CHENG, J., TIYABOONCHAI, A., YAMASHITA, Y. M. & HUNT, A. J. 2011. Asymmetric division of cyst stem cells in Drosophila testis is ensured by anaphase spindle repositioning. *Development,* 138**,** 831-7.

CLERMONT, Y. 1966. Renewal of Spermatogonia in Man. *Am J Anat,* 118**,** 509-24.

CLERMONT, Y. & LEBLOND, C. 1955. SPERMIOGENESIS OF MAN, MONKEY, RAM AND OTHER TUAMJIIALS AS SHOWN BY THE "PER1OL)IC ACID-SCHIFF TECHNIQUE. *Am J Anat,* 96**,** 229-53.

CLIFT, D. & MARSTON, A. L. 2011. The role of shugoshin in meiotic chromosome segregation. *Cytogenet Genome Res,* 133**,** 234-42.

CORNWALL, G. A. 2009. New insights into epididymal biology and function. *Hum Reprod Update,* 15**,** 213-27.

DAVIES, E. L. & FULLER, M. T. 2008. *Regulation of Self-renewal and Differentiation in Adult Stem Cell Lineages: Lessons from the Drosophila Male Germ Line*, Cold Spring Harbour Lab Press.

DE CUEVAS, M. & MATUNIS, E. L. 2011. The stem cell niche: lessons from the Drosophila testis. *Development,* 138**,** 2861-9.

DE ROOIJ, D. G. 2017. The nature and dynamics of spermatogonial stem cells. *Development,* 144**,** 3022-3030.

DE ROOIJ, D. G. & RUSSELL, L. D. 2000. All You Wanted to Know About Spermatogonia but Were Afraid to Ask. *J. Androl.,* 21**,** 776-98.

DJUREINOVIC, D., FAGERBERG, L., HALLSTROM, D., A, D., LINDSKOG, C., UHLEN, M. & PONTEN, F. 2014. The human testis-specific proteome defined by transcriptomics and antibody-based profiling. *Mol Hum Reprod,* 20**,** 476-88.

DRABOVICH, A. P., SARAON, P., JARVI, K. & DIAMANDIS, E. P. 2014. Seminal plasma as a diagnostic fluid for male reproductive system disorders. *Nat Rev Urol,* 11**,** 278-88.

EDDY, E. M., TOSHIMORI, K. & O'BRIEN, D. A. 2003. Fibrous sheath of mammalian spermatozoa. *Microsc Res Tech,* 61**,** 103-115.

EISENBERG, M. L., LI, S., BEHR, B., CULLEN, M. R., GALUSHA, D., LAMB, D. J. & LIPSHULTZ, L. I. 2014. Semen quality, infertility and mortality in the USA. *Hum Reprod,* 29**,** 1567-74.

ESCALIER, D., GALLO, J. M., ALBERT, M., MEDURI, G., BERMUDEZ, D., DAVID, G. & SCHREVEL, J. 1991. Human acrosome biogenesis: immunodetection of proacrosin in primary spermatocytes and of its partitioning pattern during meiosis. *Development,* 113**,** 779-88.

FABIAN, L. & BRILL, J. A. 2012. Drosophila spermiogenesis: Big things come from little packages. *Spermatogenesis,* 2**,** 197-212.

FABRIZIO, J. J., HIME, G. R., LEMMON, S. K. & BAZINET, C. 1998. Genetic dissection of sperm individualization in Drosophila melanogaster. *Development,* 125**,** 1833-43.

FAGERBERG, L., HALLSTROM, B. M., OKSVOLD, P., KAMPF, C., DJUREINOVIC, D., ODEBERG, J., HABUKA, M., TAHMASEBPOOR, S., DANIELSSON, A., EDLUND, K., ASPLUND, A., SJOSTEDT, E., LUNDBERG, E., SZIGYARTO, C. A., SKOGS, M., TAKANEN, J. O., BERLING, H., TEGEL, H., MULDER, J., NILSSON, P., SCHWENK, J. M., LINDSKOG, C., DANIELSSON, F., MARDINOGLU, A., SIVERTSSON, A., VON FEILITZEN, K., FORSBERG, M., ZWAHLEN, M., OLSSON, I., NAVANI, S., HUSS, M., NIELSEN, J., PONTEN, F. & UHLEN, M. 2014. Analysis of the human tissue-specific expression by genome-wide integration of transcriptomics and antibody-based proteomics. *Mol Cell Proteomics,* 13**,** 397-406.

FÁRI, K., TAKÁCS, S., UNGÁR, D. & SINKA, R. 2016. The role of acroblast formation during Drosophila spermatogenesis. *Biol Open,* 5**,** 1102-10.

FAWCETT, D. W. & PHILLIPS, D. 1969. The Fine Structure and Development of the Neck Region of the Mammalian Spermatozoon. *Anat Rec,* 165**,** 153-83.

FIJAK, M., BHUSHAN, S. & MEINHARDT, A. 2011. Immunoprivileged Sites: The Testis. *Methods Mol Biol,* 677**,** 459-470.

FULLER, M. T. 1993. Spermatogenesis. *In:* BATE, M. & ARIAS, A. M. (eds.) *The Development of Drosophila melanogaster.* New York: Cold Spring Harbour Laboratory Press.

GERVASI, M. G. & VISCONTI, P. E. 2017. Molecular changes and signaling events occurring in spermatozoa during epididymal maturation. *Andrology,* 5**,** 204-218.

GLAZER, C. H., BONDE, J. P., EISENBERG, M. L., GIWERCMAN, A., HAERVIG, K. K., RIMBORG, S., VASSARD, D., PINBORG, A., SCHMIDT, L. & BRAUNER, E. V. 2017. Male Infertility and Risk of Nonmalignant Chronic Diseases: A Systematic Review of the Epidemiological Evidence. *Semin Reprod Med,* 35**,** 282-290.

GÖNCZY, P. & DINARDO, S. 1996. The germ line regulates somatic cyst cell proliferation and fate during Drosophila spermatogenesis. *Development,* 122**,** 2437-47.

GREENBAUM, M. P., IWAMORI, T., BUCHOLD, G. M. & MATZUK, M. M. 2011. Germ Cell Intercellular Bridges. *Cold Spring Harb Perspect Biol,* 3**,** 1-16.

GRISWOLD, M. D. 1998. The central role of Sertoli cells in spermatogenesis. *Sem. in Cell and Dev. Biol.,* 9**,** 411-416.

GUNES, S., SENGUPTA, P., HENKEL, R., ALGURAIGARI, A., SIIGALGLIA, M. M., KAYAL, M., JOUMAH, A. & AGARWAL, A. 2018. Microtubular Dysfunction and Male Infertility. *World J Mens Health,* 38**,** 9-23.

GUO, Y., HAI, Y., GONG, Y., LI, Z. & HE, Z. 2014. Characterization, isolation, and culture of mouse and human spermatogonial stem cells. *J Cell Physiol,* 229**,** 407-13.

HAGLUND, K., NEZIS, I. P. & STENMARK, H. 2011. Structure and functions of stable intercellular bridges formed by incomplete cytokinesis during development. *Commun Integr Biol,* 4**,** 1-9.

HALES, K. G. & FULLER, M. T. 1997. Developmentally Regulated Mitochondrial Fusion Mediated by a Conserved, Novel, Predicted GTPase. *Cell,* 90**,** 121-9.

HARA, K., NAKAGAWA, T., ENOMOTO, H., SUZUKI, M., YAMAMOTO, M., SIMONS, B. D. & YOSHIDA, S. 2014. Mouse spermatogenic stem cells continually interconvert between equipotent singly isolated and syncytial states. *Cell Stem Cell,* 14**,** 658-72.

HARDY, R. W., TOKUYASU, K. T., LINDSLEY, D. L. & GARAVITO, M. 1979. The germinal proliferation center in the testis of Drosophila melanogaster. *J Ultra Mol Struct R,* 69**,** 180-90.

HELSEL, A. R., YANG, Q. E., OATLEY, M. J., LORD, T., SABLITZKY, F. & OATLEY, J. M. 2017. ID4 levels dictate the stem cell state in mouse spermatogonia. *Development,* 144**,** 624-634.

HOLSTEIN, A.-F. & ROOSEN-RUNGE, E. 1981. *Atlas of Human Spermatogenesis,* Berlin, Grosse.

HOUSTON, B. J., CONRAD, D. F. & O'BRYAN, M. K. 2021. A framework for high-resolution phenotyping of candidate male infertility mutants: from human to mouse. *Hum Genet,* 140**,** 155-182.

HU, Z., XIA, Y., GUO, X., DAI, J., LI, H., HU, H., JIANG, Y., LU, F., WU, Y., YANG, X., LI, H., YAO, B., LU, C., XIONG, C., LI, Z., GUI, Y., LIU, J., ZHOU, Z., SHEN, H., WANG, X. & SHA, J.

2011. A genome-wide association study in Chinese men identifies three risk loci for non-obstructive azoospermia. *Nat Genet,* 44**,** 183.

HUCKINS, C. 1971. The spermatogonial stem cell population in adult rats. I. Their morphology, proliferation and maturation. *Anat Rec,* 169**,** 533-57.

INABA, K. & MIZUNO, K. 2016. Sperm dysfunction and ciliopathy. *Reprod Med Biol,* 15**,** 77-94.

JAMSAI, D. & O'BRYAN, M. K. 2011. Mouse models in male fertility research. *Asian J Androl,* 13**,** 139-51.

JENSEN, T. K., JACOBSEN, R., CHRISTENSEN, K., NIELSEN, N. C. & BOSTOFTE, E. 2009. Good semen quality and life expectancy: a cohort study of 43,277 men. *Am J Epidemiol,* 170**,** 559-65.

JUTTE, N. H., GROOTEGOED, J. A., ROMMERTS, F. F. & VAN DER MOLEN, H. J. 1981. Exogenous lactate is essential for metabolic activities in isolated rat spermatocytes and spermatids. *J Reprod Fertil,* 62**,** 399-405.

KERREBROCK, A. W., MOORE, D. P., WU, J. S. & ORR-WEAVER, T. L. 1995. Mei-S332, a Drosophila protein required for sister-chromatid cohesion, can localize to meiotic centromere regions. *Cell,* 83**,** 247-56.

KHAWAR, M. B., GAO, H. & LI, W. 2019. Mechanism of Acrosome Biogenesis in Mammals. *Front. Cell Dev. Biol,* 7**,** 1-12.

KIERSZENBAUM, A. L., RIVKIN, E. & TRES, L. L. 2003. Acroplaxome, an F-Actin–Keratin-containing Plate, Anchors the Acrosome to the Nucleus during Shaping of the Spermatid Head. *Mol Biol Cell,* 14**,** 4628-40.

KIERSZENBAUM, A. L. & TRES, L. L. 2004. The acrosome-acroplaxome-manchette complex and the shaping of the spermatid head. *Arch Histol Cytol,* 67**,** 271-284.

KIM, S. & DYNLACHT, B. D. 2013. Assembling a primary cilium. *Curr Opin Cell Biol,* 25**,** 506-11.

KITAJIMA, T. S., SAKUNO, T., ISHIGURO, K., IEMURA, S., NATSUME, T., KAWASHIMA, S. A. & WATANABE, Y. 2006. Shugoshin collaborates with protein phosphatase 2A to protect cohesin. *Nature,* 441**,** 46-52.

KOBAYASHI, D. & TAKEDA, H. 2012. Ciliary motility: the components and cytoplasmic preassembly mechanisms of the axonemal dyneins. *Differentiation,* 83**,** S23-29.

KONDYLIS, V. & RABOUILLE, C. 2009. The Golgi apparatus: Lessons from Drosophila. *FEBS Lett,* 583**,** 3827-38.

KRAUSZ, C. & RIERA-ESCAMILLA, A. 2018. Genetics of male infertility. *Nat Rev Urol*.

KUBOTA, H., M.R., A. & BRINSTER, R. L. 2004. Growth Factors Essential for Self-Renewal and Expansion of Mouse Spermatogonial Stem Cells. *Proc Natl Acad Sci U S A,* 101**,** 16489-94.

KWITNY, S., KLAUS, A. V. & HUNNICUT, G. R. 2010. The annulus of the mouse sperm tail is required to establish a membrane diffusion barrier that is engaged during the late steps of spermiogenesis. *Biol Reprod,* 82**,** 669-78.

LEE, N. P. & CHENG, C. Y. 2004. Ectoplasmic specialization, a testis-specific cell-cell actin-based adherens junction type: is this a potential target for male contraceptive development? *Hum Reprod Update,* 10**,** 349-69.

MAJEWSKA, M. M., SUSZCZYNSKA, A., KOTWICA-ROLINSKA, J., CZERWIK, T., PATERCZYK, B., POLANSKA, M. A., BERNATOWICZ, P. & BEBAS, P. 2014. Yolk proteins in the male reproductive system of the fruit fly Drosophila melanogaster: Spatial and temporal patterns of expression. *Insect Biochemistry and Molecular Biology,* 47**,** 23-35.

MCKEE, B. D., YAN, R. & TSAI, J. H. 2012. Meiosis in male Drosophila. *Spermatogenesis,* 2**,** 167-184.

MEISTRICH, M. L., MOHAPATRA, B., SHIRLEY, C. R. & ZHAO, M. 2003. Roles of transition nuclear proteins in spermiogenesis. *Chromosoma,* 111**,** 483-8.

MENCARELLI, C., LUPETTI, P. & DALLAI, R. 2008. New insights into the cell biology of insect axonemes. *Int Rev Cell Mol Biol,* 268**,** 95-145.

MERONI, S. B., GALARDO, M. N., RINDONE, G., GORGA, A., RIERA, M. F. & CIGORRAGA, S. B. 2019. Molecular Mechanisms and Signaling Pathways Involved in Sertoli Cell Proliferation. *Front. Endocrinol,* 10**,** 224.

MORENO, R. D., RAMALHO-SANTOS, J., SUTOVSKY, P., CHAN, E. K. & SCHATTEN, G. 2000. Vesicular traffic and golgi apparatus dynamics during mammalian spermatogenesis: implications for acrosome architecture. *Biol Reprod,* 63**,** 89-98.

NOGUCHI, T., KOLZUMI, M. & HAYASHI, S. 2011. Sustained Elongation of Sperm Tail Promoted by Local Remodeling of Giant Mitochondria in Drosophila. *Curr Biol,* 21**,** 805-14.

O'DONNELL, L., NICHOLLS, P. K., O'BRYAN, M. K., MCLACHLAN, R. I. & STANTON, P. G. 2011. Spermiation: The process of sperm release. *Spermatogenesis,* 1**,** 14-35.

OATLEY, M. J., KAUCHER, A. V., RACICOT, K. E. & OATLEY, J. M. 2011. Inhibitor of DNA binding 4 is expressed selectively by single spermatogonia in the male germline and regulates the self-renewal of spermatogonial stem cells in mice. *Biol Reprod,* 85**,** 347-56.

OKAMOTO, K. & SHAW, J. M. 2005. Mitochondrial Morphology and Dynamics in Yeast and Multicellular Eukaryotes. *Annu Rev Genet,* 39**,** 503-36.

OLIVA, R. 2006. Protamines and male infertility. *Hum Reprod Update,* 12**,** 417-35.

OLIVA, R. & DIXON, G. H. 1991. Vertebrate Protamine Genes and the Histone-to-Protamine Replacement Reaction. *Prog Nucleic Acid Res Mol Biol,* 40**,** 25-94.

ORR-WEAVER, T. L. 1995. Meiosis in Drosophila: seeing is believing. *Proc Natl Acad Sci U S A,* 92**,** 10443-9.

ORTH, J. M., GUNSALUS, G. L. & LAMPERTI, A. A. 1988. Evidence From Sertoli Cell-Depleted Rats Indicates That Spermatid Number in Adults Depends on Numbers of Sertoli Cells Produced During Perinatal Development. *Endocrinology,* 122**,** 787-94.

OTANI, H., TANAKA, O., KASAI, K.-I. & YOSHIOKA, T. 1988. Development of Mitochondrial Helical Sheath in the Middle Piece of the Mouse Spermatid Tail: Regular Dispositions and Synchronized Changes. *Anat Rec,* 222**,** 26-33.

PANDEY, U. B. & NICHOLS, C. D. 2011. Human disease models in Drosophila melanogaster and the role of the fly in therapeutic drug discovery. *Pharmacol Rev,* 63**,** 411-36.

PEROTTI, M. E. 1975. Ultrastructural aspects of fertilization in Drosophila. *In:* AFZELINS, B. A. (ed.) *The Functional Anatomy of the Spermatozoan, Proceedings of the Second International Symposium.* Oxford: Pergamon Press.

PHILLIPS, D. 1970. Insect Sperm: Their Structure and Morphogenesis. *Cell Biol,* 44**,** 243-77.

PLEUGER, C., LEHTI, M. S., DUNLEAVY, J. E. M., FIETZ, D. & O'BRYAN, M. K. 2020. Haploid male germ cells—the Grand Central Station of protein transport. *Hum Reprod Update,* 26**,** 474-500.

RATHKE, C., BAARRENDS, W. M., AWE, S. & RENKAWITZ-POHL, R. 2014. Chromatin dynamics during spermiogenesis. *Biochimica et Byophysica Acta,* 1839**,** 155-68.

RATHKE, C., BARCKMANN, B., BURKHARD, S., JAYARAMAIAH-RAJA, S., ROOTE, J. & RENKAWITZ-POHL, R. 2010. Distinct functions of Mst77F and protamines in nuclear shaping and chromatin condensation during Drosophila spermiogenesis. *Eur J Cell Biol,* 89**,** 326-38.

RATO, L., ALVES, M. G., SOCORRO, S., DUARTE, A. I., CAVACO, J. E. & OLIVEIRA, P. F. 2012. Metabolic regulation is important for spermatogenesis. *Nat Rev Urol,* 9**,** 330-8.

RATTNER, J. B. & BRINKLEY, B. R. 1972. Ultrastructure of Mammalian Spermiogenesis III. The Organization and Morphogenesis of the Monchette during Rodent Spermiogenesis. *J Ultrastruct Res,* 41**,** 209-18.

RIPARBELLI, M. G., CALLAINI, G. & MEGRAW, T. L. 2012. Assembly and persistence of primary cilia in dividing Drosophila spermatocytes. *Dev. Cell,* 23**,** 425-32.

RUSSELL, L. D. 1979. Spermatid-Sertoli Tubulobulbar Complexes as Devices for Elimination of Cytoplasm from the Head Region of Late Spermatids of the Rat. *Anat. Rec,* 194.

RUSSELL, L. D. & MALONE, J. P. 1980. A study of Sertoli-Spermatid Tubulobulbar complexes in selected mammals. *Tissue Cell,* 12**,** 263-85.

SHARMA, R. & AGARWAL, A. 2018. Chapter 14 - Defective Spermatogenesis and Sperm DNA Damage. *In:* ZINI, A. & AGARWAL, A. (eds.) *A Clinician's Guide to Sperm DNA and Chromatin Damage.* Cham: Springer.

SHARMA, S., HANUKOGLU, A. & HANUKOGLU, I. 2018. Localization of epithelial sodium channel (ENaC) and CFTR in the germinal epithelium of the testis, Sertoli cells, and spermatozoa. *J Mol Histol,* 49**,** 195-208.

SIDDALL, N. A. & HIME, G. R. 2017. A Drosophila toolkit for defining gene function in spermatogenesis. *Reproduction,* 153**,** R121-R132.

SOUMILLON, M., NECSULEA, A., WEIER, M., BRAWAND, D., ZHANG, X., GU, H., BARTHES, P., KOKKINAKI, M., NEF, S., GNIRKE, A., DYM, M., DE MASSY, B., MIKKELSEN, T. S. &

KAESSMANN, H. 2013. Cellular source and mechanisms of high transcriptome complexity in the mammalian testis. *Cell Rep,* 3**,** 2179-90.

STEGER, K., REY, R., KLIESCH, S., LOIUS, F., SCHLERICHER, G. & BERGMANN, M. 1996. Immunohistochemical detection of immature Sertoli cell markers in testicular tissue of infertile adult men: a preliminary study. *Int J Androl,* 19**,** 122-8.

SUN, M. S., WEBER, J., BLATTNER, A. C., CHAURASIA, S. & LEHNER, C. F. 2019. MNM and SNM maintain but do not establish achiasmate homolog conjunction during Drosophila male meiosis. *PLoS Genet,* 15**,** e1008162.

TAKEMORI, N. & YAMAMOTO, M.-T. 2009. Proteome mapping of the Drosophila melanogaster male reproductive system. *Proteomics,* 9**,** 2484-2493.

THOMAS, S. E., SOLTANI-BEJNOOD, M., ROTH, P., DORN, R., LOGSDON, J. M., JR. & MCKEE, B. D. 2005. Identification of two proteins required for conjunction and regular segregation of achiasmate homologs in Drosophila male meiosis. *Cell,* 123**,** 555-68.

TOKUYASU, K. T. 1972. Dynamics of spermiogenesis in Drosophila melanogaster I. Individualization process. *Z Zellforsch Mik Ana,* 124**,** 479-506.

TOKUYASU, K. T. 1974. Dynamics of spermiogenesis in Drosophila melanogaster: IV. Nuclear transformation. *J Ultra Mol Struct R,* 48**,** 284-303.

TOKUYASU, K. T. 1975. Dynamics of spermiogenesis in Drosophila melanogaster. VI. Significance of “onion” nebenkern formation. *J Ultra Mol Struct R,* 53**,** 93-112.

TOKUYASU, K. T., PEACOK, W. & HARDY, R. W. 1972. Dynamics of Spermiogenesis n Drosophilamelanogaster*II. Coiling Process. *Z Zellforch Mikrosk Anat,* 127**,** 492-525.

TOURE, A., RODE, B., HUNNICUT, G. R., ESCALIER, D. & GACON, G. 2011. Septins at the annulus of mammalian sperm. *Biol. Chem.,* 392**,** 799-803.

TOURNAYE, H., KRAUSZ, C. & OATES, R. D. 2017. Novel concepts in the aetiology of male reproductive impairment. *The Lancet Diabetes & Endocrinology,* 5**,** 544-553.

UHLEN, M., FAGERBERG, L., HALLSTROM, B. M., LINDSKOG, C., OKSVOLD, P., MARDINOGLU, A., SIVERTSSON, A., KAMPF, C., SJOSTEDT, E., ASPLUND, A., OLSSON, I., EDLUND, K., LUNDBERG, E., NAVANI, S., SZIGYARTO, C. A., ODEBERG, J., DJUREINOVIC, D., TAKANEN, J. O., HOBER, S., ALM, T., EDQVIST, P. H., BERLING, H., TEGEL, H., MULDER, J., ROCKBERG, J., NILSSON, P., SCHWENK, J. M., HAMSTEN, M., VON FEILITZEN, K., FORSBERG, M., PERSSON, L., JOHANSSON, F., ZWAHLEN, M., VON HEIJNE, G., NIELSEN, J. & PONTEN, F. 2015. Proteomics. Tissue-based map of the human proteome. *Science,* 347**,** 1260419.

WAHEEB, R. & HOFMANN, M. C. 2011. Human spermatogonial stem cells: a possible origin for spermatocytic seminoma. *Int J Androl,* 34**,** e296-305; discussion e305.

WARD, W. S. 2009. Function of sperm chromatin structural elements in fertilization and development. *Mol Hum Reprod,* 16**,** 30-36.

WEBER, J., KABAKCI, Z., CHAURASIA, S., BRUNNER, E. & LEHNER, C. F. 2020. Chromosome separation during Drosophila male meiosis I requires separase-mediated cleavage of the homolog conjunction protein UNO. *PLoS Genet,* 16**,** e1008928.

WHITE-COOPER, H. & BAUSEK, N. 2010. Evolution and spermatogenesis. *Philos Trans R Soc Lond B Biol Sci,* 365**,** 1465-80.

WILSON, K. L., FITCH, K. R., BAFUS, B. T. & WAKIMOTO, B. T. 2006. Sperm plasma membrane breakdown during Drosophila fertilization requires sneaky, an acrosomal membrane protein. *Development,* 133**,** 4871-9.

WONG, E. W. P., MRUK, D. D. & CHENG, C. Y. 2008. Biology and regulation of ectoplasmic specialization, an atypical adherens junction type, in the testis. *Biochim Biophys Acta.,* 1778**,** 692-708.

XAVIER, M. J., SALAS-HUETOS, A., OUD, M. S., ASTON, K. I. & VELTMAN, J. A. 2021. Disease gene discovery in male infertility: past, present and future. *Hum Genet,* 140**,** 7-19.

YAMASHITA, Y. M., FULLER, M. T. & JONES, D. L. 2005. Signaling in stem cell niches: lessons from the Drosophila germline. *J Cell Sci,* 118**,** 665-72.

YAN, R., THOMAS, S. E., TSAI, J. H., YAMADA, Y. & MCKEE, B. D. 2010. SOLO: a meiotic protein required for centromere cohesion, coorientation, and SMC1 localization in Drosophila melanogaster. *J Cell Biol,* 188**,** 335-49.

YASSINE, S., ESCOFFIER, J., MARTINEZ, G., COUTTON, C., KARAOUZÈNE, T., ZOUARI, R., RAVANAT, J.-L., METZLER-GUILLEMAIN, C., LEE, H. C., FISSORE, R., HENNEBICQ, S., RAY, P. F. & ARNOULT, C. 2015. Dpy19l2-deficient globozoospermic sperm display altered genome packaging and DNA damage that compromises the initiation of embryo development. *Mol Hum Reprod,* 21**,** 169-185.

YASUNO, Y., KAWANO, J., INOUE, Y. H. & YAMAMOTO, M. 2013. Distribution and morphological changes of the Golgi apparatus during Drosophila spermatogenesis. *Dev Growth Differ.,* 55**,** 635-47.

YU, J., WU, H., WEN, Y., LIU, Y., ZHOU, T., NI, B., LIN, Y., DONG, J., ZHOU, Z., HU, Z., GUO, X., SHA, J. & TONG, C. 2015. Identification of seven genes essential for male fertility through a genome-wide association study of non-obstructive azoospermia and RNA interference-mediated large-scale functional screening in Drosophila. *Hum Mol Genet,* 24**,** 1493-503.

ZHAO, M., SHIRLEY, C. R., MOUNSEY, S. & MEISTRICH, M. L. 2004. Nucleoprotein Transitions During Spermiogenesis in Mice with Transition Nuclear Protein Tnp1 and Tnp2 Mutations.pdf. *Biol Reprod,* 71**,** 1016-25.

ZHAO, W., LI, Z., PING, P., WANG, G., YUAN, X. & SUN, F. 2018. Outer dense fibers stabilize the axoneme to maintain sperm motility. *J. Cell. Mol. Med.,* 22**,** 1755-68.

ZICKLER, D. & KLECKNER, N. 2015. Recombination, Pairing, and Synapsis of Homologs during Meiosis. *Cold Spring Harb Perspect Biol,* 7**,** a016626.

ZOLLER, R. & SCHULZ, C. 2012. The Drosophila cyst stem cell lineage: Partners behind the scenes? *Spermatogenesis,* 2**,** 145-157.

Chapter 2: The discovery of novel fertility genes from infertile patients using Drosophila

2.1 Introduction

Fly (*Drosophila melanogaster)* models are widely used for studying mammalian spermatogenesis, as the processes of spermatogenesis is highly conserved (reviewed in Bonilla and Xu (2008) and White-Cooper and Bausek (2010).

Over 75% of human disease genes have known *Drosophila* orthologues (Pandey and Nichols, 2011). The high conservation of spermatogenesis between mammals and flies makes *Drosophila* an excellent model system for studying potential male fertility genes. *Drosophila* are cheaper and have a faster generation time than mouse models, and have a wide variety of well-defined genetic tools (reviewed in Siddall and Hime (2017)). A study by Yu et al. (2015) perfectly demonstrates the utility of *Drosophila* in screening for infertility genes. Using a non-obstructive azoospermia Genome-wide association study in a Han Chinese population, Yu et al. was able to analyse single nucleotide variations (SNVs) without the need for validation in multiple patients. Using a *Drosophila* model, the fly orthologues of candidate fertility genes were screened for roles in male fertility using RNA interference (RNAi) (Hu et al., 2011b). Seven novel essential male fertility genes were discovered using this approach (Yu et al., 2015). Furthermore, the ease of targeted gene knockout in *Drosophila* allows for the replacement of the *Drosophila* gene with its human orthologue, in order to determine whether the function of the human gene is sufficient to replace the function of the *Drosophila* orthologue. Using a similar technique, the functional impact of specific SNVs can be tested by replacing the fly gene with a mutated version of the human orthologue.

The objective of this chapter was to test the potential of candidate male infertility mutations, which have been previously highlighted by our collaborators through whole exome sequencing

of infertile men. This was undertaken through the International Male Infertility Genomics Consortium (IMIGC), a collaboration between clinicians and researchers from all over the world, including Australia, UK, US, and Europe. The aim is to expedite the discovery of novel infertility-causing mutations by using patient data to drive basic research and translating these results back into patient care.

Through this collaboration Professor Don Conrad from Oregon Health and Science University provided a list of genes found to be mutated in the exomes of infertile men. These patients were a part of the GEMINI consortium, as outlined in Hardy et al. (2021). In short, the infertile male patients were identified through reproductive history analysis and physical examination as outlined in Schlegel et al. (2021). Whole exome sequencing was undertaken to identify SNVs with an allele frequency of <1% according to GnomAD (https://gnomad. broad institute. org/). Affected genes were then cross referenced against known gene candidates that had already been shown to be associated with human male infertility (Oud et al., 2019).

The present research involved using animal models and human tissues to validate the expression and function of these genes. In this chapter, *Drosophila* were used to screen these candidate genes by knockdown in the testis using RNAi. The genes which showed the most promise were then characterised in more detail in human samples, and a knockout mouse model was generated for the best candidate fertility gene (Chapter 3).

2.2 Experimental procedures

2.2.1 BLAST analysis of candidate genes

A list (Table 1) of candidate infertility-causing variants was identified through whole exome sequencing of infertile males by our collaborators (GEMINI Consortium, Don Conrad, Oregon Health and Science University). A DRSC integrative ortholog prediction tool (DIOPT) analysis was used to define the *Drosophila* orthologues of each mutated gene (Hu et al., 2011a). DIOPT is a tool which combines orthologue predictions from multiple orthologue predictor tools simultaneously. The DIOPT score is the number of tools which predicted orthologous similarity between the human and the *Drosophila* gene. A DIOPT score of >3 was chosen as the threshold for a true orthologue (Table 1), as this indicated a moderate to high predicted orthology. This resulted in the identification of 10 *Drosophila* orthologues of the 35 human genes. For the selected *Drosophila* genes, 15 UAS-RNAi lines were ordered, with one or two lines ordered per gene of interest, depending on availability.

The *Gal4*-UAS system is a commonly used method in *Drosophila* biology which targets the knockdown of a gene (via RNAi) in a specific cell or tissue. The *Gal4* is attached to a "driver" which is expressed within a specific tissue or cell type while the RNAi is attached to an upstream activator sequence (Figure 1)

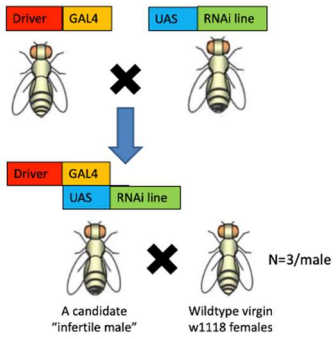

Figure 1: Diagram of the male fertility assay. *Drosophila* with *Gal4*-drivers (in this thesis, targeted to the testis) are crossed with UAS-RNAi lines. This expresses the RNAi line in the specific cell targeted by the driver in the resulting offspring, which generates candidate infertile males. These candidates are crossed with 3 virgin w^{1118} females.

2.2.2 *Drosophila* stocks

All stocks used are outlined in Table 2 with a brief description of function. w^{1118} (BL3605, Bloomington stock Center) flies were used as wild-type controls, as well as for the source of virgin females used to test the fertility of mutant males. The *nanos-Gal4/UAS-Gal4* (*nos-Gal4*) and *trafficjam-Gal4* (*tj-Gal4*) driver lines were donated by Prof. Gary Hime of University of Melbourne (Siddall and Hime, 2017). The *gDj:*GFP*;*nos-Gal4 and *Tj-Gal4,gDj:GFP/Cyo* lines were generated in-house by Dr Sebastian Judd-Mole. The 15 *Drosophila* UAS-RNAi lines used were ordered from Bloomington *Drosophila* Stock Center and are listed in Table 2. All *Drosophila* stocks were maintained in 30 ml vials on Cordonbleu food media (Supp Table 1) and kept at 22°C unless otherwise specified

Table 1: DIOPT scores for the fertility genes of interest from the GEMINI consortium													
Human GeneID	**Human Gene ID**	**HGNCID**	**Human Symbol**	**Species**	**Fly Gene ID**	**FlyBaseID**	**Fly Symbol**	**DIOPT Score**	**Weighted score**	**Rank**	**Best Score**	**Best Score Reverse**	**Prediction Derived From**
ASB11	140456	17186	ASB11	Fly	38037	FBgn0035113	pyx	1	0.91	low	Yes	Yes	Phylome
ATP8B3	**148229**	**13535**	**ATP8B3**	**Fly**	**41469**	**FBgn0037989**	**ATP8B**	**5**	**4.92**	**moderate**	**Yes**	**No**	**OrthoDB, OrthoFinder, orthoMCL, Panther, Phylome**
ATP8B3	148229	13535	ATP8B3	Fly	36488	FBgn0259221	CG42321	3	2.81	low	No	No	eggNOG, OrthoDB, orthoMCL
ATP8B3	148229	13535	ATP8B3	Fly	32609	FBgn0030746	CG9981	3	2.8	low	No	No	eggNOG, OrthoFinder, orthoMCL
AXDND1	126859	26564	AXDND1					0	0	None			
CXCR3	2833	4540	CXCR3	Fly	44126	FBgn0266429	AstA-R1	1	0.91	low	Yes	No	Phylome
CXCR3	2833	4540	CXCR3	Fly	40019	FBgn0036789	AstC-R2	1	0.91	low	Yes	No	Phylome
DCAF12L1	**139170**	**29395**	**DCAF12L1**	**Fly**	**41460**	**FBgn0037980**	**DCAF12**	**11**	**10.87**	**moderate**	**Yes**	**No**	**Compara, Hieranoid, Inparanoid, OMA, OrthoDB, OrthoFinder, OrthoInspector, orthoMCL, Panther, Phylome, TreeFam**
ESX1	80712	14865	ESX1	Fly	31807	FBgn0030058	CG11294	2	2.06	high	Yes	Yes	Panther, TreeFam
FAAH2	**158584**	**26440**	**FAAH2**	**Fly**	**36340**	**FBgn0033717**	**CG8839**	**15**	**14.75**	**high**	**Yes**	**Yes**	**Compara, eggNOG, Hieranoid, Homologene, Inparanoid, Isobase, OMA, OrthoDB, OrthoFinder, OrthoInspector, orthoMCL, Panther, Phylome, RoundUp, TreeFam**
FAAH2	158584	26440	FAAH2	Fly	43083	FBgn0039341	CG5112	8	7.76	moderate	No	Yes	Compara, eggNOG, Isobase, OrthoDB, OrthoFinder, Panther, Phylome, TreeFam
FAAH2	158584	26440	FAAH2	Fly	42431	FBgn0038803	CG5191	6	5.92	moderate	No	Yes	eggNOG, Isobase, OrthoDB, OrthoFinder, Panther, TreeFam
FAAH2	158584	26440	FAAH2	Fly	40956	FBgn0037547	CG7910	6	5.92	moderate	No	Yes	eggNOG, Isobase, OrthoDB, OrthoFinder, Panther, TreeFam
FAAH2	158584	26440	FAAH2	Fly	40957	FBgn0037548	CG7900	5	4.97	moderate	No	Yes	eggNOG, OrthoDB, OrthoFinder, Panther, TreeFam
FANCM	**57697**	**23168**	**FANCM**	**Fly**	**42543**	**FBgn0038889**	**Fancm**	**12**	**11.79**	**high**	**Yes**	**Yes**	**Compara, eggNOG, Hieranoid, Inparanoid, OrthoDB, OrthoFinder, OrthoInspector, orthoMCL, Panther, Phylome, RoundUp, TreeFam**
FRMPD3	**84443**	**29382**	**FRMPD3**	**Fly**	**41817**	**FBgn0261859**	**CG42788**	**7**	**6.83**	**moderate**	**Yes**	**No**	**Compara, eggNOG, OrthoDB, OrthoFinder, OrthoInspector, RoundUp, TreeFam**
GBP3	2635	4184	GBP3	Fly	42934	FBgn0039213	atl	1	0.9	low	Yes	No	eggNOG

Table 1: DIOPT scores for the fertility genes of interest from the GEMINI consortium (continued…)													
Search Term	**Human Gene ID**	**HGNCID**	**Human Symbol**	**Species**	**Fly Gene ID**	**FlyBaseID**	**Fly Symbol**	**DIOPT Score**	**Weighted score**	**Rank**	**Best Score**	**Best Score Reverse**	**Prediction Derived From**
GUCA1C	9626	4680	GUCA1C	Fly	32799	FBgn0083228	Frq2	2	1.91	moderate	Yes	No	eggNOG, OrthoDB
GUCA1C	9626	4680	GUCA1C	Fly	43126	FBgn0039380	CG5890	2	1.91	moderate	Yes	No	eggNOG, OrthoDB
GUCA1C	9626	4680	GUCA1C	Fly	32797	FBgn0030897	Frq1	2	1.91	moderate	Yes	No	eggNOG, OrthoDB
GUCA1C	9626	4680	GUCA1C	Fly	40187	FBgn0036926	CG7646	2	1.91	moderate	Yes	No	eggNOG, OrthoDB
GUCA1C	9626	4680	GUCA1C	Fly	40186	FBgn0013303	Nca	2	1.91	moderate	Yes	No	eggNOG, OrthoDB
GUCA1C	9626	4680	GUCA1C	Fly	32063	FBgn0265595	CG44422	2	1.91	moderate	Yes	No	eggNOG, OrthoDB
HAVCR1	26762	17866	HAVCR1					0	0	None			
HIF3A	**64344**	**15825**	**HIF3A**	**Fly**	**43580**	**FBgn0266411**	**sima**	**8**	**7.81**	**moderate**	**Yes**	**No**	**Compara, eggNOG, Hieranoid, OrthoDB, OrthoInspector, Panther, Phylome, TreeFam**
HIF3A	64344	15825	HIF3A	Fly	38065	FBgn0262139	trh	2	1.9	low	No	No	eggNOG, OrthoFinder
MAGEA6	4105	6804	MAGEA6	Fly	40860	FBgn0037481	MAGE	6	5.97	moderate	Yes	No	eggNOG, Hieranoid, Inparanoid, OrthoDB, Panther, Phylome
MAGEB4	4115	6811	MAGEB4	Fly	40860	FBgn0037481	MAGE	7	6.93	moderate	Yes	No	eggNOG, Hieranoid, Inparanoid, OrthoDB, Panther, Phylome, TreeFam
MS4A14	84689	30706	MS4A14					0	0	None			
MUM1L1	139221	26583	MUM1L1					0	0	None			
OCM	654231	8105	OCM	Fly	38092	FBgn0035161	CG13898	1	0.9	low	Yes	No	eggNOG
OCM	654231	8105	OCM	Fly	44913	FBgn0011273	Acam	1	0.9	low	Yes	No	eggNOG
OCM	654231	8105	OCM	Fly	36195	FBgn0010423	TpnC47D	1	0.9	low	Yes	No	eggNOG
OCM	654231	8105	OCM	Fly	37405	FBgn0034592	CG9406	1	0.9	low	Yes	No	eggNOG
OCM	654231	8105	OCM	Fly	319047	FBgn0051960	CG31960	1	0.9	low	Yes	No	eggNOG
OCM	654231	8105	OCM	Fly	47878	FBgn0004910	Eip63F-1	1	0.9	low	Yes	No	eggNOG
OCM	654231	8105	OCM	Fly	31050	FBgn0040351	CG11638	1	0.9	low	Yes	No	eggNOG
OCM	654231	8105	OCM	Fly	35751	FBgn0033238	azot	1	0.9	low	Yes	No	eggNOG
OCM	654231	8105	OCM	Fly	33603	FBgn0051958	CR31958	1	0.9	low	Yes	No	eggNOG
OCM	654231	8105	OCM	Fly	246577	FBgn0050378	CG30378	1	0.9	low	Yes	No	eggNOG
OCM	654231	8105	OCM	Fly	35498	FBgn0033027	TpnC4	1	0.9	low	Yes	No	eggNOG
OCM	654231	8105	OCM	Fly	37278	FBgn0034481	CG11041	1	0.9	low	Yes	No	eggNOG
OCM	654231	8105	OCM	Fly	35473	FBgn0013348	TpnC41C	1	0.9	low	Yes	No	eggNOG
OCM	654231	8105	OCM	Fly	42465	FBgn0038830	CG17272	1	0.9	low	Yes	No	eggNOG
OCM	654231	8105	OCM	Fly	36905	FBgn0004580	Cbp53E	1	0.9	low	Yes	No	eggNOG
OCM	654231	8105	OCM	Fly	43117	FBgn0039373	CG5024	1	0.9	low	Yes	No	eggNOG
OCM	654231	8105	OCM	Fly	33752	FBgn0031692	TpnC25D	1	0.9	low	Yes	No	eggNOG
OCM	654231	8105	OCM	Fly	36329	FBgn0000253	Cam	1	0.9	low	Yes	No	eggNOG

Table 1: DIOPT scores for the fertility genes of interest from the GEMINI consortium (continued…)													
Search Term	**Human Gene ID**	**HGNCID**	**Human Symbol**	**Species**	**Fly Gene ID**	**FlyBaseID**	**Fly Symbol**	**DIOPT Score**	**Weighted score**	**Rank**	**Best Score**	**Best Score Reverse**	**Prediction Derived From**
OCM	654231	8105	OCM	Fly	43118	FBgn0039374	CG17770	1	0.9	low	Yes	No	eggNOG
OCM	654231	8105	OCM	Fly	39916	FBgn0010424	TpnC73F	1	0.9	low	Yes	No	eggNOG
OCM	654231	8105	OCM	Fly	37613	FBgn0034774	CG13526	1	0.9	low	Yes	No	eggNOG
P2RY4	5030	8542	P2RY4	Fly	40019	FBgn0036789	AstC-R2	1	0.91	low	Yes	No	Phylome
P2RY4	5030	8542	P2RY4	Fly	40020	FBgn0036790	AstC-R1	1	0.91	low	Yes	No	Phylome
PFKFB1	**5207**	**8872**	**PFKFB1**	**Fly**	**32938**	**FBgn0027621**	**Pfrx**	**10**	**9.69**	**moderate**	**Yes**	**No**	**Compara, eggNOG, Hieranoid, Inparanoid, OrthoDB, OrthoInspector, orthoMCL, Phylome, RoundUp, TreeFam**
PKHD1L1	93035	20313	PKHD1L1					0	0	None			
PNLDC1	154197	21185	PNLDC1					0	0	None			
PRRG3	79057	30798	PRRG3					0	0	None			
SCML1	6322	10580	SCML1	Fly	41168	FBgn0003334	Scm	1	1.1	low	Yes	No	Panther
SCML1	6322	10580	SCML1	Fly	31254	FBgn0024993	CG2662	1	1.1	low	Yes	No	Panther
SCML1	6322	10580	SCML1	Fly	44889	FBgn0004860	ph-d	1	0.95	low	Yes	No	Isobase
SCML1	6322	10580	SCML1	Fly	43288	FBgn0002441	l(3)mbt	1	0.9	low	Yes	No	eggNOG
SPIDR	23514	28971	SPIDR					0	0	None			
TDRD9	**122402**	**20122**	**TDRD9**	**Fly**	**41919**	**FBgn0003483**	**spn-E**	**15**	**14.75**	**high**	**Yes**	**Yes**	**Compara, eggNOG, Hieranoid, Homologene, Inparanoid, Isobase, OMA, OrthoDB, OrthoFinder, OrthoInspector, orthoMCL, Panther, Phylome, RoundUp, TreeFam**
TFDP3	**51270**	**24603**	**TFDP3**	**Fly**	**36461**	**FBgn0011763**	**Dp**	**10**	**9.86**	**moderate**	**Yes**	**No**	**Compara, eggNOG, Hieranoid, Inparanoid, OrthoDB, OrthoFinder, OrthoInspector, Panther, Phylome, TreeFam**
TRIM63	84676	16007	TRIM63	Fly	34453	FBgn0051721	Trim9	2	1.84	moderate	Yes	No	Compara, Phylome
VSIG1	340547	28675	VSIG1	Fly	318958	FBgn0051814	CG31814	1	0.91	low	Yes	No	Phylome
ZCCHC16	340595	25214	RTL4	Fly	19835207	FBgn0266534	CG45095	1	1.01	low	Yes	Yes	OrthoDB
ZCCHC5	203430	22997	RTL3					0	0	None			
ZFR2	**23217**	**29189**	**ZFR2**	**Fly**	**39764**	**FBgn0263603**	**Zn72D**	**11**	**10.76**	**moderate**	**Yes**	**No**	**Compara, eggNOG, Hieranoid, Inparanoid, OrthoDB, OrthoFinder, OrthoInspector, orthoMCL, Panther, Phylome, TreeFam**

Table 1: DIOPT scores for the fertility genes of interest from the GEMINI consortium (continued…)

Search Term	Human Gene ID	HGNCID	Human Symbol	Species	Fly Gene ID	FlyBase ID	Fly Symbol	DIOPT Score	Weighted score	Rank	Best Score	Best Score Reverse	Prediction Derived From
ZNF512B	57473	29212	ZNF512B	Fly	2768990	FBgn0053265	Muc68E	1	1.03	low	Yes	No	RoundUp
ZNF512B	57473	29212	ZNF512B	Fly	317939	FBgn0052249	CG32249	1	0.95	low	Yes	No	Isobase
ZNF512B	57473	29212	ZNF512B	Fly	34812	FBgn0028544	CG16884	1	0.9	low	Yes	Yes	orthoMCL
ZNF543	125919	25281	ZNF543	Fly	41530	FBgn0038047	CG5245	2	2.1	moderate	Yes	No	Hieranoid, Panther
ZNF543	125919	25281	ZNF543	Fly	34592	FBgn0020309	crol	2	1.81	moderate	Yes	No	orthoMCL, Phylome
ZNF674	641339	17625	ZNF674	Fly	33657	FBgn0031610	CG15436	1	1	low	Yes	No	Hieranoid
ZNF674	641339	17625	ZNF674	Fly	41530	FBgn0038047	CG5245	1	1	low	Yes	No	Hieranoid
ZNF674	641339	17625	ZNF674	Fly	40414	FBgn0037120	CG11247	1	1	low	Yes	No	Hieranoid
ZNF674	641339	17625	ZNF674	Fly	31410	FBgn0025679	Klf15	1	0.91	low	Yes	No	Phylome

Human Gene ID = Gene name according to Entrez; HGNCID = Gene ID according to HUGO Gene Nomenclature Committee (HGNC); Human Symbol = Gene name according to HGNC, Species = Species of interest; Fly Gene ID = Gene ID according to NCBI; FlyBase ID = FlyBase ID number; Fly symbol = Gene name according to FlyBase; DIOPT Score = Number of orthologue predictor tools suggesting orthologous genes; Weighted Score = weighted DIOPT score based on number of tools predicting orthologous genes; Rank = likelihood of orthologous genes; Prediction Derived From = List of predictor tools predicting orthologous genes.

2.2.3 Initial screen of infertility candidate genes

The 15 UAS-RNAi lines (Table 2) were crossed separately with either *tj-Gal4* or *nos-Gal4* transgenic lines to generate adult male flies with expression of each target gene knocked down in the somatic or germline cells respectively. For each genotype, three males were individually housed, each with three virgin w^{1118} females and allowed to mate for three days at 29°C. Subsequently, they were tipped into a fresh vial twice, each time being allowed to mate for three days. At the end of the third mating period, the flies were discarded. After the males were removed from each vial, the vial was transferred to 27°C after the adults were removed, as previous work had shown low incidence of non-specific sperm defects in flies raised at 29°C but not at 27°C (Rohmer et al., 2004).

Table 2: *Drosophila* stocks used for the fertility screen

Fly line	Function	Fly gene	Patient Orthologue
w^{1118}	Wild-type control	N/A	N/A
Tj-Gal4	Cyst cell driver	N/A	N/A
Nos-Gal4;UAS-Gal4	Germ cell driver	N/A	N/A
BL5417	gdj:GFP	N/A	N/A
Tj-Gal4, gDj:GFP/CyO	Cyst cell driver & sperm GFP	N/A	N/A
gDj:GFP;nos-GAL4	Germ cell driver & sperm GFP	N/A	N/A
Bloomington stocks			
68160	UAS-RNAi	*DCAF12*	*DCAF12L1*
65140	UAS-RNAi	*CG8839*	*FAAH2*
33889	UAS-RNAi	*Fancm*	*FANCM*
35380	UAS-RNAi	*Pfrx*	*PFKFB1*
57222	UAS-RNAi	*Pfrx*	*PFKFB1*
32620	UAS-RNAi	*spn-E*	*TDRD9*
34808	UAS-RNAi	*spn-E*	*TDRD9*
31767	UAS-RNAi	*Dp*	*TFDP3*
33372	UAS-RNAi	*Dp*	*TFDP3*
55635	UAS-RNAi	*Zn72D*	*ZFR2*
63037	UAS-RNAi	*ATP8B*	*ATP8B3*
31556	UAS-RNAi	*CG42788*	*FRMPD3*
34594	UAS-RNAi	*CG42788*	*FRMPD3*
26207	UAS-RNAi	*sima*	*HIF3A*
33894	UAS-RNAi	*sima*	*HIF3A*

The offspring were counted 7 days after the adults were removed from each vial. The males were considered infertile if no offspring were produced, and sub-fertile if there was a statistically significant reduction in the number of offspring produced compared to control. After the initial screen of the 15 UAS-RNAi lines the same experiment was repeated with 10 individually housed males in order to increase statistical power, focussing on a smaller number of candidate genes which had shown signs of disrupted fertility in the initial screen.

2.2.4 Histological analysis of *Drosophila* testes

After the mating assay, infertile and sub-fertile lines were examined histologically. Testes were dissected from 3-5 day old flies in 1 x PBS. The testes were fixed in 4% PFA for 30 mins at room temperature, then washed in 1 x PBS. Testis nuclei were stained with 1 mg/ml DAPI and 2 µl/ml Alexa Fluor 555 phalloidin (F-actin) in PBS for 30 mins at room temperature, in a dark chamber, then washed in 1 x PBS. Testes were mounted with Fluromount-G (Invitrogen, Thermofisher) mounting medium on microscope slides with coverslips. Fluorescent images were taken using a Cell Voyager confocal microscope (CV1000, Yokogawa, Tokyo, Japan)

2.2.5 Biopsies

Human testis biopsies were obtained (with written informed consent) from patients who presented with obstructive (OA) or non-obstructive azoospermia (NOA) at the Centre of Reproductive Medicine and Andrology of the University Hospital in Münster (Germany) and the Department of Urology and Andrology of the University Hospital in Giessen. Immediately following surgical removal, testicular tissue for histological analysis were fixed in Bouin's solution and ultimately embedded in paraffin. 5-µm-thick sections were cut with a microtome and placed on a microscope slide. Histological analysis including score count analysis was

performed as outlined in Bergmann and Kliesch (2010). OA patients were defined as having intact spermatogenesis (score 10, NSP) whereas NOA patients used in this study showed a Sertoli Cell Only (SCO) defined by a complete loss of germ cells.

2.2.6 Quantifying *ZFR2* and *DCAF12L1* expression human testes

Total candidate gene mRNA levels were quantified by semi-quantitative RT-PCR as described previously (Pleuger et al., 2017), as below. The PCR primers used are outlined in Table 3. mRNA was extracted from Bouin's fixed and paraffin embedded testicular biopsies using the RNeasy FFPE Kit (Qiagen), which included a treatment with Proteinase K, which removed the formalin that can crosslink the DNA, increasing the yield. The extracted mRNA was purified from remaining genomic DNA by incubating with 2 µL of 10 U/µL RNase-free DNase I (Peqlab Biotechnology), 1 µL RNase-free incubation buffer (500 mM, Roche), 0.25 µL RNase inhibitor (40 U/µL), per 6.65 µL of mRNA, for 25 mins at 37°C.

For cDNA synthesis, 9 µl of 200 ng/µL mRNA was mixed with 51 µl of RT-Mix (all components came from Applied Biosystems by ThermoFisher Scientific), including 6 µl of GeneAmp 10x PCR Gold Buffer, 6 µl of nucleotide mix (10mM), 3 µl of random hexamer

Table 3: Sequences of primers for RT-PCR and In-situ hybridization

Gene	Ascension No.	Forward Primer (5'-3')	Reverse Primer (5'-3')	PCR Product length
DCAF12	NM_015397.4	CAGTTTGGCTGGGATCACTC	TCAGGAGACTGGGAAGTTGC	163bp
DCAF12L1	NM_178470.5	TGGACTGCTATGAAAACAGG	AGTGCCCAAACATCTAAGG	149bp
GAPDH	NM_002046.3	CCAGGTGGTCTCCTCTGACTTC	GTGGTCGTTGAGGGCAATG	81bp

primers (50 µM), 3 µl of RNase Inhibitor (20U/µl), 3 µl of MultiScribe Reverse Transcriptase (50 U/µl) and 18 µl of sterile distilled water.

1 µl of the generated cDNA was then mixed with 2.5 µl of GeneAmp 10x PCR Gold Buffer, 2 µl of $MgCl_2$ (25 mM), 1 µl of each of the forward and reverse primers (10 pmol/mL), 1 µl of nucleotide mix (10 mM each), 0.15 µl of AmpliTaq Gold polymerase, and 16.35 µl of sterile distilled water. Primers for *GAPDH, DCAF12* and *DCAF12L1* were used. RT-PCR was undertaken under the following cycle conditions: 9 mins at 95°C, 38 x [45 secs at 94°C, 45 secs at 58°C, 45 secs 72°C] and 7 mins at 72°C. 4µl of GelGreen Nucleic Acid Stain (Biotium) were added to each PCR product, and the PCR product was size separated on a 1.5% agarose gel at 120 V for 65 mins, using a 50 base-pair ladder as a reference.

2.2.7 Qualifying *ZFR2* expression human testes using immunohistochemistry

Slides with 5µm-thick testicular biopsy sections were boiled in 1x citrate buffer (pH 6.0) for 20 mins. Slides were then incubated in 3% H_2O_2 in methanol for 15 mins in order to block any endogenous peroxidases. In order to prevent non-specific binding, the slides were incubated in 1.5% BSA for 45 mins. ZFR2 antibody (rabbit, polyclonal. Sigma HPA0055678) was incubated on the slides overnight in a dark chamber at a dilution of 1:200 in 1.5% BSA. After several wash steps, goat anti-rabbit biotinylated immunoglobulin 1.6 g/L (Dako A/S, E0466) was added at a dilution of 1:200 for 60 mins in a dark chamber. The sections were subsequently incubated with Vectastain Elite ABC Standard Kit (Vector Laboratories) for 1 hour. Immunohistochemical staining was performed using Peroxidase Substratkit AEC (BioLogo Dr. Hartmut Schultheiss e.K) for up to 30 mins. Nuclei were counterstained with haematoxylin, and slides were mounted with Kaiser's glycerol gelatine.

2.2.8 Statistical Analysis

GraphPad Prism 7 was used for statistical analysis, and to generate all graphs. An ordinary one-way ANOVA, comparing candidate gene RNAi knockdown to the w^{1118} control, using a Dunnett's multiple comparison test was used, to analyse the significance of the decrease in the number of offspring in the fly infertility screen.

2.3 Results

2.3.1 Knockdown of *Zn72D* and *DCAF12* cause sterility and subfertility in the fly, respectively

A list of 35 candidate gene variants identified from whole exome sequencing as potentially causing infertility in men, was sent to the O'Bryan lab. BLAST analysis determined that 10 of these candidate genes had possible *Drosophila* orthologues (denoted by a DIOPT score of greater than 3; see Table 1). From these 10 fly orthologues, 15 *Drosophila* RNAi lines were sourced and tested for fertility status with *nanos-Gal4* and *trafficjam-Gal4* testis specific drivers using the Gal4-UAS system. The number of offspring were recorded for each knockdown. The initial screen, using 3 individually housed males did not provide a reliable result as there was noticeable variation in many of the lines of interest (Figure 2). *CG8839* and *CG42788* RNAi lines crossed with the *tj-Gal4* driver resulted in lethality. For this reason, the experiment was repeated on the RNAi lines which in the original screen, showed potentially reduced fertility, using 10 males per gene to gain more statistical power (Figure 3). Only the RNAi/*Gal4* combinations which showed the most promise were repeated in the second screen.

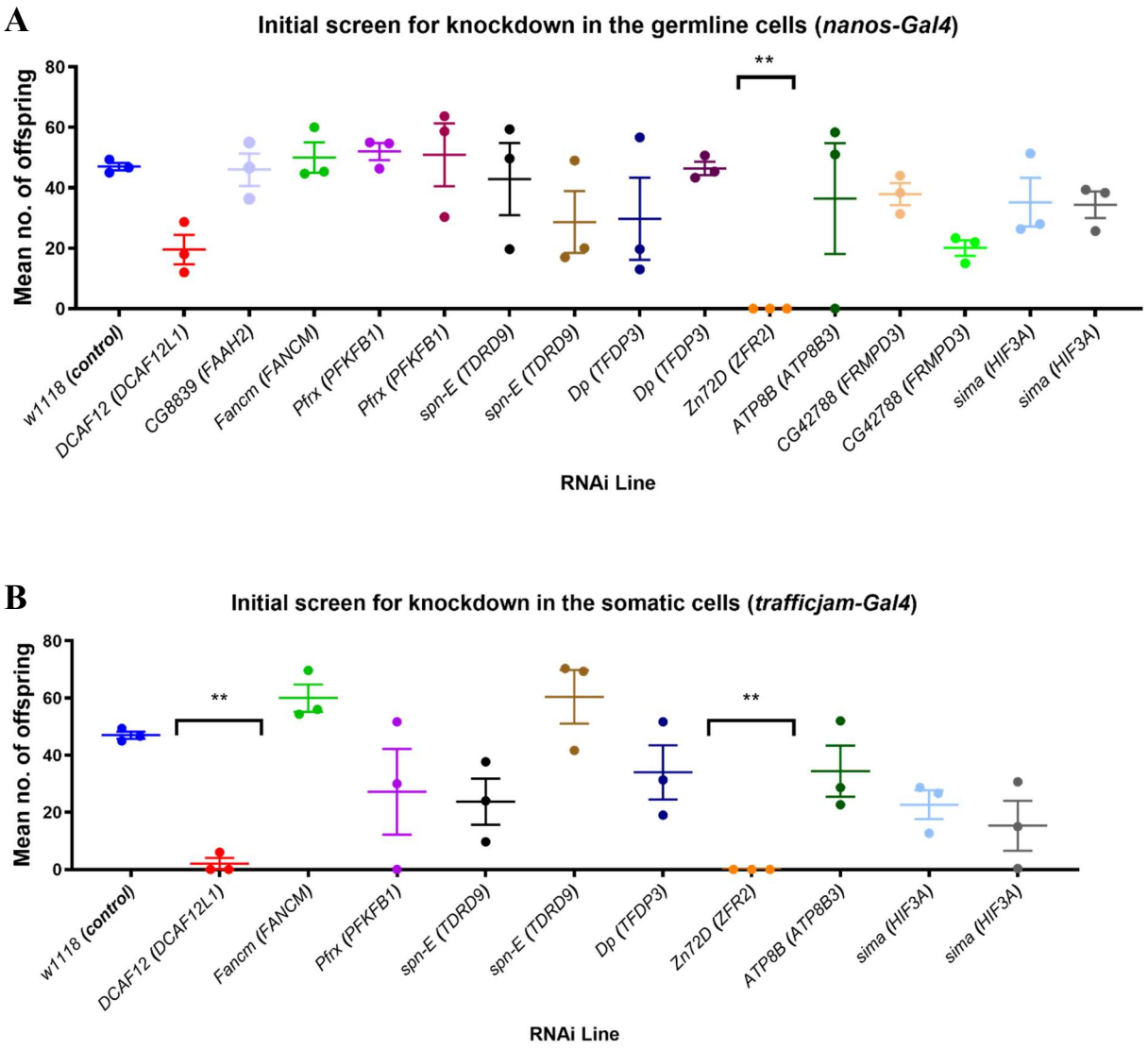

Figure 2: Initial screen to assess the role of individual candidate genes in *Drosophila* male fertility. A screen for potential candidate infertility genes in the **(A)** germline cells of the testis, using a *nanos-Gal4* line and **(B)** in the somatic cells of the testis, using a *trafficjam-Gal4***.** The genes of interest are indicated by "*Drosophila* gene (patient orthologue)". Each bar represents the average number of offspring from a cross from three single transgenic male, each with 3 w^{1118} females, over three 3-day lays. The error bars indicate the standard error of the mean for each male. (**= $p<0.01$)

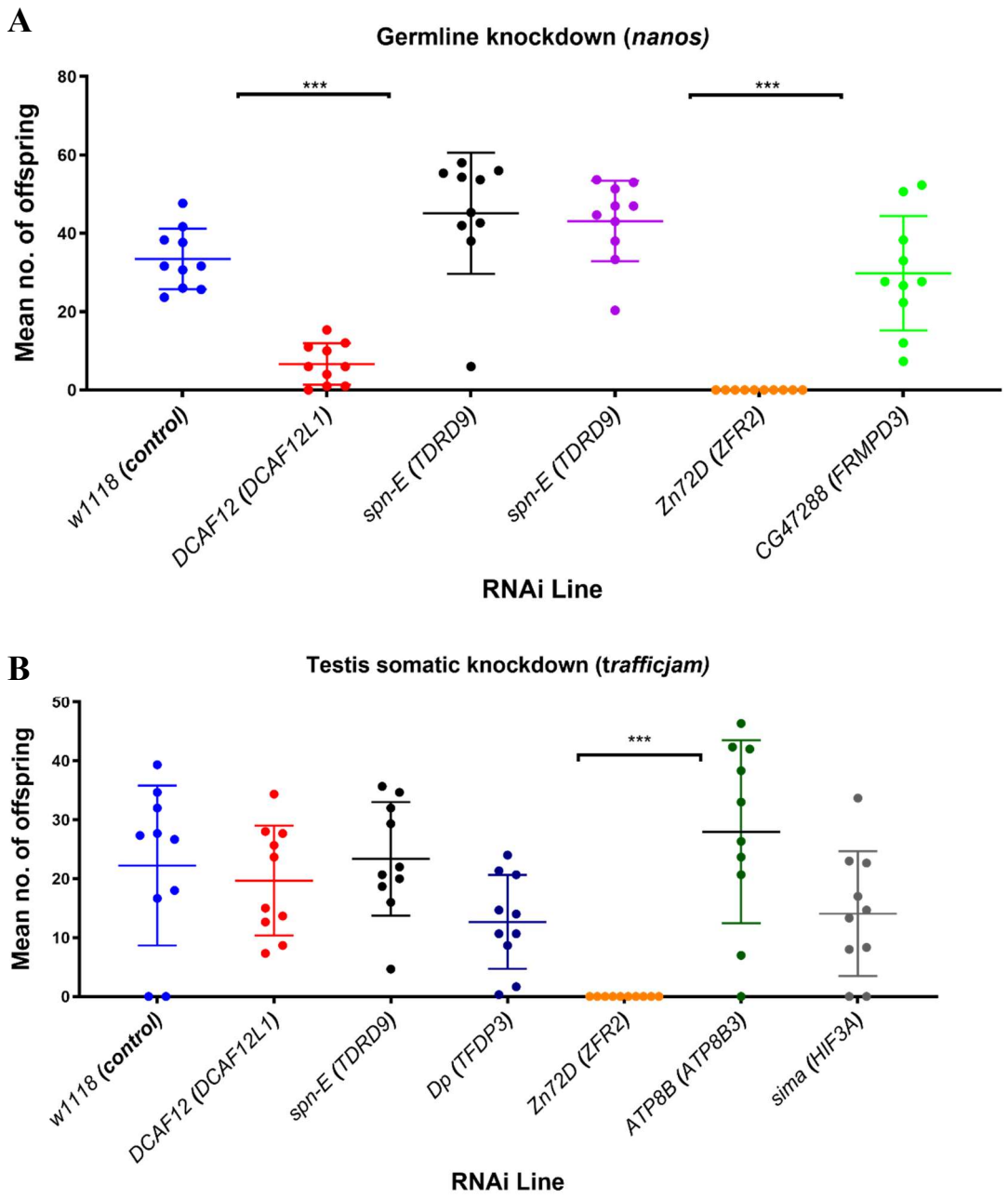

Figure 3: Follow-up screen to assess the role of individual candidate genes in *Drosophila* male fertility. A screen for potential candidate infertility genes in the **(A)** germline cells of the testis, using a *nanos-Gal4* line and **(B)** in the somatic cells of the testis, using a *trafficjam-Gal4***.** The genes of interest are indicated by "*Drosophila* gene (patient orthologue)". Each bar represents the average number of offspring from a cross from three single transgenic male, each with 3 w^{1118} females, over three 3-day lays. The error bars indicate the standard error of the mean for each male. (***= $p<0.001$)

When *Zn72D* was knocked down in either the germline (Figure 3A), or the somatic (Figure 3B) cells, the male flies were sterile ($p<0.001$). *Dcaf12* knockdown in the germline resulted in sub-fertility (control mean = 33 offspring per male, *Dcaf12* = 7, $p<0.001$), but no significant reduction in progeny was observed with knockdown in the somatic cells. These results suggest that the human *Zn72D* and *DCAF12* warranted further analysis.

2.3.2 Histological analysis of *Zn72D* and *DCAF12* testicular knockdown in flies

To examine the histological effect of *Zn72D* and *DCAF12* knockdown on male fertility, the *nos*-Gal4 and *tj*-Gal4 transgenes were combined with a *don juan (dj)-GFP* transgene, which expresses GFP in the sperm tails. After dissection, the testes were fixed and stained with phalloidin (red) which targets F-actin and DAPI (blue) which stains DNA.

When *Zn72D* was knocked down in the germ cells of the *Drosophila* testis, sperm were still produced. In the proximal region of the testis, spermatogenesis presented as disorganised sperm heads, (DAPI, blue) with no actin cones present (Phalloidin, red) (Figure 4E-H). A similar phenotype was observed when *Zn72D* was knocked down in the somatic cells (Figure 4I-L). However, near the distal end of the testis, there was a noticeable reduction in the number of sperm produced, relative to the w^{1118} control (Figure 4A-D). Furthermore, there was a distinct lack of sperm in the seminal vesicle (Figure 5E-H), as indicated by a lack of tails (green) and sperm heads (blue) and the dramatic reduction in the overall seminal vesicle size. The lack of sperm in the seminal vesicles clearly shows why the flies in the screen were sterile.

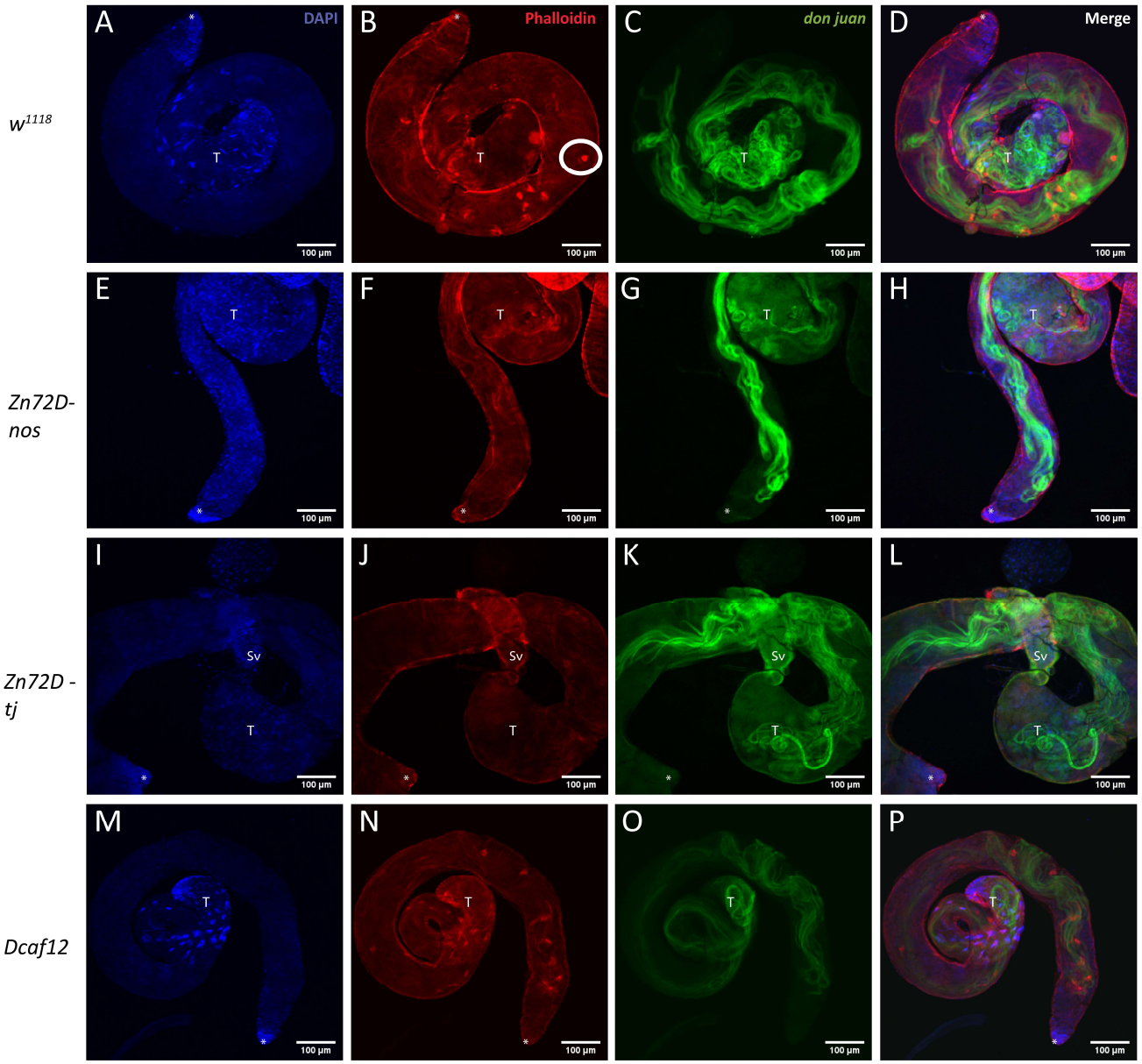

Figure 4: Analysis of *Zn72D* and *DCAF12* germ cell knockdown in the *Drosophila testis*. (A-D) *dj-GFP;nos-Gal4/w*^{1118}, **(E-H)** *dj-GFP;nos-Gal4/UAS-Zn72Di,* **(I-L)** *dj-GFP;tj-Gal4/Zn72Di,* **(M-P)** *dj-GFP;nos-Gal4/DCAF12i*. All samples were stained with DAPI (nuclei, blue) and Phalloidin (actin, red). The *dj (donjuan)-GFP* caused green fluorescence in the sperm tails. White circle = actin cones, * = hub, Te = testis, Sv = Seminal vesicle

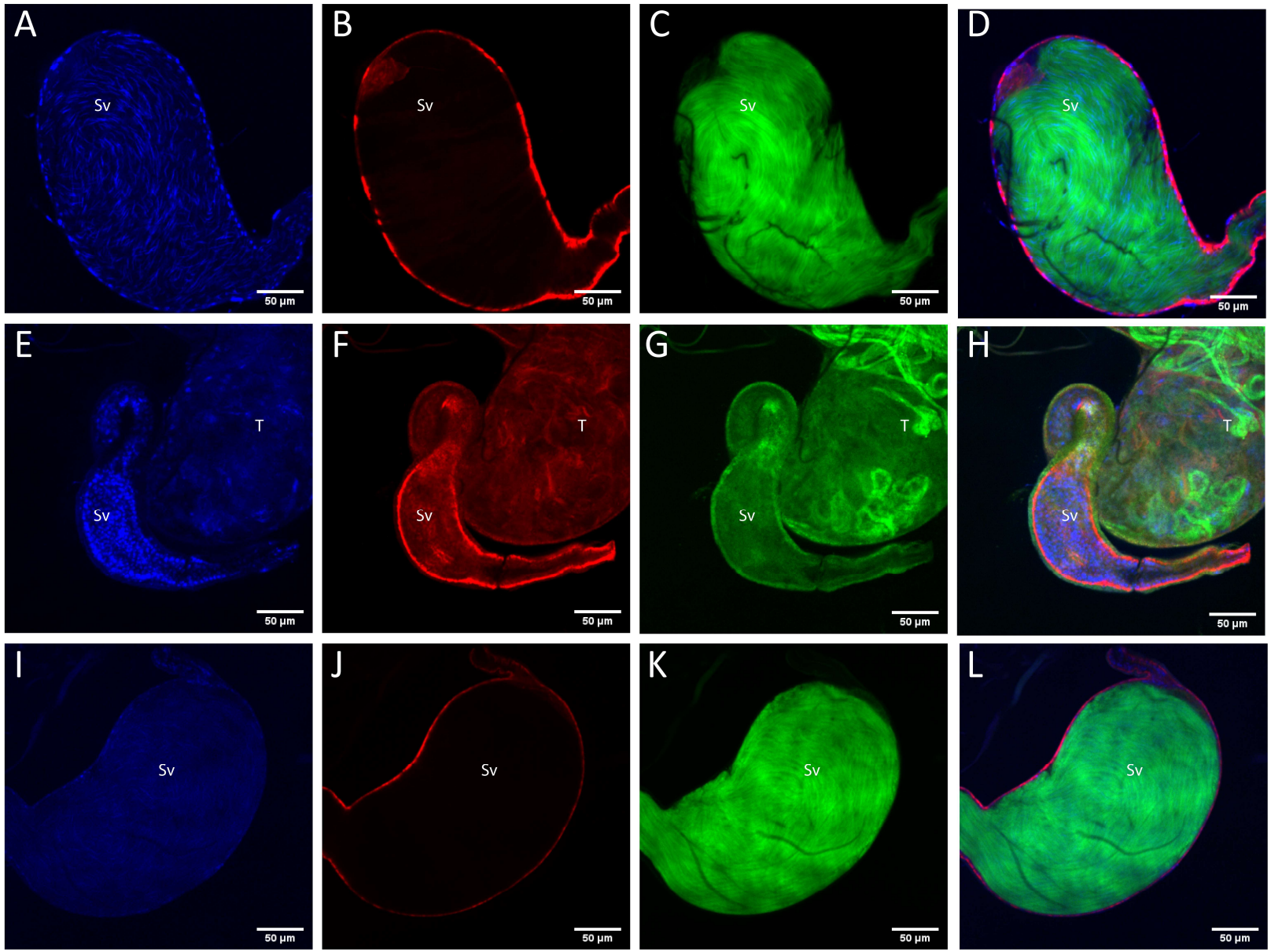
A
B
C
D
E
F
G
H
I
J
K
L
Sv
T
50 µm
w1118
Zn72D
DCAF12

Figure 5: Seminal vesicle analysis of *Zn72D* and *DCAF12* germ cell knockdown in the *Drosophila testis*. **(A-D)** *dj-GFP;nos-Gal4/w*^{1118}, **(E-H)** *dj-GFP;nos-Gal4/UAS-Zn72Di,* **(I-L)** *dj-GFP;nos-Gal4/DCAF12i*. All samples were stained with DAPI (nuclei, blue) and Phalloidin (actin, red). The *dj (donjuan)-GFP* caused green fluorescence in the sperm tails.

When *DCAF12* was knocked down in the germ cells of the testis, sperm were present in the testis (Figure 4M-P), however there were noticeably fewer than in the control (Figure 4A-D). The seminal vesicle however is full of sperm (Figure 5I-L).

2.3.3 *ZFR2* and *DCAF12L1* are both expressed in the human testis

In order to determine the expression of these genes in the mammalian testis, testicular single-cell sequencing data was used. Analysis of data from Jung et al. (2019) (mouse) and Mahyari et al. (2021) (human) demonstrated that both *ZFR2* and *DCAF12L1* were expressed in the testis. In both mice and humans, *DCAF12L1* expression was highest in Sertoli cells (Figure 6). In the human, in addition to Sertoli cell expression, there was also notable *DCAF12L1* expression in spermatogonia (Figure 6B). The single-cell sequencing data of *ZFR2* will be discussed in detail in the next chapter, however *ZFR2* was shown to be expressed in the testes of both humans and mice. The patient *ZFR2* and *DCAF12L1* mutations identified by our collaborators are outlined in Table 4. Testes from patients with normal spermatogenesis (NSP)

Table 4: *ZFR2* and *DCAF12L1* mutations in the patients

Gene	Genomic position	cDNA pos.	Protein pos.	Genotype	Phenotype
ZFR2	g.Chr19: 3810840G>A	c.C2341T	p.R781X	Homozygous	Azoospermia
DCAF12L1	X: 125685967C>G	c.G625C	p.V209L	Hemizygous	No biopsy
	X: 126552176G>A	c.C433T	p.Q145X	Hemizygous	Maturation arrest
	X: 126552202AA/-	c.406_407del	p.L136AX	Hemizygous	No biopsy
	X 126551264-/C	c.1344dupG	p.P449AX	Hemizygous	Spermatocyte arrest

and Sertoli cell (SCO) phenotypes were analysed, in order to examine expression of these genes. RT-PCR determined that both DCAF12L1, and its homologue, DCAF12 were expressed in the testes of human patients with both NSP and SCO phenotypes (Figure 7).

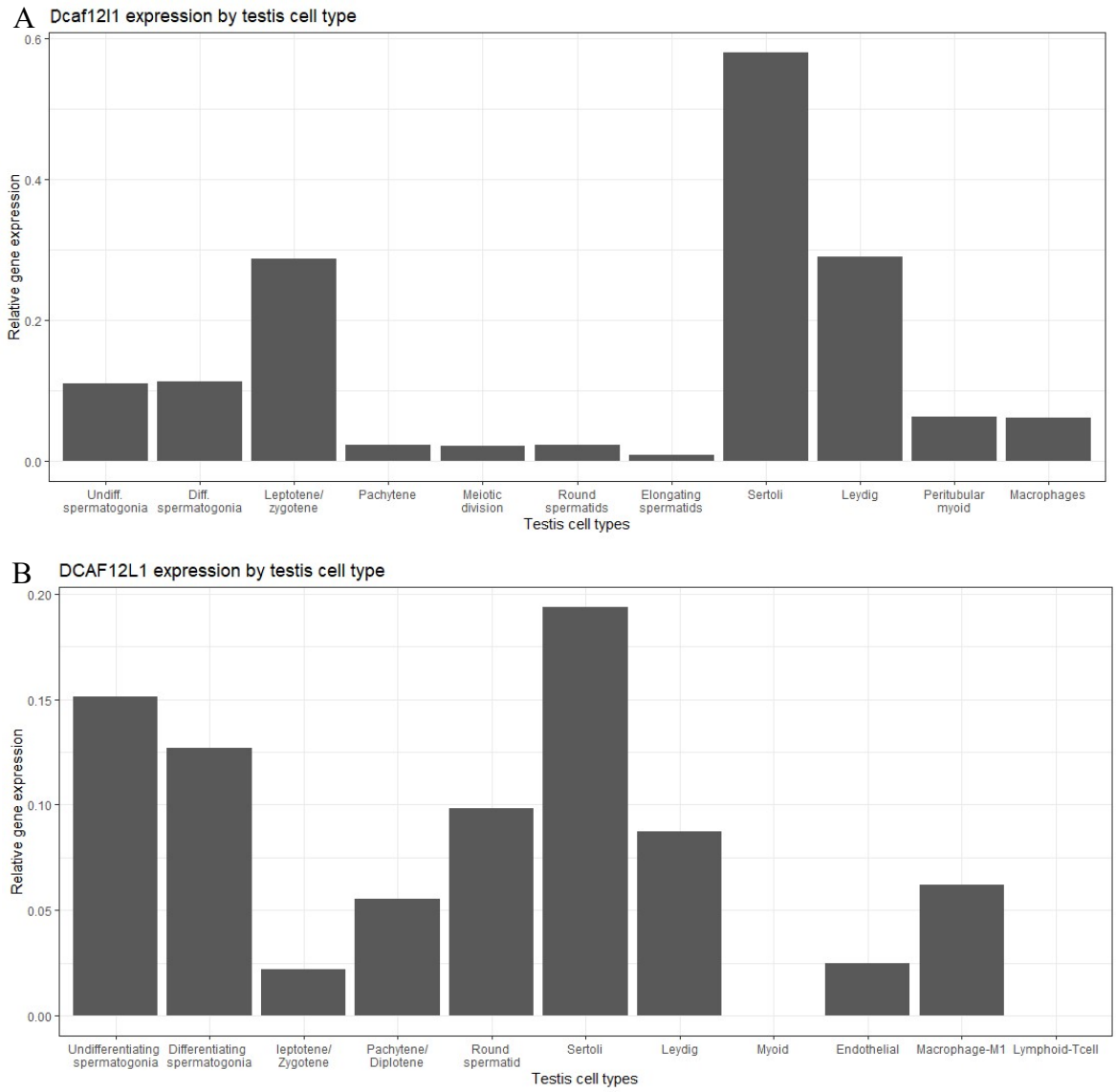

Figure 6: Relative *DCAF12L1* expression in by testis cell type using RNA seq in (A) mouse and (B) human. (A) Relative expression of *Dcaf12l1* in the mouse was low in the germline cells, and higher in somatic cells, particularly Sertoli cells. (B) In the human, relative expression of *DCAF12L1* in germline cells was highest in spermatogonia, and in somatic cells, was highest in Sertoli cells. Data extracted from Jung et al. (2019) and Mahyari et al. (2021).

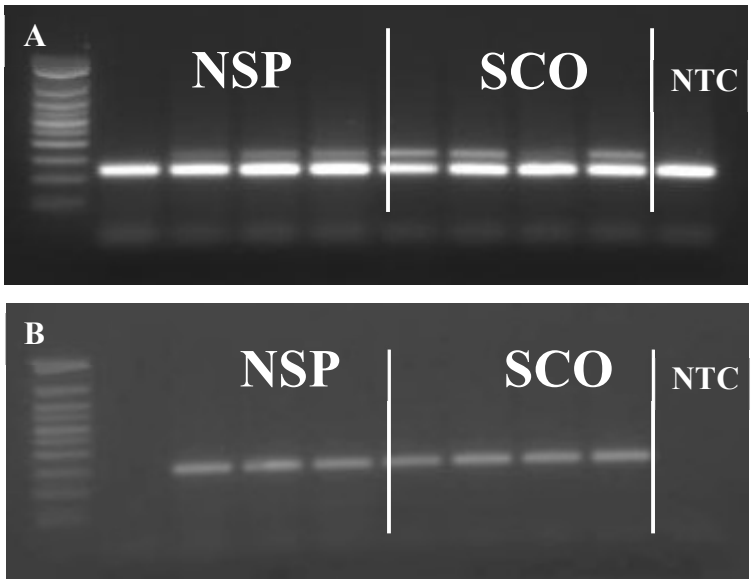

Figure 7: Qualitative RT-PCR using specific DCAF12 (A) and DCAF12L1 (B) primers in cryo-preserved testicular biopsies showing NSP and SCO. For RT-PCR, n = 8 samples revealing NSP and n = 8 samples showing SCO. PCR was run at 58°C for 40 cycles. This shows cDNA from cryo-preserved testis. NTC is the negative water control.

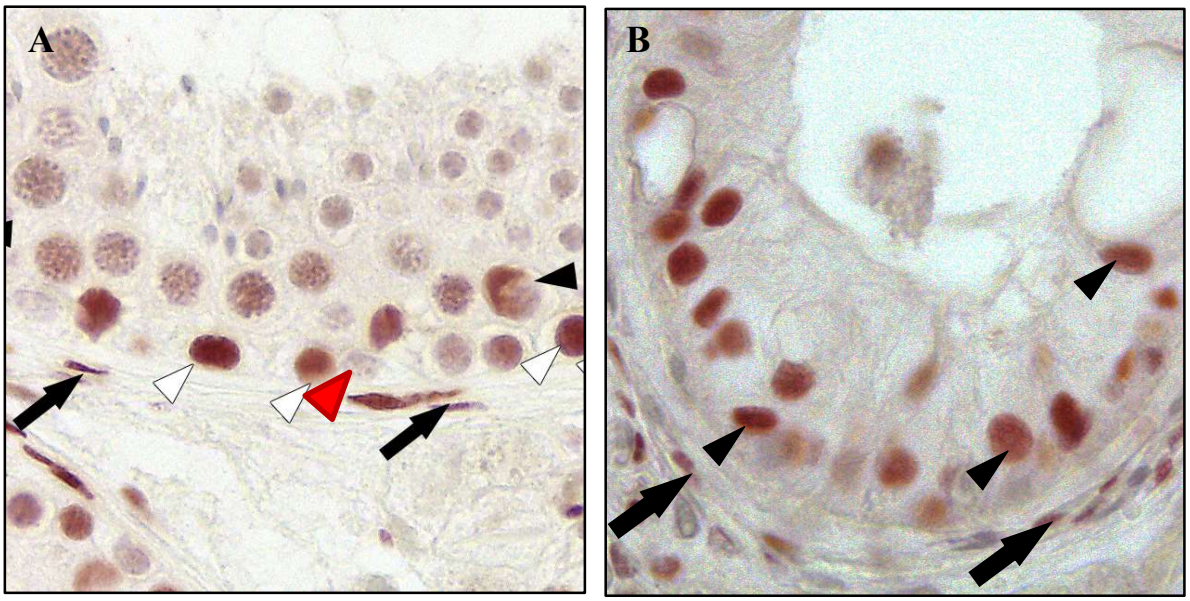

Figure 8: Human Zinc Finger RNA-binding protein 2 (ZFR2) immunohistochemical antibody staining in normal human spermatogenesis (NSP, A) and Sertoli cell only testis samples (SCO, B). A) In NSP, subtypes of spermatogonia (A_{pale} and B spermatogonia, black lined arrowhead), Sertoli cells (black arrowhead), and peritubular cells (black arrows) are strongly stained whereas staining was weaker in primary spermatocytes. Note absent staining in A_{dark} spermatogonia (red arrowheads). B) In SCO, Sertoli cell and peritubular cell nuclei are stained. AEC staining, primary magnification, x400.

Immunohistochemical ZFR2 antibody staining of human testis tissue with NSP (Fig 8A) and SCO (Fig 8B) confirmed the RNAseq data (outlined in Chapter 3), by demonstrating that ZFR2 protein was localised to both somatic and germline cells. With somatic cells, ZFR2 was localised in somatic Sertoli and peritubular cells, and in germline A_{pale} and B spermatogonia, until staining begins to fade in pachytene spermatocytes. In A_{dark} spermatogonia and spermatids staining was absent. This is also aligned with the RNAseq data.

2.4 Discussion

Our collaborators identified a list of 35 genes which were highlighted as potential fertility genes, utilising whole exome sequencing of infertile men. In order to investigate the role of these genes in male fertility, the orthologues of these genes were tested using *Drosophila* knockdown models. From these experiments, two fly genes of interest were discovered: *Zn72D*, with the patient orthologue *ZFR2*, and *DCAF12* with the patient orthologue *DCAF12L1*. The patients in which these mutations were found have been outlined in Table 4.

As mutations in both these genes were associated with azoospermia in all cases, it was expected that something similar would be seen in the *Drosophila*. In order to test specifically whether these two genes were required in somatic or germline testis cells, a *nos-Gal4* driver, which targets the spermatogonia and a *tj-Gal4* driver, which targets the cyst stem cells in the testis were employed for RNAi-induced knockdown. It is important to note however, that *tj-Gal4* is also expressed in neurons, which may explain why some of the RNAi lines tested with the *tj-Gal4* driver (*CG8839* and *CG42788*) resulted in lethality and could therefore not be used to examine adult male fertility (Figure 2B).

When *Zn72D* was knocked down in either the soma or the germline of the testis, the males were sterile. This was further verified by the histology of the seminal vesicle, which clearly showed an absence of sperm (Figure 5L). Interestingly however, there were sperm produced in the testis. While the proximal part of the testis, including the stem cell hub and early spermatids looked relatively normal, the distal end of the testis contained fewer late spermatids, compared to the control. The distal part of the control testis had an abundance of coiled spermatids, whereas the *Zn72D* knockdown had very few coiled sperm (Figure 4H and 5H). This is an indicator that *Zn72D* plays a vital role in male fertility, and therefore its orthologue, *ZFR2*, should be further examined in the human and in an appropriate mammalian model.

According to InterPro (IPR013087), both *ZFR2* and its homologue *ZFR* contain three zinc finger C_2H_2 transcription-factor domains and a DZF domain at the C-terminus. C_2H_2 domains are the most common type of transcription factor domain, and are characterised by their ability to bind to longer sequences of DNA and RNA (20-40bp), unlike other transcription factor domains, which tend to bind to much shorter sequences (Fedotova et al., 2017). To date, the role of the DZF domain is unknown.

The two major papers detailing the function of *Zn72D* suggest that this gene is involved in the process of RNA splicing within the Males Sex Lethal (MSL) complex (Worringer et al., 2009, Worringer and Panning, 2007). In *Drosophila* males, the MSL complex is responsible for dosage compensation on the single X chromosome, where it upregulates X-linked genes to equalise the production of X-linked gene products in males to the levels found in normal "XX" females. One of the genes which make up this complex, *maleless* (*mle*), was found to be dependent on *Zn72D* for mle production in its correctly spliced form. In the absence of *Zn72D*, *mle* levels are not sufficient to allow the MSL complex to localise to the X chromosome,

thereby preventing the dosage compensation processes from occurring (Worringer and Panning, 2007).

Zn72D has previously been implicated in *Drosophila* male fertility (Biwot et al., 2019). While Biwot et al. also found that knockdown of *Zn72D* with a *nos-Gal4* driver lead to male infertility, there were some differences and similarities between their findings and the results presented in this thesis.

One of the similarities between the Biwot et al. paper and the present thesis was the presence of scattered spermatid nuclei (Figure 3E and F from Biwot et al. (2019)) and Figure 4E-H from the present study). The Biwot et al. study also outlined the lack of actin cones, which was also found in the present study (Figure 4F). These actin cones are responsible for the individualisation of sperm bundles at the end of spermatogenesis. However, if the spermatid heads are not properly aligned earlier in spermiogenesis, the actin cones would not be able to form later in spermiogenesis. This suggests that *Zn72D* is playing a role earlier in spermatogenesis than when the actin cones are formed.

While Biwot et al. observed no sperm in the seminal vesicle, a low (non-zero) egg hatch rate was found, indicating that there must have been some sperm in the seminal vesicles during the reproductive lifespan of the *Zn72D* knockdown males. In contrast, while we also found no sperm in the seminal vesicles, the *Zn72D* knockdown males showed sterility in our fertility assay.

Furthermore, the *nos-Gal4>w*$^{-}$ flies from the Biwot et al. paper appeared to have a noticeably small seminal vesicle (Figure 3A from Biwot et al. (2019)), compared to the seminal vesicles

observed in the present thesis (Figure 5A-D). The histology in the present thesis is also more compelling, as it also shows the presence of sperm tails within the testis, thus providing more information regarding which part of spermatogenesis the germ cells stop maturing, in the absence of *Zn72D*.

As the *Zn72D* knockdown caused such a strong sterility phenotype in the fly, the function of the patient gene *ZFR2* was further analysed in a mammalian model. The generation and analysis of a *Zfr2*$^{-/-}$ mouse knockout line is described in Chapter 3.

At present, the exact function of *ZFR2* is unknown, although it has been linked to cervical cancer progression where higher expression was correlated with better survival compared to patients with lower expression (Zhang et al., 2018). *ZFR2* has also been shown to be differentially methylated in prostate tumour tissue between patients with more aggressive prostate cancer compared to those with less aggressive prostate cancer (Rubicz et al., 2019). Most interestingly however, is a descriptive study by (Norling et al., 2014), which outlines *ZFR2* mutations as a potential cause of Primary Ovarian Insufficiency (POI). This study used high-resolution array comparative genomic hybridization analysis to identify candidate POI-causing mutations. One particular patient had a deletion in chromosome 19, which affected six different genes (including *ZFR2*) associated with a complete lack of oocytes and follicles. Of those genes, all but *ZFR2* had previously been studied using mouse models or had been previously identified as having more severe mutations than only infertility. For this reason, it was concluded that *ZFR2* mutation may be causative of female primary ovarian insufficiency (Norling et al., 2014).

While there is little known in the literature on ZFR2, its mammalian paralogue, ZFR, has been studied in much greater detail. Zinc-finger proteins in general have long been known to play an important role in the regulation of development and growth (Klug and Rhodes, 1987). Specifically, ZFR has recently been implicated in pancreatic cancer (Zhao et al., 2016b), as it was found that expression was significantly higher in pancreatic tumours than in normal pancreatic tissue. Furthermore, knockdown of *ZFR* caused a significant reduction in viability of pancreatic cancer cells, through arrest of the cell cycle at G0/G1 phases (Zhao et al., 2016b). ZFR has also been implicated within a consanguineous family, potentially contributing to spastic paraplegia (Novarino et al., 2014).

The original discovery of ZFR was in a screen for RNA-binding proteins expressed during murine spermatogenesis (Meagher et al., 1999). This study found that ZFR was expressed most highly in pachytene spermatocyte nuclei during meiosis, where it associated with the chromosomes. Strong nuclear staining was also found in the Sertoli cells. As the paper outlines, this is significant, as after meiosis the conformation of the chromatin changes in order to allow tighter packaging of DNA into the sperm head through transition proteins and protamines. The lack of spermatozoa seen in the *ZFR2* mutant patient, the ZFR2 antibody staining (Figure 8), and the single-cell RNA sequencing data in Figure 6, strongly suggest that ZFR2 may be playing a similar role to that, previously discovered for ZFR i.e., in the packaging of DNA.

The other gene of interest from the *Drosophila* screen was *DCAF12*, with the patient orthologue, *DCAF12L1*. So far been 4 infertile patients have been identified with various missense and nonsense *DCAF12L1* mutations (Table 4). While knockdown of *DCAF12* in the fly testis somatic cells did not affect fertility (Figure 3B), knockdown in the germline cells resulted in a clear and significant reduction in fertility (Figure 3A). A *Dcaf12l1* knockout

mouse model was generated by the O'Bryan Lab, however the homozygous mutant mice were healthy and fertile (Unpublished data, Houston et al.).

While the infertility screen determined that *Drosophila DCAF12* germline knockdown caused severe sub-fertility, the histological analysis indicated that there were still sperm in the testis (Figures 4M-P) and the seminal vesicles (Figures 5I-L). However, while the size of the *DCAF12* seminal vesicle looked to be relatively similar to the w^{1118} control (Figure 5D), there appeared to be a slightly lower concentration of sperm, as the heads were not as distinct in the knockdown (Figure 5I) compared to the control (Figure 5A).

Both *DCAF12L1* and the highly similar *DCAF12* were shown to be expressed in both SCO and NSP patients (Figure 7). Furthermore, the single-cell RNA sequencing data indicates that relative expression of *Dcaf12l1* in the mouse was low in germ cells, and higher in the Sertoli cells (Figure 6A), while in the humans, expression was highest in the spermatogonia and in the Sertoli cells (Figure 6B). The most important motif in DCAF12L1 is a WD-40 domain, a short motif of approximately 40 amino acids, ending with a tryptophan-aspartic acid dipeptide (hence WD). These domains are usually involved in apoptosis or cell cycle control, with four to sixteen repeating units within the motif (Hwangbo et al., 2016). It has been suggested that its human paralogue, DCAF12 plays a role as a regulator of programmed cell death and apoptosis. When mutated, it enhanced tumour growth through the loss of neoplastic tumour suppressors and prevent the elimination of supernumerary cells through a wide range of pro-apoptotic pathways (Hwangbo et al., 2016).

A previous study (Ramasamy et al., 2014) has suggested *DCAF12L1* as a potential fertility gene. This study identified genes which were both hypermethylated in fibroblasts from non-

obstructive azoospermia patients, and highly expressed in the testis. *DCAF12L1* was outlined as one of these genes of interest. However, this study used fibroblasts isolated from testis biopsies, and found *DCAF12L1* was not expressed in fibroblasts, hence they did not study this gene any further. This finding, in conjunction with the results from the single cell RNA sequencing (Figure 6) and the RT-PCR (Figure 7) suggest that *DCAF12L1* remains a candidate gene of interest in studying fertility genes.

In summary, the purpose of this chapter was to screen a large number of genes which had been implicated in causing infertility in men. From the 10 genes initially screened, *Zn72D,* with the patient orthologue *ZFR2*; and *DCAF12,* with the patient orthologue *DCAF12L1* were found to cause infertility when knocked down in the fly testis. *ZFR2* was further analysed in a mouse model, outlined in Chapter 3. The data from human testis samples and single cell RNA sequencing data suggests that *ZFR2* is expressed early in spermatogenesis, particularly in meiosis. This also matches the purported role of ZFR2 in RNA binding. *DCAF12L1* was found to be expressed in both somatic and germline cells of the testis.

This chapter demonstrates the validity of using *Drosophila* as a model organism in screening a large number of genes implicated in male reproduction, in order to concentrate focus on a smaller number of genes.

2.5 References

BERGMANN, M. & KLIESCH, S. 2010. Testicular Biopsy and Histology. *In:* NIESCHLAG, E., BEHRE, H. M. & NIESCHLAG, S. (eds.) *Andrology: Male Reproductive Health and Dysfunction.* Berlin: Springer.

BIWOT, J. C., ZHANG, H. B., CHEN, M. Y. & WANG, Y. F. 2019. A new function of immunity-related gene Zn72D in male fertility of Drosophila melanogaster. *Arch Insect Biochem Physiol,* 102**,** e21612.

BONILLA, E. & XU, E. Y. 2008. Identification and characterization of novel mammalian spermatogenic genes conserved from fly to human. *Mol Hum Reprod,* 14**,** 137-42.

FEDOTOVA, A. A., BONCHUK, A. N., MOGLIA, V. A. & GEORGIEV, P. G. 2017. C2H2 Zinc Finger Proteins: The Largest but Poorly Explored Family of Higher Eukaryotic Transcription Factors. *Acta Naturae,* 9**,** 47-58.

HARDY, J. J., WYRWOLL, M. J., MCFADDEN, W., MALCHER, A., ROTTE, N., POLLOCK, N. C., MUNYOKI, S., VEROLI, M. V., HOUSTON, B. J., XAVIER, M. J., KASAK, L., PUNAB, M., LAAN, M., KLIESCH, S., SCHLEGEL, P., JAFFE, T., HWANG, K., VUKINA, J., BRIENO-ENRIQUEZ, M. A., ORWIG, K., YANOWITZ, J., BUSZCZAK, M., VELTMAN, J. A., OUD, M., NAGIRNAJA, L., OLSZEWSKA, M., O'BRYAN, M. K., CONRAD, D. F., KURPISZ, M., TUTTELMANN, F., YATSENKO, A. N. & CONSORTIUM, G. 2021. Variants in GCNA, X-linked germ-cell genome integrity gene, identified in men with primary spermatogenic failure. *Hum Genet,* 140**,** 1169-1182.

HU, Y., FLOCKHART, I., VINYAGAM, A., BERGWITZ, C., BERGER, D., PERRIMON, N. & MOHR, S. E. 2011a. An integrative approach to ortholog prediction for disease-focused and other functional studies. *BMC Bioinformatics,* 12**,** 1-16.

HU, Z., XIA, Y., GUO, X., DAI, J., LI, H., HU, H., JIANG, Y., LU, F., WU, Y., YANG, X., LI, H., YAO, B., LU, C., XIONG, C., LI, Z., GUI, Y., LIU, J., ZHOU, Z., SHEN, H., WANG, X. & SHA, J. 2011b. A genome-wide association study in Chinese men identifies three risk loci for non-obstructive azoospermia. *Nat Genet,* 44**,** 183.

JUNG, M., WELLS, D., RUSCH, J., AHMAD, S., MARCHINI, J., MYERS, S. R. & CONRAD, D. F. 2019. Unified single-cell analysis of testis gene regulation and pathology in five mouse strains. *Elife,* 8.

KLUG, A. & RHODES, D. 1987. Zinc Fingers: A Novel Protein Fold for Nucleic Acid Recognition. *Cold Spring Harbor Symposia on Quantitative Biology,* 52**,** 473-82.

MAHYARI, E., GUO, J., LIMA, A. C., LEWINSOHN, D. P., STENDAHL, A. M., VIGH-CONRAD, K. A., NIE, X., NAGIRNAJA, L., ROCKWEILER, N. B., CARRELL, D. T., HOTALING, J. M., ASTON, K. I. & CONRAD, D. F. 2021. Comparative single-cell analysis of biopsies clarifies pathogenic mechanisms in Klinefelter syndrome. *Am J Hum Genet,* 108**,** 1924-1945.

MEAGHER, M. J., SCHUMACHER, J. M., LEE, K., HOLDCRAFT, R. W., EDELHOFF, S., DISTECHE, C. & BRAUN, R. E. 1999. Identification of ZFR, an ancient and highly conserved murine chromosome-associated zinc finger protein. *Gene,* 228**,** 197-211.

NORLING, A., HIRSCHBERG, A. L., RODRIGUEZ-WALLBERG, K. A., IWARSSON, E., WEDELL, A. & BARBARO, M. 2014. Identification of a duplication within the GDF9 gene and novel candidate genes for primary ovarian insufficiency (POI) by a customized high-resolution array comparative genomic hybridization platform. *Human Reproduction,* 29**,** 1818-1827.

NOVARINO, G., FENSTERMAKE, A. G., ZAKI, M. S., HOFREE, M., SILHAVY, J. L., HEIBERG, A. D., ABDELLATEEF, M., ROSTI, B., SCOTT, E., MANSOUR, L., MASRI, A., KAYSERILI, H., AL-AAMA, J. Y., ABDEL-SALAM, G. M. H., KARMINEJAD, A., KARA, M., KARA, B., BOZORGMEHRI, B., VBEN-OMRAN, T., MOJAHEDI, F., EL DIN MAHMOUD, I. G., BOUSLAM, N., BOUHOUCHE, A., BENOMAR, A., HANEIN, S., RAYMOND, L., FORLANI, S., MASCARAO, M., SELIM, L., SEHATA, N., AL-ALLAWI, N., BINDU, P. S., AZAM, M.,

GUNEL, M., CAGLAYAN, A., BILGUVAR, K., TOLUN, A., ISSA, M. Y., SCHROTH, J., SPENCER, E. G., ROSTI, R. O., AKIZU, N., VAUX, K. K., A., J., KOH, A. A., MEGAHED, H., DURR, A., BRICE, A., STEVANIN, G., GRABRIEL, S. B., IDEKER, T. & GLEESON, J. G. 2014. Exome Sequencing Links Corticospinal Motor Neuron Disease to Common Neurodegenerative Disorders. *Science,* 343**,** 506-11.

OUD, M. S., VOLOZONOKA, L., SMITS, R. M., VISSERS, L., RAMOS, L. & VELTMAN, J. A. 2019. A systematic review and standardized clinical validity assessment of male infertility genes. *Hum Reprod,* 34**,** 932-941.

PANDEY, U. B. & NICHOLS, C. D. 2011. Human disease models in Drosophila melanogaster and the role of the fly in therapeutic drug discovery. *Pharmacol Rev,* 63**,** 411-36.

PLEUGER, C., FIETZ, D., HARTMANN, K., SCHUPPE, H. C., WEIDNER, W., KLIESCH, S., BAKER, M., O'BRYAN, M. K. & BERGMANN, M. 2017. Expression of ciliated bronchial epithelium 1 during human spermatogenesis. *Fertil Steril,* 108**,** 47-54.

RAMASAMY, R., RIDGEWAY, A., LIPSHULTZ, L. I. & LAMB, D. J. 2014. Integrative DNA methylation and gene expression analysis identifies discoidin domain receptor 1 association with idiopathic nonobstructive azoospermia. *Fertility and Sterility,* 102**,** 968-973.e3.

ROHMER, C., DAVID, J. R., MORETEAU, B. & JOLY, D. 2004. Heat induced male sterility in Drosophila melanogaster: adaptive genetic variations among geographic populations and role of the Y chromosome. *J Exp Biol,* 207**,** 2735-43.

RUBICZ, R., ZHAO, S., GEYBELS, M., WRIGHT, J. L., KOLB, S., KLOTZLE, B., BIBIKOVA, M., TROYER, D., LANCE, R., OSTRANDER, E. A., FENG, Z., FAN, J. B. & STANFORD, J. L. 2019. DNA methylation profiles in African American prostate cancer patients in relation to disease progression. *Genomics,* 111**,** 10-16.

SCHLEGEL, P. N., SIGMAN, M., COLLURA, B., DE JONGE, C. J., EISENBERG, M. L., LAMB, D. J., MULHALL, J. P., NIEDERBERGER, C., SANDLOW, J. I., SOKOL, R. Z., SPANDORFER, S. D., TANRIKUT, C., TREADWELL, J. R., ORISTAGLIO, J. T. & ZINI, A. 2021. Diagnosis and Treatment of Infertility in Men: AUA/ASRM Guideline Part I. *J Urol,* 205**,** 36-43.

SIDDALL, N. A. & HIME, G. R. 2017. A Drosophila toolkit for defining gene function in spermatogenesis. *Reproduction,* 153**,** R121-R132.

WHITE-COOPER, H. & BAUSEK, N. 2010. Evolution and spermatogenesis. *Philos Trans R Soc Lond B Biol Sci,* 365**,** 1465-80.

YU, J., WU, H., WEN, Y., LIU, Y., ZHOU, T., NI, B., LIN, Y., DONG, J., ZHOU, Z., HU, Z., GUO, X., SHA, J. & TONG, C. 2015. Identification of seven genes essential for male fertility through a genome-wide association study of non-obstructive azoospermia and RNA interference-mediated large-scale functional screening in Drosophila. *Hum Mol Genet,* 24**,** 1493-503.

ZHANG, L., JIANG, Y., LU, X., ZHAO, H., CHEN, C., WANG, Y., HU, W., ZHU, Y., YAN, H. & YAN, F. 2018. Genomic characterization of cervical cancer based on human papillomavirus status. *Gynecol Oncol*.

ZHAO, X., CHEN, M. & TAN, J. 2016. Knockdown of ZFR suppresses cell proliferation and invasion of human pancreatic cancer. *Biol Res,* 49**,** 1-8.

2.6 Supplementary Figures

Supp Table 1: Cordonbleu medium recipe for 15 L of food	
Water (Hot)	1062 mL
Potassium tartrate	108 g
Calcium Chloride	6.75 g
Agar	72 g
Yeast	162 g
Dextrose	720 g
Sugar (raw)	360 g
Bring to boil	
Water (cold)	2700 mL
Semolina	900 g
Bring to boil	
Water	1800 mL
Cool to ~60°C	
Nipagen	108 mL
Propionic Acid	54 mL
Makes ~18 trays of food	

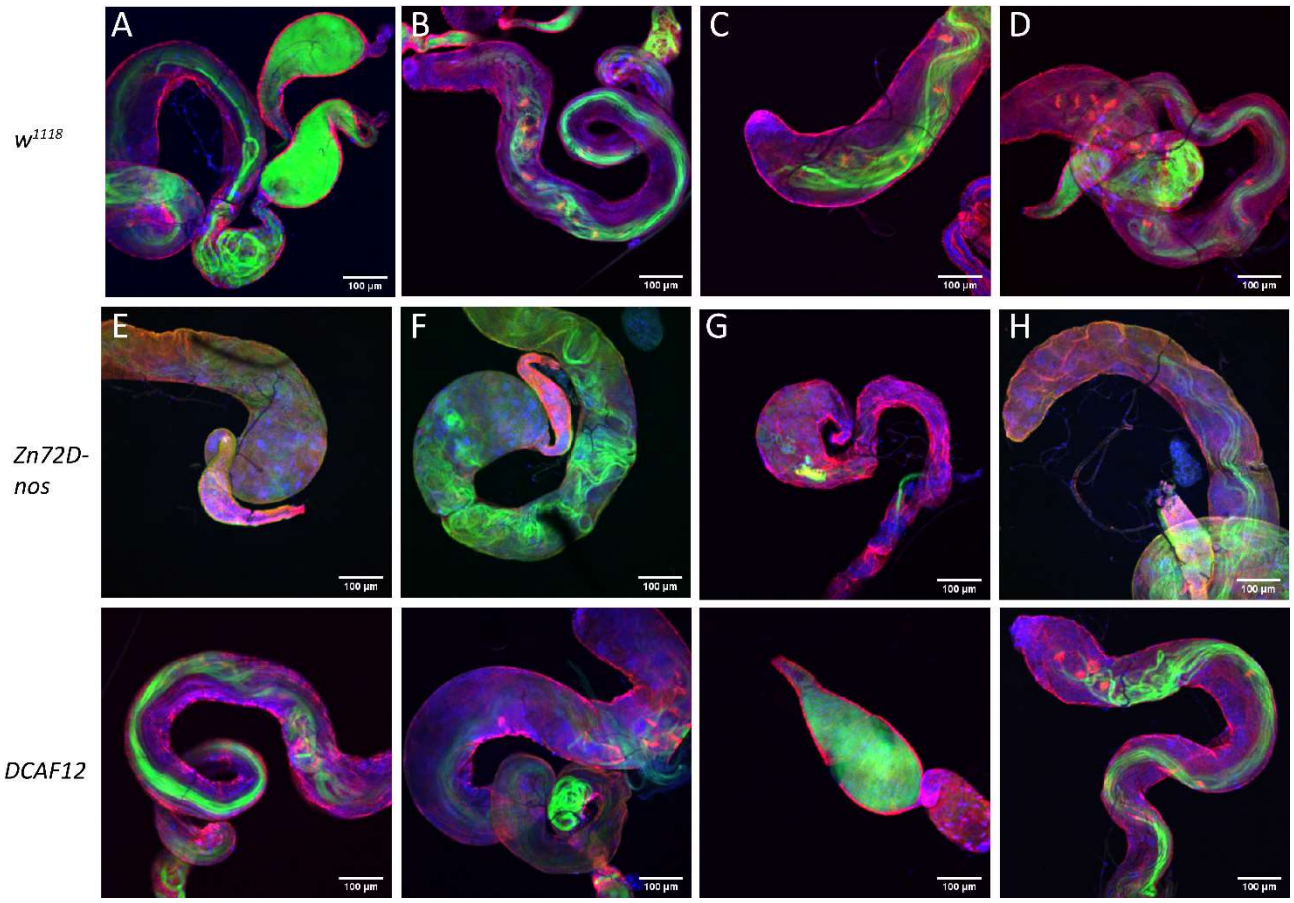

Supp Figure 1: Extra histology images for the *Drosophila* knockdown

Chapter 3: Zinc finger RNA-binding protein 2 (Zfr2) is not required for male fertility in the mouse

Paper submitted to Developmental Biology

Preamble

Chapter 2 of this thesis described the use of *Drosophila* to rapidly screen the fly orthologues of candidate human male fertility genes identified by our collaborators as being mutated in the exomes of infertile men. Ten such genes were analysed through the targeted knockdown in somatic and germline cells of the *Drosophila* testis, and two were found to be essential for male fly fertility; *Zn72D* (patient orthologue *ZFR2*) and *DCAF12* (patient orthologue *DCAF12L1*). These two genes were therefore considered excellent candidates for further knockout studies in the mouse. The *Dcaf12l1* knockout mouse was analysed by Dr Brendan Houston and found to be fertile and healthy. This chapter, currently submitted to Developmental Biology, outlines my detailed analysis of the *Zfr2*$^{-/-}$ knockout mouse, which was also found to be healthy and fertile.

Title: Zinc finger RNA binding protein 2 (ZFR2) is not required for male fertility in the mouse

Authors: Lachlan M Cauchi[1,2], Brendan J Houston[3,*], Liina Nagirnaja[4], Anne E O'Connor[3], D Jo Merriner[3], Kenneth I Aston[5], Peter N Schlegel[6], Don F Conrad[4], Richard Burke[1], Moira K O'Bryan[3]

Affiliations: 1) School of Biological Science, Monash University, Clayton, Australia. 2) Institute for Veterinary Anatomy, Histology and Embryology, Justus-Liebig University, Giessen, Germany. 3) The School of BioSciences and Bio21 Institute, The University of Melbourne, Parkville, Australia 4) Oregon National Primate Research Center, Oregon Health & Science University, Oregon, USA. 5) Andrology and IVF Laboratory, Division of Urology, Department of Surgery, University of Utah School of Medicine, Utah, USA. 6) Weill Cornell Medicine, Department of Urology, New York, USA.

*Correspondence: Brendan Houston, The School of BioSciences and Bio21 Institute, The University of Melbourne, Parkville, Australia. Email: brendan.houston@unimelb.edu.au

Funding information: This work was supported in part by Monash University and by Deutsche Forschungsgemeinschaft Grant GRK 1871 for the International Research Training Group "Molecular pathogenesis of male reproductive disorders" between Monash University (Clayton, VIC, Australia) and Justus Liebig University (Giessen, Germany) and by a National Health and Medical Research Council Australia, Grant (APP1120356) to MKOB, KIA and DFC.

Abstract

Background: Thousands of genes are expressed during spermatogenesis and male infertility has a strong genetic component. Within this study, we focus on the role of *Zfr2* in male fertility, a gene previously implicated in infertile men. To date, very little is known about the role of *ZFR2* in either humans or mice. To this end, the requirement for ZFR2 in male fertility was assessed using a knockout mouse model.

Results: *Zfr2* was found to be expressed in the testes of both humans and mice. Deletion of *Zfr2* was achieved via removal of exon 2 using CRISPR-Cas9 methods. The absence of *Zfr2* did not result in a reduction in any fertility parameters assessed. Knockout males were capable of fostering litter sizes equal to wild type males, and there were no effects of *Zfr2* knock out on sperm number or motility. We note *Zfr2* knockout females were also fertile.

Conclusions: The absence of *Zfr2* alone is not sufficient to cause a reduction in male fertility in mice.

Introduction

Male infertility is a complex disorder that effects approximately 7% of men in Western cultures (1). The complexity lies in the fact that it can be caused by both genetic and environmental factors, or a combination of both. It is estimated that approximately 20,000 genes are expressed in spermatogenesis (2) with thousands enriched in the testis, according to the Human Protein Atlas (3-5). This suggests that the genetic causes of infertility are likely to be common and diverse in their molecular origin. Male infertility has also been associated with increased morbidity and younger mortality, as it has been demonstrated that a decrease in sperm and semen quality is associated with younger mortality, and that the degree of impact scaled with semen compromise, with azoospermia being the most severe (6). This, and more recent research suggests semen quality, and male fertility are biomarkers of overall health (7). This relationship between the efficiency of spermatogenesis and overall health exemplifies the importance of deepening our understanding of the genetic causes of male fertility.

Here, we explore the function of an uncharacterised gene, zinc finger RNA-binding protein 2 (*Zfr2*), a candidate male infertility gene found in an infertile patient presenting with azoospermia (no sperm in the ejaculate (8). Very little has been published regarding *ZFR2*, and to our knowledge, its function has not been tested. *ZFR2* is expressed in the human adult testis and foetal brain, with little to no expression in other tissues (KIAA1086 (9)). *ZFR,* the paralogue of *ZFR2* has also been identified. Both genes contain three classical C_2H_2 type zinc finger domains (InterPro IPR013087). C_2H_2 domains are the most common regulatory protein in mammals, and most often bind to DNA, but have also been found to bind RNA and proteins (reviewed in Iuchi, 2001 (10)).

Within this study, we aimed to test the requirement of *Zfr2* expression for normal male fertility in mice. Knockout males were healthy and fertile, and loss of *Zfr2* had no effect on any male fertility parameters compared to wildtype males. Therefore, we can conclude that *Zfr2* activity is not an absolute requirement for male fertility in the mouse.

Experimental procedures

Analysis of RNA sequencing data

To explore the expression of *ZFR2* in human testes and *Zfr2* in mouse testes, RNA sequencing (RNA seq) data was sourced from Jung et al. (11) and Mahyari et al. (12) using R studio. Expression data are show for major germ cell types and Sertoli cells. Data are presented as normalised expression values.

Animal ethics

All animal experiments were completed following approval by the Monash University Animal Experimentation Ethics Committee (number BSCI/2017/31) and followed animal ethics guidelines stated by the Australian National Health and Medical Research Council (NHMRC)

Generation of the *Zfr2* knockout (*Zfr2*$^{-/-}$) mouse

Zfr2$^{-/-}$ mice were generated on a C57BL/6J background using CRISPR/Cas9 technology, through the Monash University Genome Modification Platform (a partner of the Australian Phenomics Network). Excision of exon 2 (895 bp deletion) of the canonical transcript (ENSMUST00000117798.8) was achieved via injection of zygotes with CRISPR reagents and CRISPR guide sequences (GCTCTGGGCTCCGCAACTGA**AGG** and GACTGCATTAGTGTTGCATG**GGG**) targeting regions flanking exon 2 (Figures 2A and B).

Zygotes were transferred to recipient females to generate mutant pups, the DNA of which were then Sanger sequenced to validate the genetic modification. This modification led to a premature stop codon in exon 3, which is expected to lead to nonsense-mediated decay (13). This genetic modification does not allow for any other transcripts (*Zfr2*-202-207) to return to in frame. In the case that *Zfr2*-201 is alternatively spliced following genetic modification, exons 2-9 would be spliced out, resulting in a truncated protein that does not contain any of the functional C2H2 domains (encoded by exons 4-8). This protein would be only ~45% of the full-length coding sequence.

Genotyping was performed using the following conditions: 94 °C for 2 min, 35 cycles of (94 °C for 20 sec, 56 °C for 20 sec and 72 °C for 15 sec), 72 °C for 5 min using the primers indicated in Table 1. *Zfr2*$^{+/-}$ mice were mated to generate knockout and wild type animals.

Table 1. Primer pairs used to genotype *Zfr2* knockouts and quantify *Zfr2* and *Zfr* expression

Genotype	**Forward Primer (5'-3')**	**Reverse Primer (5'-3')**		**Band size (bp)**
Wild type	ACCATCCCATGCAACAAGAT	CTAATGCAGTCCCTGGTGGT		186
Knockout	CCTGCCTAAGTAAGGGTCTGG	GGAGGTATCACCGTGGTAGG		230
qPCR	**Forward Primer (5'-3')**	**Reverse Primer (5'-3')**	**Target (exons)**	**Band size (bp)**
P1 – *Zfr2*	ACACTGTGCAGTTTACCCCC	CTATACCCCACCGCAACTCC	2	103
P2 – *Zfr2*	CACGGAGTGTCACCTACACC	CCATGCATTGTCTGCAGCTC	6+7	163
P3 – *Zfr2*	CCTCTGATGCGGGAAGATCC	GAGCCTGGAACCACTTAGCA	13-15	133
P4 – *Zfr*	GGGAAGATGCCAAAATGGCG	AGCTACTGGAGCCTGATGGA		164
P5 – *Zfr*	CGACCGGCAACTACTTTGGA	GCTACTGGAGCCTGATGGAC		145
Ppia	CAGTGCTCAGAGCTCGAAAGTTT	TCTCCTTCGAGCTGTTTGCA		66

Determining the fertility of the *Zfr2*$^{-/-}$ mice

Wild type (*Zfr2*$^{+/+}$) and *Zfr2*$^{-/-}$ knockout males were assessed for fertility status using the approaches previously outlined (14). Males were first mated at 10-12 weeks of age, and copulatory plugs were used as an indication of successful mating and reproductive behaviour. Litter sizes were recorded after each mating. In addition, we tested the fertility of males over an age range of 10-35 weeks via mating with adult wild type females aged 9-35 weeks. The two combinations assessed were wild type male x wild type female and *Zfr2*$^{-/-}$ male x wild type female. Collectively, we assessed 23 litters across 5 males for the wild type and 27 litters across 6 males for the *Zfr2*$^{-/-}$. We also tested the fertility of *Zfr2*$^{-/-}$ females by setting up mating pairs with wild type or knockout males.

Assessment of male fertility parameters

In order to assess the male reproductive tissues, mice were humanely killed by cervical dislocation. Whole body, testis and epididymis weights were recorded, and mice were analysed for any overt pathologies. Testes were either snap-frozen on dry ice and stored at -80 °C, or fixed in Bouin's fixative (Amber Scientific) for 5 hours. Epididymides were either fixed in 4% paraformaldehyde, or the cauda used to harvest sperm from 10-12 week old males via the backflushing method (15). Sperm were released into MT6 medium, and their motility was assessed using computer assisted sperm analysis (Hamilton-Thorne) as described in (16). To investigate sperm morphology, the remaining cells were pelleted at 500 x *g* for 5 mins, then resuspended in PBS, and dried onto SuperFrost slides.

Daily sperm production was calculated using the Triton-X-100 solubilization method as previously outlined (17). A minimum of 3 biological replicates per genotype were analysed per assay.

Quantifying *Zfr2* expression

Quantitative PCR (qPCR) was used to determine *Zfr2* expression levels in knockout and wild type mice. Snap frozen testes were thawed in TRIzol reagent (Thermo Fisher Scientific, Australia) under RNase-free conditions, RNA was isolated using methods previously outlined (18), converted to cDNA using SuperScript III (Thermo Fisher Scientific) and used for qPCR with SYBR Green qPCR master mix (Thermo Fisher Scientific) in a QuantStudio3 PCR machine (Thermo Fisher Scientific). Three PCR primer sets were designed to target different parts of *Zfr2* to assess mRNA stability (Table 1): targeting exon 2 (P1); targeting parts of exons 6 and 7 (P2); and targeting parts of exons 13 to 15 (P3). The P1 primer pair was used to determine the absence of exon 2 in the *Zfr2*$^{-/-}$ line. Primers were also designed for *Zfr* to investigate if gene compensation occurred. Expression of *Zfr2* was normalised to the housekeeper gene *Ppia*. All primers were assessed via PCR on wild type testis cDNA followed by gel electrophoresis to ensure only one band was present at the predicted size

Histological analysis

Fixed testes and epididymides were alcohol processed and embedded into paraffin wax using standard methods, and 5 µm sections were cut using a microtome. These sections were collected on SuperFrost slides and dried at 37 °C.

Testis and epididymal sections were dewaxed using standard procedures. Sperm dried to slides were rehydrated in PBS and then fixed in 10% neutral buffer formalin. Sperm and epididymal sections were each stained with haematoxylin and eosin. Testis sections were stained with

periodic acid-Schiff's reagent and haematoxylin. All slides were dehydrated and mounted under a glass coverslip with DPX (Sigma-Aldrich, USA). Sperm morphology and tissue histology were analysed via light microscopy, referring to the gold standard manual (19). Microscopy was performed using an Olympus BX-53 microscope equipped with an Olympus 392 DP80 camera (Olympus America, Center Valley, PA, USA).

Statistical Analysis

All statistical tests were performed using GraphPad Prism 9. Multiple t-tests (α=0.05) were used to compare wild type and *Zfr2*$^{-/-}$ data. A linear regression was used to compare the fertility of each genotype over time.

Results

Zfr2 loss-of-function does not cause male infertility

The *ZFR2* variant found in the infertile man was a premature stop mutation (Table 2), predicted to lead to a truncated protein product (<10% of total protein remaining) and likely inducing nonsense-mediated decay of *ZFR2* transcripts.

The infertile man was a 34-year-old of Kuwaiti descent, presenting with non-obstructive azoospermia. Maturation arrest was found in 100% of tubules. Intratubular germ cell neoplasia, now known as germ cell neoplasia *in situ*, peritubular fibrosis and inflammation were all absent. All assessed hormone levels were within normal ranges (8). The stop mutation was predicted to result in nonsense-mediated decay.

Table 2. *ZFR2* mutation in the patient					
Gene	Genomic position	cDNA position	Protein position	Genotype	Phenotype
ZFR2	g.Chr19: 3810840G>A	c.C2341T	p.R781X	homozygous	azoospermia

Single cell sequencing data has been used to show that *Zfr2* is expressed in the testes of both mice (11) and humans (12). In mice *Zfr2* expression is highest in pre-mitotic cells and spermatocytes, as well as Sertoli cells (Figure 1A). Similar expression was seen in the human testis, however the relative expression in the Sertoli and Leydig cells was lower (Figure 1B).

Given the predicted highly deleterious nature of this human mutation (Figure 2A and B), and the lack of knowledge around the function of ZFR2, we generated a knockout mouse to further investigate the role of *Zfr2* in male fertility.

To confirm the loss of *Zfr2* expression, *Zfr2*$^{-/-}$ and wild type testes were analysed using primers targeted to three different regions along the *Zfr2* transcript (Figure 2B). A significant reduction in *Zfr2* expression in the *Zfr2*$^{-/-}$ mice was seen with all 3 primer pairs, confirming that *Zfr2* was successfully removed in *Zfr2*$^{-/-}$ animals and no alternatively spliced sequences were present (Figure 3A). Expression of the *Zfr2* paralogue *Zfr* was not altered by the loss of *Zfr2* indicating that there is no compensatory upregulation of *Zfr* in the *Zfr2* knockout (Figure 3B).

Breeding experiments revealed *Zfr2*$^{-/-}$ males were fertile. No differences in litter size between wild type and *Zfr2*$^{-/-}$ males were revealed. To test for age-related effects of *Zfr2* deletion on male fertility, we assessed the fertility of *Zfr2* knockout and wild type males up to 6 months of age (Figure 4). We found no significant difference in the litter size between genotypes at any

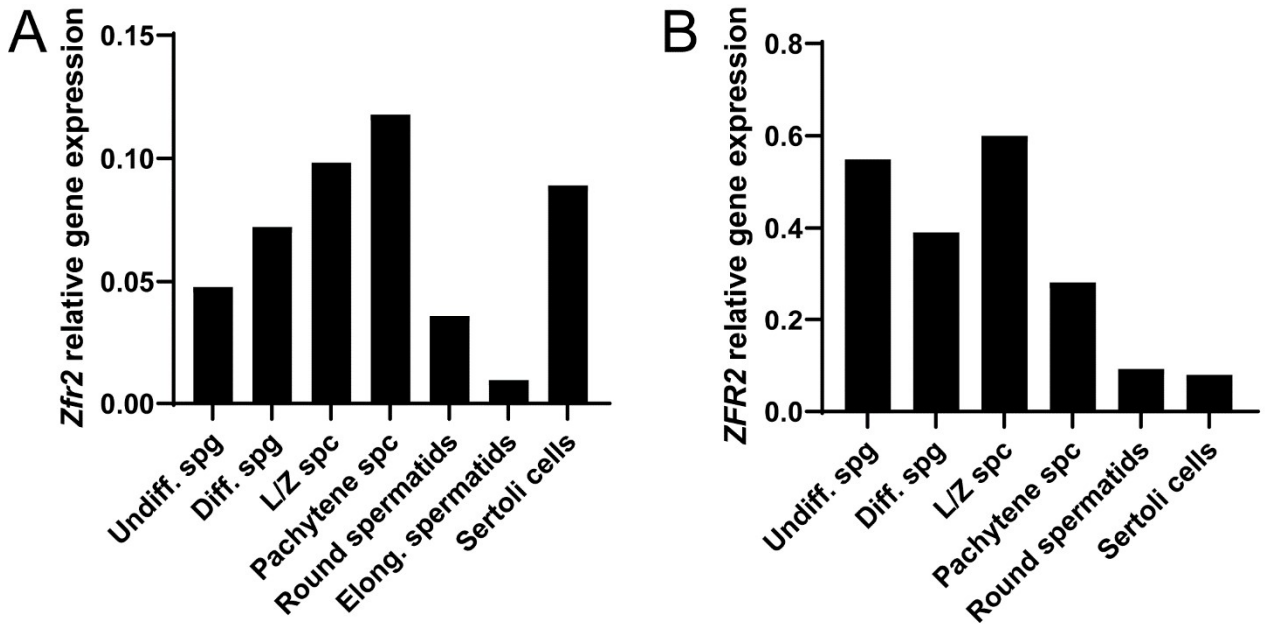

Figure 1. Relative *Zfr2*/*ZFR2* expression in male germ cells and Sertoli cells using single cell RNA sequencing in mice and men. **A)** In the mouse there is higher relative expression increases from undifferentiated (Undiff.) spermatogonia through differentiated (Diff.) spermatogonia, leptotene and zygotene spermatocytes, and pachytene spermatocytes. Expression decreases as cells enter spermiogenesis, with low expression in spermatids (round and elongating). High relative expression is seen in Sertoli cells. **B)** In men, high relative expression was found in spermatogonia, and leptotene/zygotene spermatocytes, with decreased relative expression in pachytene spermatocytes. Low expression was seen in round spermatids and Sertoli cells. Data extracted from Jung et al. (2019) [17] and Mahyari et al. (2021) [18].

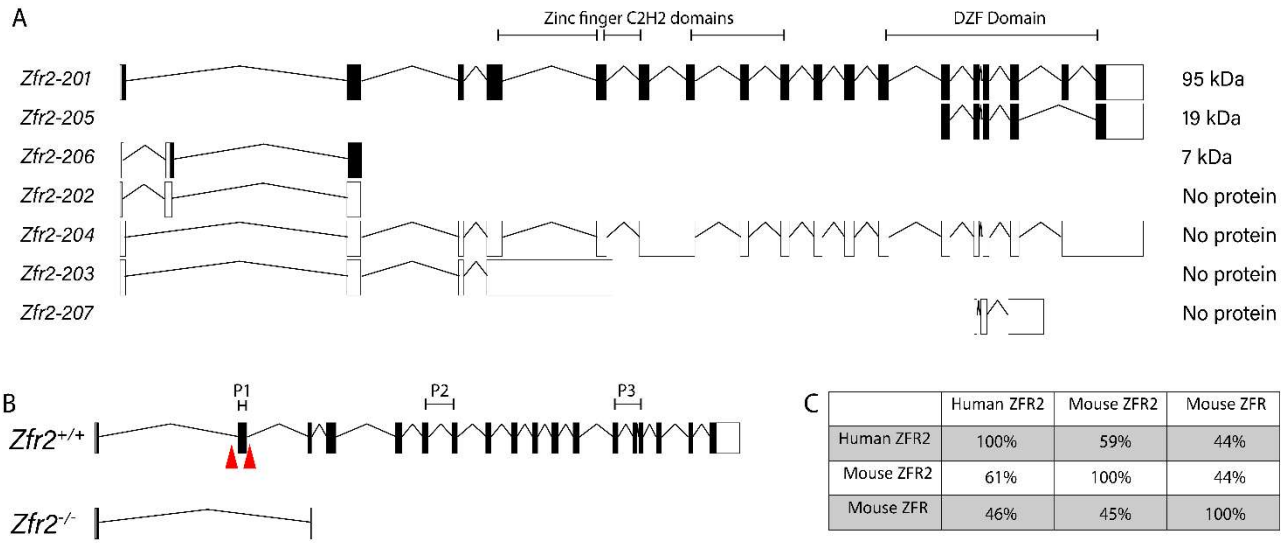

C

	Human ZFR2	Mouse ZFR2	Mouse ZFR
Human ZFR2	100%	59%	44%
Mouse ZFR2	61%	100%	44%
Mouse ZFR	46%	45%	100%

Figure 2. Generation of a *Zfr2* knockout mouse. A) Mouse *Zfr2* transcript variants as sourced from *Ensembl*: gene ENSMUSG00000034949.19. Black boxes indicate protein coding sequence (exons), white boxes indicate the untranslated regions. **B)** Comparison of *Zfr2* mRNA in wild-type ($Zfr2^{+/+}$) mice and the *Zfr2* knockout mutant ($Zfr2^{-/-}$). Red arrowheads indicate the predicted CRISPR/Cas9 cut sites, flanking exon 2. Location of the three *Zfr2* primer pairs (P1, P2, P3) used to quantify *Zfr2* transcript levels are indicated. **C)** Human *ZFR2*, Mouse *Zfr2* and Mouse *Zfr* protein identity comparison.

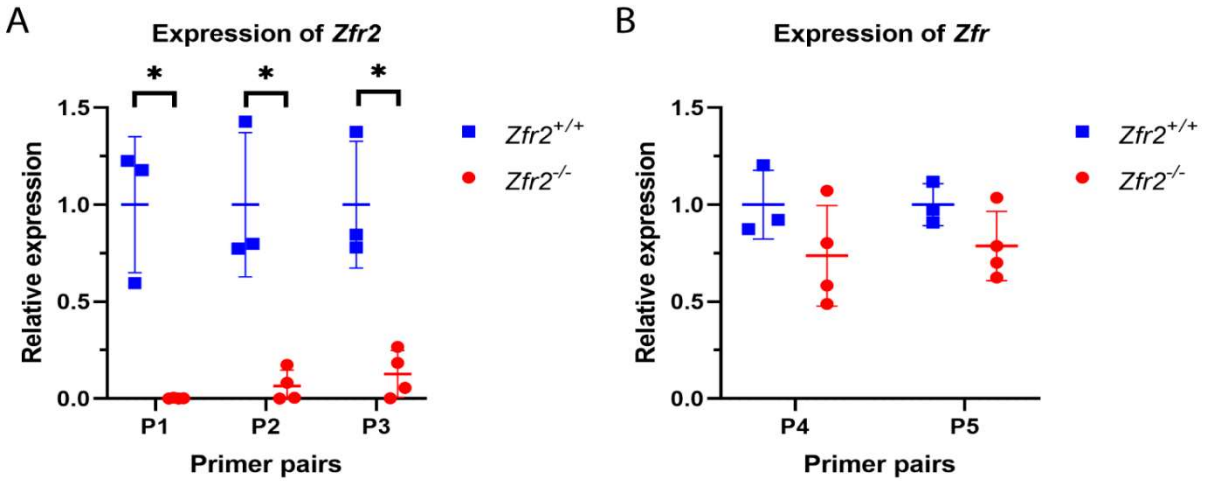

Figure 3. qPCR confirms ablation of Zfr2 gene in knockout testes. A) *Zfr2* transcript levels were assessed with primer pairs targeting three different sequences in *Zfr2* (P1, P2 and P3) using qPCR on cDNA from wild type (blue squares) and *Zfr2* knockout (red circles) testes. **B)** Comparison of *Zfr* expression (P4 and P5) between wild type and *Zfr2* knockout testes. * Indicates $p<0.05$

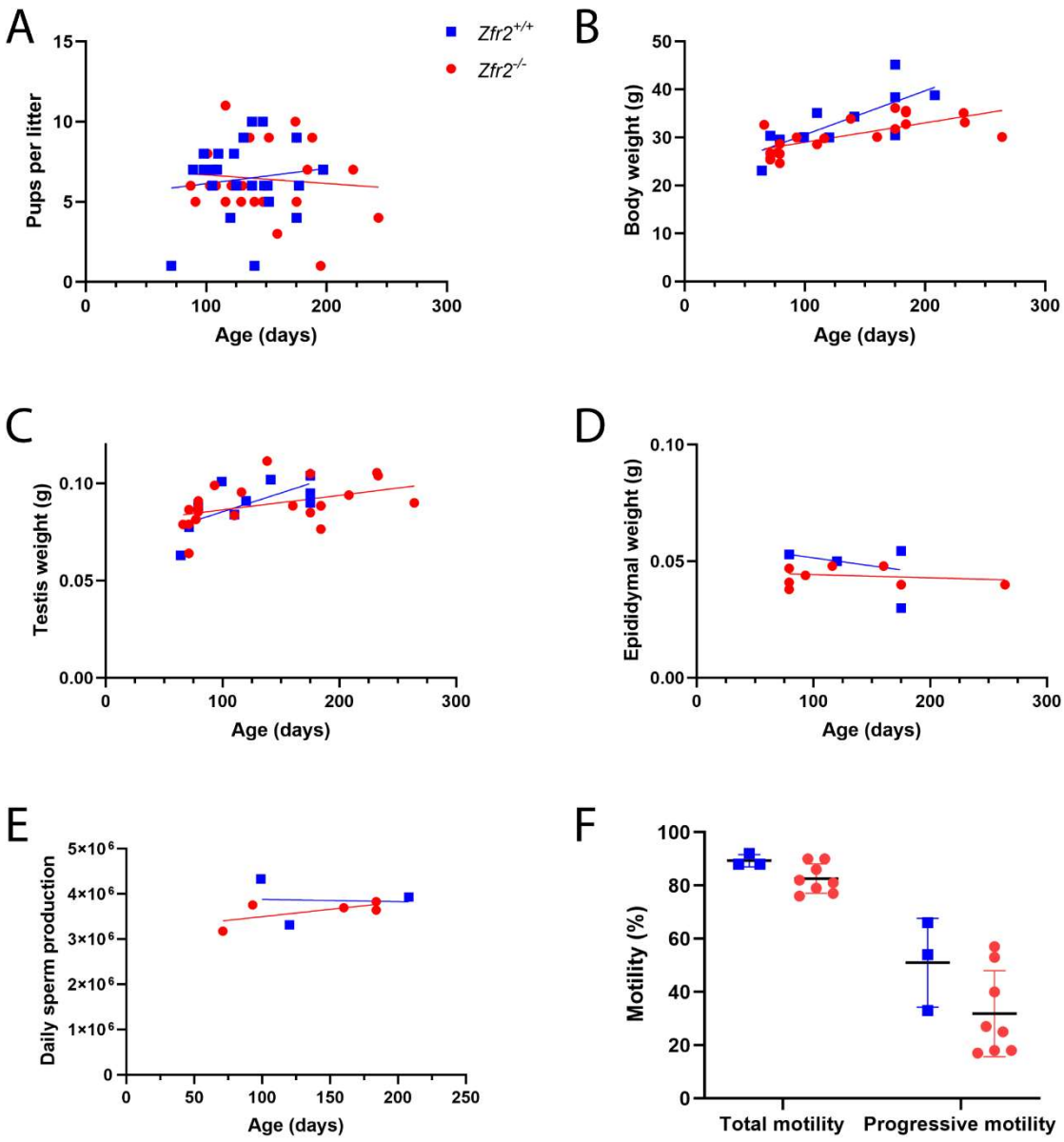

Figure 4. Fertility of *Zfr2* mice. Blue squares represent wild type (*Zfr2*$^{+/+}$) males, red circles represent *Zfr2* knockout (*Zfr2*$^{-/-}$) males. **A)** A linear regression of litter size as a function of male age. **B-D)** Body, testis and epididymal weight as a function of age, respectively; no significant change was found for any of these parameters. **E)** Daily sperm production as a function of male age. **F)** Sperm motility in 10 to 12 week-old males, assessed using computer assisted sperm analysis. Motility represents any twitching spermatozoa, while progressive motility denotes the percentage of sperm swimming in a forward motion.

age tested (Figure 4A). We also note that *Zfr2*$^{-/-}$ females were fertile and litters were generated with both wild type and *Zfr2*$^{-/-}$ males (not shown). Furthermore, as a function of age, *Zfr2*$^{-/-}$ males and wild type males had comparable body weights (Figure 4B), testis weights (Figure 4C) and epididymis weights (Figure 4D). There was no difference in daily sperm production between genotypes (Figure 4E), and sperm motility was comparable (Figure 4F). In accordance, there was no discernible difference in the histology of the testis or epididymis between genotypes, and the morphology of sperm from *Zfr2*$^{-/-}$ males was normal (Figure 5).

Discussion

To our knowledge, this is the first study to test the essential nature of *ZFR2* in any mammalian model. *ZFR2* was nominated as a high confidence human male infertility gene using whole exome sequencing of an infertile male (8). The data presented here clearly demonstrates that a loss of *Zfr2* in isolation does not compromise survival or male fertility in the mouse.

While the function of ZFR2 is unknown, previous studies have found that it may play a role in cervical (20) and prostate cancer (21), but not testicular cancer (22). Interestingly *Zfr2* mutation has also been identified as a candidate cause of primary ovarian insufficiency in women, however this has not been explored further and is also not supported by our findings in female mice (23).

The infertile man in which the *ZFR2* variant was discovered, presented with non-obstructive azoospermia, i.e., no sperm in the ejaculate, wherein the mutation was expected to cause a complete loss of gene function. The present study did not, however, replicate this phenotype using a mouse model. Reasons for this discrepancy include the presence of other, unknown damaging variants in the non-coding region of the patient, compensation for *Zfr2* by other

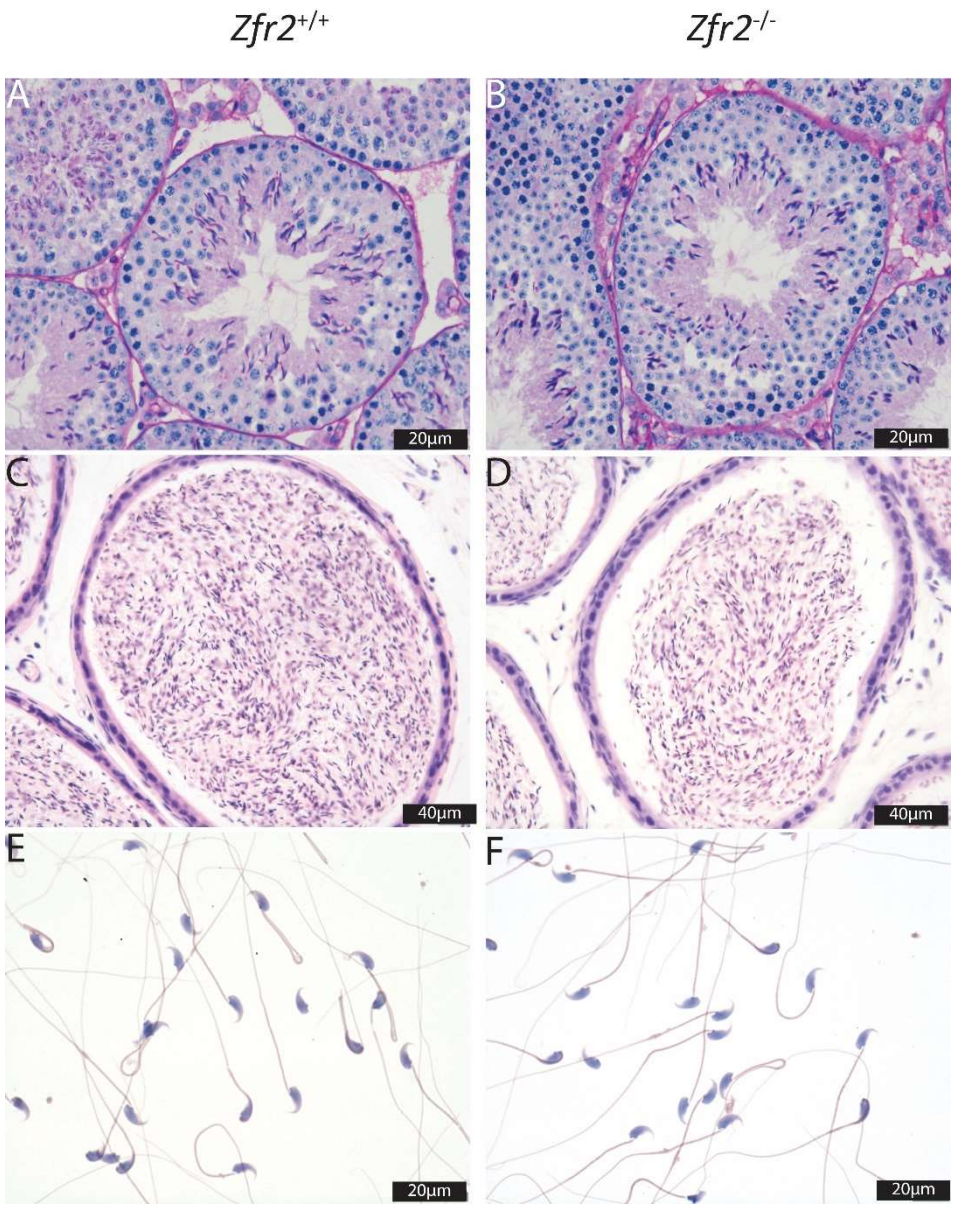

Figure 5. Testis, epididymis, and sperm histology of *Zfr2*$^{-/-}$ knockout mice. A+B) Testis sections were stained with periodic acid-Schiff reagents and hematoxylin. **C+D)** Epididymal sections were stained with hematoxylin and eosin, and were assessed for morphology and presence of sperm. Cauda epididymis sections are shown. **E+F)** Sperm were stained with hematoxylin and eosin. Scale is indicated on scale bars.

genes in the mouse that are not present in humans, the presence of a compounding loss-of-function variants in other male infertility genes, or the presence of genetic-environmental interactions. While the latter is not supported by the absence of an effect on fertility with increasing age, mice living in a high-barrier animal house, and humans are exposed to very different ranges of environmental factors. The identity of such interactions may become known as the uptake of exome and genome sequencing as a diagnostic for male infertility or whole life environmental exposures are documented more closely. Alternatively, ZFR2 may serve different functions in humans and mice. This hypothesis is not however supported by the 61% protein identity between human and mouse, and the conservation of expression pattern. In conclusion, *Zfr2* is not absolutely required for male fertility in mice.

Acknowledgements

The authors would like to acknowledge the Monash University Genome Modification Platform (a partner of the Australian Phenomics Network) for the design of the knockout strategy and generation of the mice. We thank Amy Luan for extracting the expression data for Figure 1.

Supplementary Tables

Supplementary Table 1. *Zfr2* transcripts targeted by the *Zfr2* primers	
Primer pair	**Targeted transcripts**
P1	*Zfr2-201, Zfr2-202, Zfr2-203, Zfr2-204, Zfr2-206*
P2	*Zfr2-201, Zfr2-204*
P3	*Zfr2-201, Zfr2-204, Zfr2-205, Zfr2-207*

References

1. Krausz C, Riera-Escamilla A. Genetics of male infertility. Nat Rev Urol. 2018.

2. Soumillon M, Necsulea A, Weier M, Brawand D, Zhang X, Gu H, et al. Cellular source and mechanisms of high transcriptome complexity in the mammalian testis. Cell Rep. 2013;3(6):2179-90.
3. Djureinovic D, Fagerberg L, Hallstrom D, A D, Lindskog C, Uhlen M, et al. The human testis-specific proteome defined by transcriptomics and antibody-based profiling. Mol Hum Reprod. 2014;20:476-88.
4. Fagerberg L, Hallstrom BM, Oksvold P, Kampf C, Djureinovic D, Odeberg J, et al. Analysis of the human tissue-specific expression by genome-wide integration of transcriptomics and antibody-based proteomics. Mol Cell Proteomics. 2014;13(2):397-406.
5. Uhlen M, Fagerberg L, Hallstrom BM, Lindskog C, Oksvold P, Mardinoglu A, et al. Proteomics. Tissue-based map of the human proteome. Science. 2015;347(6220):1260419.
6. Jensen TK, Jacobsen R, Christensen K, Nielsen NC, Bostofte E. Good semen quality and life expectancy: a cohort study of 43,277 men. Am J Epidemiol. 2009;170(5):559-65.
7. Choy JT, Eisenberg ML. Male infertility as a window to health. Fertil Steril. 2018;110(5):810-4.
8. Nagirnaja L, Lopes AM, Charng W-L, Miller B, Stakaitis R, et al. Diverse Monogenic Subforms of Human Spermatogenic Failure. Unpublished data.
9. Kikuno R, Nagase T, Ishikawa K, Hirosawa M, Miyajima N, Tanaka A, et al. Prediction of the coding sequences of unidentified human genes. XIV. The complete sequences of 100 new cDNA clones from brain which code for large proteins in vitro. DNA Res. 1999;6(3):197-205.
10. Iuchi S. Three classes of C2H2 zinc finger proteins. Cell Mol Life Sci. 2001(58):625-35.
11. Jung M, Wells D, Rusch J, Ahmad S, Marchini J, Myers SR, et al. Unified single-cell analysis of testis gene regulation and pathology in five mouse strains. Elife. 2019;8.
12. Mahyari E, Guo J, Lima AC, Lewinsohn DP, Stendahl AM, Vigh-Conrad KA, et al. Comparative single-cell analysis of biopsies clarifies pathogenic mechanisms in Klinefelter syndrome. Am J Hum Genet. 2021;108(10):1924-45.
13. Lindeboom RGH, Supek F, Lehner B. The rules and impact of nonsense-mediated mRNA decay in human cancers. Nat Genet. 2017;48(10):1112-18
14. Houston BJ, Conrad DF, O'Bryan MK. A framework for high-resolution phenotyping of candidate male infertility mutants: from human to mouse. Hum Genet. 2021;140(1):155-82.
15. Baker MA, Hetherington L, Weinberg A, Velkov T. Phosphopeptide analysis of rodent epididymal spermatozoa. J Vis Exp. 2014(94).
16. Gibbs GM, Orta G, Reddy T, Koppers AJ, Martinez-Lopez P, de la Vega-Beltran JL, et al. Cysteine-rich secretory protein 4 is an inhibitor of transient receptor potential M8 with a role in establishing sperm function. Proc Natl Acad Sci U S A. 2011;108(17):7034-9.
17. Dunleavy JEM, O'Connor AE, Okuda H, Merriner DJ, O'Bryan MK. KATNB1 is a master regulator of multiple katanin enzymes in male meiosis and haploid germ cell development. *Development*. Accepted 16th November 2021.
18. Houston BJ, Nagirnaja L, Merriner DJ, O'Connor AE, Okuda H, Omurtag K, et al. The Sertoli cell expressed gene secernin-1 (Scrn1) is dispensable for male fertility in the mouse. Dev Dyn. 2021;250(7):922-31.
19. Russell LD, Ettlin RA, Hikim APS, Clegg ED. Histological and Histopathological Evaluation of the testis. Clearwater, Florida: Cache River Press; 1990.
20. Zhang L, Jiang Y, Lu X, Zhao H, Chen C, Wang Y, et al. Genomic characterization of cervical cancer based on human papillomavirus status. Gynecol Oncol. 2018.

21. Rubicz R, Zhao S, Geybels M, Wright JL, Kolb S, Klotzle B, et al. DNA methylation profiles in African American prostate cancer patients in relation to disease progression. Genomics. 2019;111(1):10-6.
22. Chang Y, Wang X, Xu Y, Yang L, Qian Q, Ju S, et al. Comprehensive characterization of cancer-testis genes in testicular germ cell tumor. Cancer Med. 2019;8(7):3511-9.
23. Norling A, Hirschberg AL, Rodriguez-Wallberg KA, Iwarsson E, Wedell A, Barbaro M. Identification of a duplication within the GDF9 gene and novel candidate genes for primary ovarian insufficiency (POI) by a customized high-resolution array comparative genomic hybridization platform. Human Reproduction. 2014;29(8):1818-27.

Post-paper discussion

Chapters 2 and 3 investigated orthologues of one gene in three different organisms: *Zn72D* in the fly, *Zfr2* in the mouse and *ZFR2* in the human. While the infertile patient had a null mutation in *ZFR2,* and knockdown of *Zn72D* in either the somatic or germline cells of the *Drosophila* testis was sufficient to cause sterility, the knockout of *Zfr2* had no discernible impact on fertility in the mouse.

As humans and flies are more evolutionarily distant from each other than humans are from mice, it would be expected that a sterility phenotype seen in both human and flies would also be present in the mouse. However, this is not the case with *Zn72D*/*ZFR2.* There are a few reasons why this may be the case.

The initial reason discussed in the paper was that *Zn72D*/*ZFR2* is not a one-to-one orthologue. Mammals have two paralogous gene, *ZFR* and *ZFR2* which are both orthologous to *Drosophila Zn72D*. Partial overlap in function between human *ZFR* and *ZFR2* could lead to redundancy between these two genes, which would not be the case in the fly, which only has a single orthologue. Therefore, the sterility observed in the *Zn72D* knockdown fly would be analogous to a double knockout of both *ZFR* and *ZFR2* in a mammal. This is a caveat with using *Drosophila* to study human genes, especially in cases such as this where there is not such a distinct one-to-one gene orthologue, and can be a significant advantage in using a simple animal model. However, redundancy is unlikely to be the case here, given the initial patient only had a mutation in *ZFR2*, and not in *ZFR*. Furthermore, there was no observed compensation (by an increase in Zfr expression) in the knockout mouse. There is also the

distinct possibility that there are other compounding genetic variants in the patient which like *Zfr2,* are not sufficient to cause a reduction in fertility by themselves.

A more likely explanation for the anomaly seen here is that *ZFR2* is a supplementary paralogue to ZFR that is chiefly required in times when the external environment is not optimal. This is based on our understanding that environmental factors play a considerable role in the pathology of male infertility. The experimental mice are raised in a largely pathogen-free environment, with ad libitum food and water, and the absence of environmental contaminants. Hence, they are not exposed to the environmental and lifestyle conditions that humans are typically subject to, such as high/low temperatures, unhealthy diet (both scarcity and abundance, nutritional content), pollutants and other everyday stressors. It is possible that only under these imperfect conditions are certain genes (such as *Zfr2)* essential for spermatogenesis.

The apparent disconnect described in this thesis between the sterility caused by *Zn72D* and *DCAF12* knockdown in the fly testis, versus the infertility of the corresponding *Zfr2* and *Dcaf12l1* knockout mice does not mean that neither *Drosophila* nor mice are useful for studying fertility. As previously mentioned, finding multiple patients with identical infertility mutations requires extremely large cohorts. These animal models provide efficient albeit imperfect models for studying these genes. Our results do however exemplify the importance of studying disease genes in multiple model organisms, as has been done here.

Chapter 4: The role of zinc and zinc transport in male fertility

4.1 Introduction

Zinc plays a role in many important biological functions, ranging from cell signalling to enzymatic activity, growth regulation and general homeostasis (Levaot and Hershfinkel, 2018). It acts primarily as an important structural co-factor in numerous proteins but can also act as a signalling molecule in its own right. Disruption of zinc transport can contribute to a wide range of diseases and cellular responses, such as Alzheimer's, cancer, and inflammation (Kerns et al., 2018). Zinc is also thought to be important for male fertility. One of the most convincing examples of a role for zinc in male fertility is a large meta-analysis and systematic review by Zhao et al. (2016), which found that the zinc levels in seminal plasma of infertile males were significantly lower than in fertile counterparts. This study also found that subfertile men who took zinc supplements demonstrated increased fertility parameters, such as increased semen volume, and improved sperm morphology and motility (Zhao et al., 2016). Previous research has determined that copper tansport has also been shown to be important for fertility (Ghaffari et al., 2019).

Within this chapter, the role of zinc transport in male fertility was examined, using the fly as a model organism. Zinc is transported in and out of the cytosol via members of two main protein families. The mammalian Zrt-, Irt-like protein (ZIP) family, also called solute carrier 39 (SLC39) family, contains 10 members that are responsible for transport of zinc ions into the cytosol from outside the cell (import/uptake) or from the lumen of intracellular organelles, such as the endoplasmic reticulum and Golgi. Conversely, the Zinc Transporter (ZnT) family, which can also be called SLC30, contains 14 members that are responsible for zinc transport from the cytosol, to outside the cell (export/efflux), or into organelles (Lichten and Cousins, 2009). For the sake of clarity, this thesis will use the ZIP/ZnT nomenclature, rather than the also valid

SLC39/30 nomenclature. While showing considerable structural similarities, members of the ZIP and ZnT families diverge into subfamilies, in regards to transcription patterns, protein cellular localisation, and even ion specificity. Moreover, the ZnTs and ZIPs are widely and differentially expressed in different human tissues and organs (Yang et al., 2013).

Zinc may be playing a number of roles in fertility, as it is detected in a range of cells important for spermatogenesis, including Leydig cells, B spermatogonia, spermatocytes, spermatids and is also found in the epididymis (Croxford et al., 2011). Zinc is essential for the secretion of testosterone from Leydig cells, hence is an important regulator of spermatogenesis (Croxford et al., 2011). It has been shown that dietary zinc deficiency can lead to testicular atrophy including compromised spermatogenesis (Merker and Günther, 1997). It is however, established that the majority of seminal zinc is secreted from the prostate (Wong et al., 2001).

There is a large amount of information regarding the *Drosophila* ZnTs and ZIPs, yet to date only one of these has been associated with a distinct role in fertility. The ZIP *fear-of-intimacy* (*foi*), orthologue of human *ZIP6* and *ZIP10*, has been shown to be important for the morphogenesis of the embryonic gonad (Van Doren et al., 2003). *foi* has also been shown to be important in the development of myoblasts, by supplying zinc to key zinc finger transcription factors (Carrasco-Rando et al., 2016). *Zip42C.1, Zip42C.2* and *Zip89B* are closely related to human ZIP subfamily, containing *ZIP1, ZIP2* and *ZIP3*, and have all been shown to be involved in dietary zinc uptake in the *Drosophila* mid-gut (Richards et al., 2015, Qin et al., 2013). *Zip71B* has been found to be involved in zinc transport into the Malpighian tubes, the *Drosophila* equivalent of the kidney, and is downregulated by increased, toxic levels of cytosolic zinc (Yin et al., 2017).

The *Drosophila* ZnTs are responsible for zinc efflux from the cytosol and have also been well characterised. *ZnT63C* and *ZnT77C* were found to play a role in the *Drosophila* gut, acting as the zinc exporters to remove the zinc imported by *Zip42C.1, Zip42C.2* and *Zip89B* (Wang et al., 2009, Qin et al., 2013). *ZnT86D* has been shown to be highly expressed on the Golgi of the cell, responsible for export of zinc from the cytosol, into the Golgi (Dechen et al., 2015). To date, there is nothing known about *ZnT49B.*

Previous research in men has also found that several ZnTs and ZIPs are expressed along the human male reproductive tract, including on ejaculated sperm (Foresta et al., 2014). However, this study was limited by a narrow focus on only a few zinc transporters (*ZnT1* and *2*, and *ZIP1, 5, 6, 8* and *14*), without explanation as to why only these were chosen. The aim of this chapter was to characterise the testis function and expression of the fly zinc transporters and thus provide a basis for future research into the detailed roles of those found to be required for male fertility. Both overexpression and knockdown of each *Drosophila* ZnT and ZIP gene was investigated, providing an exhaustive analysis of the requirement for zinc transport, which has not been feasible in higher model organisms. Furthermore, as previous research has determined that dietary zinc is important in fertility (Zhao et al., 2016a), the effect of removing zinc from the *Drosophila* diet was also examined.

4.2 Experimental procedures

4.2.1 *Drosophila* stocks for fertility assays

35 UAS-RNAi or UAS-cDNA lines (Table 1) were crossed separately with either *tj-Gal4* or *nos-Gal4* transgenic lines to generate adult male flies with altered expression of each target gene in the somatic or germline cells respectively. For these infertility crosses, w^{1118} (BL3605, Bloomington stock Center) flies were used as wild-type controls, as well as for the source of

virgin females used to test the fertility of mutant males. The *nanos-Gal4/UAS-Gal4* (*nos-Gal4*) and *trafficjam-Gal4* (*tj-Gal4*) driver lines were donated by Gary Hime of University of Melbourne (Siddall and Hime, 2017). The *dj:GFP;nos-Gal4* and *tj-Gal4/dj:GFP* lines were generated in-house by Sebastian Judd-Mole. The 35 UAS-RNAi or UAS-cDNA lines were all previously generated and/or characterised by our research group (Dechen et al., 2015). The flies were kept on standard Cordonbleu medium (Table 2)

Table 1: *Drosophila* stocks used for the fertility screen (OE = overexpression, KD=knockdown)

Fly line	Function	Human orthologue
Dietary assay		
Red Dahomey	Wild-type control	
Fertility screen		
w^{1118}	Wild-type control	N/A
Tj-Gal4	Cyst cell driver	N/A
Nos-Gal4;UAS-Gal4	Germ cell driver	N/A
Tj-GAL4, gdj:GFP/CyO	Cyst cell driver & sperm tail maker (GFP)	N/A
gdj:GFP;nos-GAL4	Germ cell driver & sperm tail marker (GFP)	N/A
UAS lines		
17723_FLAG_51C	*ZnT63C* OE	*ZnT1* *ZnT10*
v2276 (3)	*ZnT63C* KD	
v105145	*ZnT63C* KD	
5130_eGFP_51C	*ZnT77C* OE	
v5390 (2)	*ZnT77C* KD	
31860-PB_FLAG_51C	*ZnT33D* OE	*ZnT2* *ZnT3* *ZnT4* *ZnT8*
v103398 (3)	*ZnT33D* KD	
3994_FLAG_96e	*ZnT35C* OE	
11163_FLAG_51C	*ZnT41F* OE	
v13311 (3)	*ZnT41F* KD	
6672_FLAG_51C	*ZnT86D* OE	*ZnT5* *ZnT6* *ZnT7*
6672_eGFP_51C	*ZnT86D* OE	
v107339	*ZnT86D* KD	
v4654	*ZnT49B* KD	*ZnT9*

Table 1: *Drosophila* stocks used for the fertility screen (OE = overexpression, KD=knockdown) cont…		
9428_FLAG_51C	*Zip42C.1* OE	*ZIP1* *ZIP2* *ZIP3*
v3986 (3) (ZIP 42C.1)	*Zip42C.1* KD	
9430_FLAG_51C	*Zip42C.2* OE	
v7338 (3)	*Zip42C.2* KD	
4334_FLAG_51C	*Zip88E* OE	
v106785 (dZIP 88E)	*Zip88E* KD	
dZIP_89B_FLAG_(2)_B	*Zip89B* OE	
6898_FLAG_51C	*Zip89B* OE	
v37358	*Zip89B* KD	
ZIP 71B FLAG	*Zip71B* OE	*ZIP5*
v44538	*Zip71B* KD	
6817_FLAG_51C	*fear-of-intimacy* OE	*ZIP6* *ZIP10*
v10102	*fear-of-intimacy* KD	
Catsup_FLAG_51C	*Catecholamines up* OE	*ZIP7*
V10095 RNAi	*Catecholamines up* KD	
2117_FLAG_51C	*Zip102B* OE	*ZIP9*
v51083 RNAi	*Zip102B* KD	
13189_STOP_FLAG_51C	*Zip48C* OE	*ZIP11*
v105650 FB	*Zip48C* KD	
7816_FLAG_51C	*Zip99C* OE	*ZIP13*
v1362	*Zip99C* KD	

4.2.2 Fertility screen of zinc overexpression and knockdown lines

Three candidate infertile males from each cross outlined in 4.2.1 were individually housed, each with three virgin w^{1118} females and allowed to mate for three days at 29°C. Subsequently, the females and their male were tipped into a fresh vial (and placed at 27°C) twice, each time being allowed to mate and lay eggs for three days. This change in temperature was due to previous research showing low incidence of non-specific sperm defects in flies raised at 29°C but not at 27°C (Rohmer et al., 2004).

At the end of the third mating period, all adults were removed. The number of offspring from each 3-day mating period were counted 7 days after the adults were removed from each vial. In order to obtain more statistically powerful data, the same experiment was repeated with 10 individually housed males, focussing on a smaller number of candidate lines which had shown signs of disrupted fertility in the initial screen of all 35 UAS lines. This included five knockdowns expressed in the germline, and six knockdowns expressed in the somatic cells of the testis. The males were considered infertile if no offspring were produced, and subfertile if there was a statistically significant reduction in the number of offspring produced, compared to control.

4.2.3 Histological analysis of *Drosophila* testes

After the mating assay, the reproductive tracts of infertile and subfertile lines were examined histologically. Testes were dissected from 3 to 5-day old flies in 1x PBS. The testes were fixed in 4% PFA for 30 mins at room temperature, then washed in 1x PBS. Testis nuclei were stained with 1 mg/mL DAPI and F-actin stained with 1:500 (final dilution) Alexa Fluor 555 phalloidin in PBS for 30 mins at room temperature in a dark chamber, then washed in 1x PBS. Testes

were mounted with Fluoromount-G mounting medium (Invitrogen, Thermofisher) on microscope slides with coverslips. Fluorescent images were taken using a Cell Voyager confocal microscope (CV1000, Yokogawa, Tokyo, Japan)

4.2.4 Human testis biopsy collection

Human testis biopsies were obtained (with written informed consent) from patients who presented with obstructive (OA) or non-obstructive azoospermia (NOA) at the Centre of Reproductive Medicine and Andrology of the University Hospital in Münster (Germany) and the Department of Urology and Andrology of the University Hospital in Giessen. Immediately following testicular biopsy, testicular tissue was fixed in Bouin's solution for approximately 24 hours and ultimately embedded in paraffin. 5-µm-thick sections were cut with a microtome and placed on a microscope slide, and stained with haematoxylin and eosin. Histological analysis including score count analysis was performed as outlined in Bergmann and Kliesch (2010). OA patients were defined as having intact spermatogenesis, with a score of 10 , denoting normal spermatogenesis (NSP) according to (Bergmann and Kliesch, 2010) whereas NOA patients used in this study showed a Sertoli Cell Only (SCO) epithelium defined by a complete loss of germ cells.

4.2.5 Quantifying *ZnT* and *ZIP* expression human testes

Total candidate gene mRNA levels were quantified by semi-quantitative RT-PCR as described previously (Pleuger et al., 2017), as below. The PCR primers used are outlined in Table 3. mRNA was extracted from Bouin's fixed and paraffin embedded testicular biopsies using the RNeasy FFPE Kit (Qiagen), which included a treatment with Proteinase K, which removed the formalin that can crosslink the DNA, increasing the yield. The extracted mRNA was purified

from remaining genomic DNA by incubating with 2 µL of 10 U/µL RNase-free DNase I (Peqlab Biotechnology), 1 µL RNase-free incubation buffer (500 mM, Roche), 0.25 µL RNase inhibitor (40 U/µL), per 6.65 µL of mRNA, for 25 mins at 37°C.

For cDNA synthesis, 9 µl of 200 ng/µL mRNA was mixed with 51 µl of RT-Mix (all components came from Applied Biosystems by ThermoFisher Scientific), including 6 µl of GeneAmp 10x PCR Gold Buffer, 6 µl of nucleotide mix (10mM), 3 µl of random hexamer primers (50 µM), 3 µl of RNase Inhibitor (20U/µl), 3 µl of MultiScribe Reverse Transcriptase (50 U/µl) and 18 µl of sterile distilled water.

1 µl of the generated cDNA was then mixed with 2.5 µl of GeneAmp 10x PCR Gold Buffer, 2 µl of $MgCl_2$ (25 mM), 1 µl of each of the forward and reverse primers (10 pmol/mL), 1 µl of nucleotide mix (10 mM each), 0.15 µl of AmpliTaq Gold polymerase, and 16.35 µl of sterile distilled water. Primers for *GAPDH, ZIP1, ZIP3, ZIP5, ZnT1 and ZnT9* were used. RT-PCR was undertaken under the following cycle conditions: 9 mins at 95°C, 38 x [45 secs at 94°C, 45 secs at 58°C, 45 secs 72°C] and 7 mins at 72°C. 4µl of GelGreen Nucleic Acid Stain

Table 3: Sequences of primers for RT-PCR and In situ hybridization

Gene	Ascension No.	Forward Primer (5'-3')	Reverse Primer (5'-3')	PCR Product length
ZIP1	NM_014437.5	TGGACCTGCTGCCTGACTAC	CAGCAGAGCCCTTGTTTCC	191bp
ZIP3	NM_213568.2	ACCGTAAGCGCCATGATCC	CCGCTCACCACTTGAGGAAG	247bp
ZIP5	NM_001135195.1	GAGGACCAGCAAAGACAAG	TCTGCCACACCTAAGAAGG	172bp
ZnT1	NM_021194.3	TGCCTCTTCCACCATCACAG	GTTTTCGGGTCTGCGGGG	240bp
ZnT9	NM_006345.4	TTGGGCATCAGTAAGTCTG	GGTTGAGGATGAAGCAATC	161bp
GAPDH	NM_002046.3	CCAGGTGGTCTCCTCTGACTTC	GTGGTCGTTGAGGGCAATG	81bp

(Biotium) were added to each PCR product, and the PCR product was size separated on a 1.5% agarose gel at 120 V for 65 mins, using a 50 base-pair ladder as a reference.

4.2.6 Probe design

DIG-labelled RNA probes for in situ hybridisation were generated as described previously (Pleuger et al., 2017) The RT-PCR product outlined in section 4.2.5 was ligated into pCR II TOPO vector (Invitrogen) and subsequently transformed into One Shot TOP 10 Chemically Competent *E. coli* (Invitrogen), followed by plasmid extraction using a QIAprep Spin Miniprep kit (Qiagen). The insertion of the PCR product was validated by double digest, using BamHI and NotI (New England Biolabs), and the sequence of the plasmid was validated by Sangar sequencing performed by Eurofins Genomic. These restriction enzymes were then used for the linearization of the plasmid DNA. For the *in vitro* transcription, RNA-DIG labelling Mix (Boehringer Mannheim) and RNA polymerase T7 and SP6 (Promega) were used according to manufacturer's instructions.

The in situ hybridization was performed using methods previously defined by our lab (Fietz et al., 2016), with the following variations. The tissue sections were incubated with Proteinase K (10 μg/mL) in sterile DEPC-treated autoclaved water for 15 minutes at 37°C. Digestion was stopped by incubation in 0.2% glycine solution (in PBS-$MgCl_2$) for 5 minutes at room temperature. The sections were then post-fixed in 4% paraformaldehyde for 10 minutes, incubated in 0.25% acetic acid in 10 nM triethanolamine solution for 10 minutes, and prehybridized in 20% glycerol solution in DEPC-treated water for 1 hour.

Each probe was used at a dilution of 1:50. Therefore, 4 mL of sense or antisense RNA was mixed with 4 μL of yeast RNA and 2 μL of salmon sperm (both Sigma-Aldrich). 10 μL of probe mix was added to 190 mL of hybridization buffer consisting of 20 μL of 20x standard saline citrate, 40 μL of dextran sulfate, 4 μL of Denhardt's reagent, 100 μL of deionized formamide, and 26 μL of DEPC water. Hybridization was performed at 44°C overnight in a humidified chamber containing 50% formamide in 2x SSC.

For post-hybridization, the sections were washed as outlined: 2x 15 minutes in 2x SSC at room temperature, 4x 15 minutes in 2x SSC at 54°C, 2x 30 minutes in 0.2x SSC at 54°C, 5 minutes in 2x SSC at room temperature, and 10 minutes in 1x TNMT (Tris, NaCl, MgCl, and Tween 20) at room temperature. To prepare for immunohistochemical detection, the sections were incubated for 1 hour in 3% bovine serum albumin (BSA; Roth) in 1x TNMT. The digoxigenin (DIG)-labelled probes were detected using a DIG-Fab antibody (Roche) at a dilution of 1:1000 in 1x TNMT and 3% BSA at 4°C overnight in a dark humid chamber. Staining was visualized using a ready-to-use 5-bromo-4-chloro-3-indolyl phosphate/nitro-blue tetrazolium chloride (BCIP/NBT) solution (Amresco).

4.2.7 *Drosophila* stocks for zinc dietary dropout assay

The Red Dahomey outbred population of *Drosophila* (Mair et al., 2005) was used for the dietary dropout assay. This line is more robust than the standard w^{1118} line used in genetic assays, and previous experiments using this diet have used an outbred population.

4.2.8 Holidic media

A holidic media was used (previously defined by Piper et al. (2014)). This is a chemically defined diet which has been optimised for lifespan and fertility and can be easily manipulated to remove individual metals, amino acids, etc. The 100N diet is used as a control, and is named such due to having 100 mM of nitrogen. 1 mL of $CuSO_4$ and $ZnSO_4$ solution were each omitted from the "100N-Cu" and "100N-Zn" respectively, and replaced with 1 mL of distilled water. Copper was used as a positive control, as Steiger et al. (2010) had previously determined that copper transport was important in fertility.

4.2.9 Collection of males and virgins

Standard density rearing was used to synchronise adult emergence and control for larval rearing density. Flies were left in embryo collection cages on apple juice agar (275mL water, 12.5 g agar, 150 mL apple juice, 10.5 mL Nipagen) at 25°C. 250 eggs were then distributed into a bottle containing standard sugar-yeast (SY) medium, consisting of 50 g of sugar, 100 g of yeast and 10 g of agar per L. All adult males and virgin females were collected and housed on SY media for 48 hours. Ten males per diet were each put on one of the three diets (100N, 100N-Cu and 100N-Zn) for 48 hours.

4.2.10 Zinc and copper dropout diet mating with recovery (4-day cycle)

At the start of the assay, each male was placed with ten virgin females and allowed to mate for 24 hours at 25°C. Previous unpublished work from the lab suggested that a male is capable of mating up to 10 females in this time. The males were tipped into fresh, individual vials containing the experimental diet (100N, 100N-Cu or 100N-Zn) and allowed to "recover" for 3 days. After the 3 days, the males were given virgin females and again allowed to mate for 24

hours at 25°C. This was repeated 7 times until the males were approximately 30 days old, at which point they were discarded, as the males would no longer mate efficiently past this age. The mated females were each individually housed (1 female per vial) on standard SY medium for 7 days. At this point, the proportion of females fertilised by each male, as well as the total number of offspring (recorded as the number of pupal cases) per male were recorded.

4.2.11 Zinc and copper dropout diet sperm depletion assay (1-day cycle)

The approach from section 4.2.10, was repeated, with the following adjustments. Rather than allowing the males 3 days to "recover" after each mating period, they were immediately given 10 fresh virgin females, with the aim to completely deplete their sperm levels. This was repeated for 7 rounds until the males were approximately 12 days old. Females were separated as previously detailed, and the number of offspring were recorded as described above.

4.2.12 Statistical Analysis

GraphPad Prism 7 was used for statistical analysis, and to generate all graphs. For the genetic fertility screen, an ordinary one-way ANOVA to compare to the w^{1118} control by a Dunnett's multiple comparison test was used to analyse the significance of the decrease in the number of offspring. An ordinary one-way ANOVA was also used to compare the mean number of offspring, and proportion of females fertilised, of males the experimental diets (100N-Cu and 100N-Zn) to the control diet (100N).

4.3 Results

4.3.1 Altering zinc transporter expression can cause infertility

In order to examine the effect of knockdown and over-expression of *Drosophila ZIP* and *ZnT* genes on male fly fertility, fly strains containing either a UAS-RNAi (knockdown) and UAS-cDNA (overexpression) transgene were mated with strains with trafficjam(tj)-Gal4 (somatic cells of the testis) and nanos(nos)-Gal4 (germline cells of the testis) drivers. These crosses generated adult males which expressed individual transgenes in their germline or somatic testicular cells, and therefore, had altered zinc transporter expression in these specific cell populations. These adult males (3 per genotype) were mated to three control w^{1118} females, and the number of offspring produced was assessed, by counting the number of resultant pupae (Figure 1). Each bar represents the average number of offspring produced from a single male the three 3-day matings, with 3 w^{1118} virgin females, using w^{1118} males as a control.

When expressed in the germline, only *ZnT86D* over-expression resulted in a significant reduction in fertility while overexpression of *Zip42C.1* and *Zip71B* as well as knockdown of *Zip42C.2* and *Zip71B* all caused a noticeable, albeit non-significant subfertility (Figure 1A). In the somatic cells, knockdown of *catecholamines up (catsup)* and overexpression of *Zip89B* and *Zip71B* resulted in sterility, whereas knockdown of *foi* and *ZnT49B*, as well as the overexpression of *ZnT63C* resulted subfertility (Figure1B). The overexpression of *Zip42C.2, ZnT77C* and *ZnT86D* were also further analysed as they showed a non-significant reduction in fertility (Figure 1B).

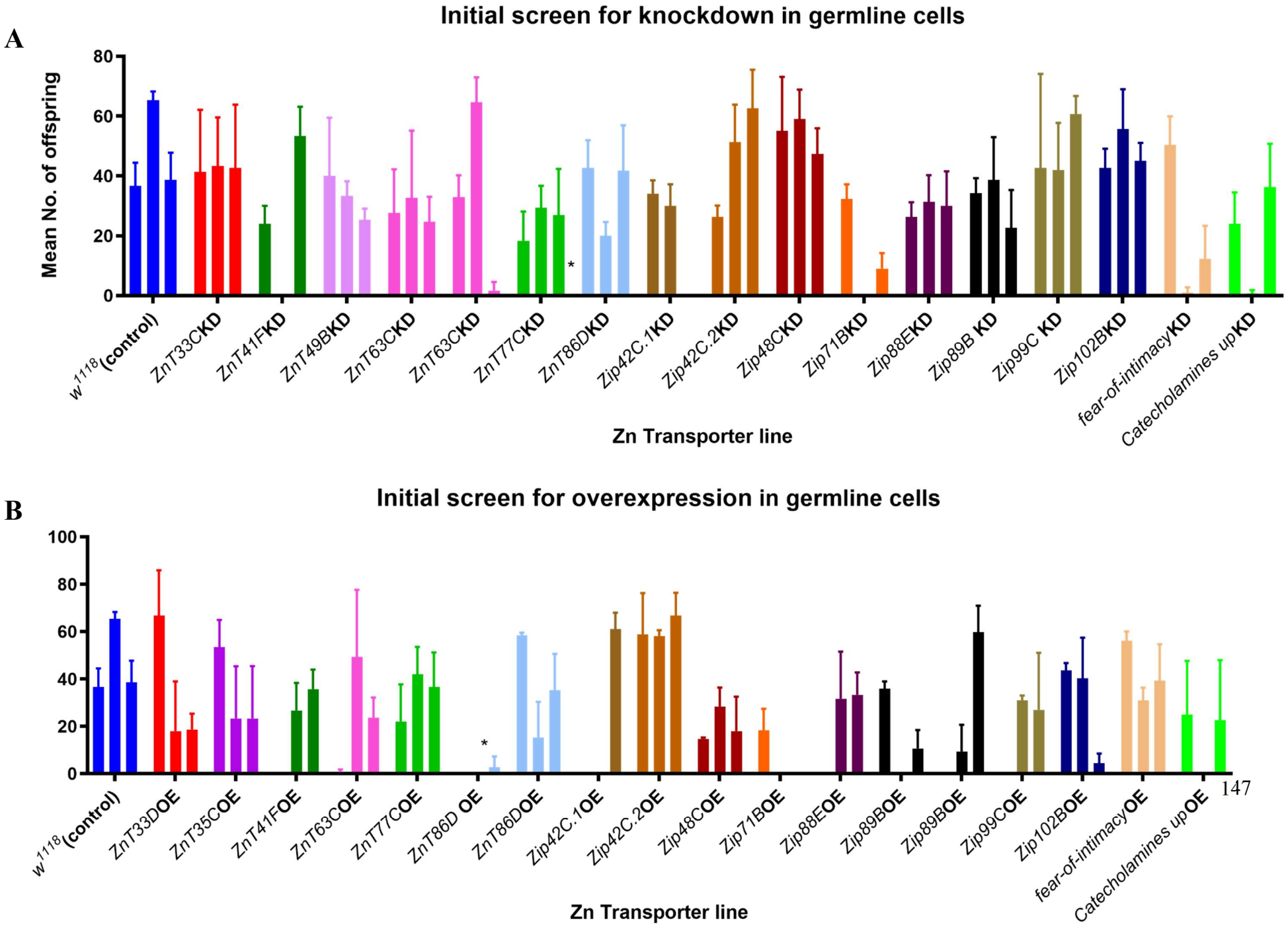
A
Initial screen for knockdown in germline cells
Mean No. of offspring
80
60
40
20
0
*
w1118(control)
ZnT33CKD
ZnT41FKD
ZnT49BKD
ZnT63CKD
ZnT63CKD
ZnT77CKD
ZnT86DKD
Zip42C.1KD
Zip42C.2KD
Zip48CKD
Zip71BKD
Zip88EKD
Zip89B KD
Zip99C KD
Zip102BKD
fear-of-intimacyKD
Catecholamines upKD
Zn Transporter line
B
Initial screen for overexpression in germline cells
100
80
60
40
20
0
*
w1118(control)
ZnT33DOE
ZnT35COE
ZnT41FOE
ZnT63COE
ZnT77COE
ZnT86D OE
ZnT86DOE
Zip42C.1OE
Zip42C.2OE
Zip48COE
Zip71BOE
Zip88EOE
Zip89BOE
Zip89BOE
Zip99COE
Zip102BOE
fear-of-intimacyOE
Catecholamines upOE
Zn Transporter line

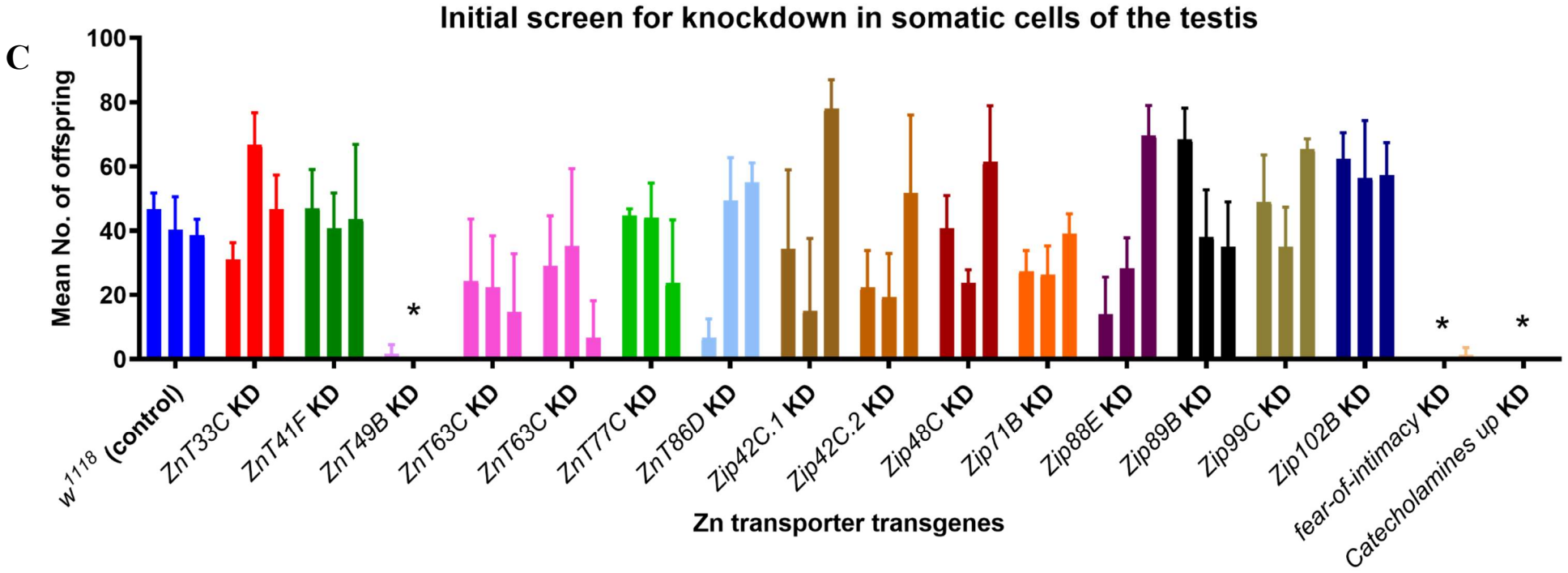
C
Initial screen for knockdown in somatic cells of the testis
Mean No. of offspring
100
80
60
40
20
0
*
*
*
w1118 (control)
ZnT33C KD
ZnT41F KD
ZnT49B KD
ZnT63C KD
ZnT63C KD
ZnT77C KD
ZnT86D KD
Zip42C.1 KD
Zip42C.2 KD
Zip48C KD
Zip71B KD
Zip88E KD
Zip89B KD
Zip99C KD
Zip102B KD
fear-of-intimacy KD
Catecholamines up KD
Zn transporter transgenes

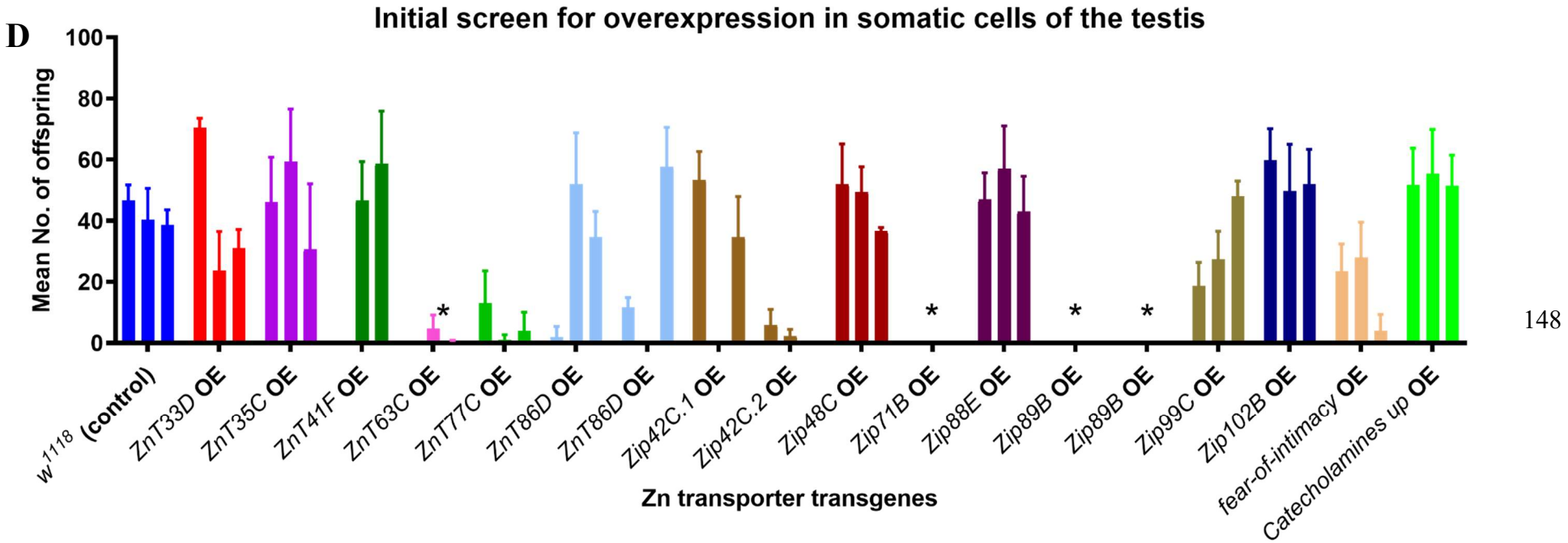
D
Initial screen for overexpression in somatic cells of the testis
Mean No. of offspring
100
80
60
40
20
0
*
*
*
*
*
w1118 (control)
ZnT33D OE
ZnT35C OE
ZnT41F OE
ZnT63C OE
ZnT77C OE
ZnT86D OE
ZnT86D OE
Zip42C.1 OE
Zip42C.2 OE
Zip48C OE
Zip71B OE
Zip88E OE
Zip89B OE
Zip89B OE
Zip99C OE
Zip102B OE
fear-of-intimacy OE
Catecholamines up OE
Zn transporter transgenes

Figure 1: Initial screen for the knockdown (KD) (A and C) or over-expression (OE) (B and D) of fertility candidate zinc transport genes in the *Drosophila* testis. The candidate infertility genes from the zinc transport screen were manipulated in the germline cells of the testis, using a *nanos*-Gal4 **(A and B)** driver and in the somatic cells of the testis, using *trafficjam*-Gal4 **(C and D).** Each bar shows the average number of offspring, resulting from a cross with three transgenic males, each with 3 w^{1118} females, over three 3-day mating periods. Error bars indicate the standard deviation for each set of 3 males. To generate the statistic, a One-Way ANOVA, with a Dunnett's Multiple comparisons test to the w^{1118} control was used. (*=$p<0.05$, ZnT = Zinc Transporter, Zip = Zrt-, Irt-like protein, OE = overexpression, KD = RNAi knockdown)

The initial fertility assay, while providing some significant results, was found to be not sensitive enough to detect subfertility effectively, hence several of the experimental lines were repeated, using 10 single-male replicates, rather than the original 3 replicates (Figure 2). In the germline, the overexpression of *Zip71B* caused sterility (Figure 2A). In the somatic cells, knockdown of *Zip42C.1* and *fear-of-intimacy*, as well as overexpression of *Zip89B* all resulted in sterility, while the overexpression of *Zip42C.2* and *Zip71B* and knockdown of *ZnT49B* KD resulted in subfertility.

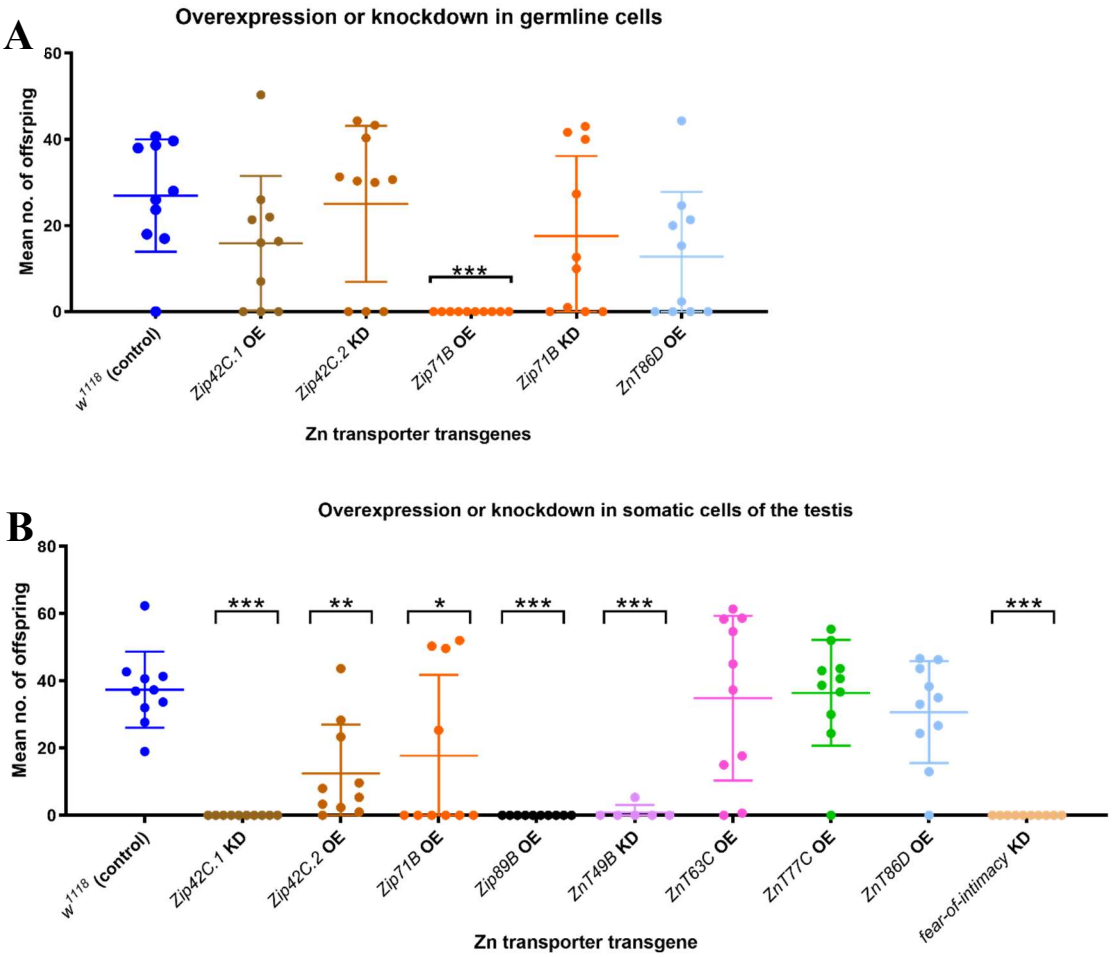

Figure 2: Knockdown (KD) or overexpression (OE) of fertility candidate zinc transport genes in the *Drosophila* testis. The candidate infertility genes from the zinc transport screen were manipulated in the germline cells of the testis, using a *nanos*-Gal4 **(A)** line and in the somatic cells of the testis, using a *trafficjam*-Gal4 **(B).** These genes were chosen as they showed promise in the original screen. Each dot represents the average number of offspring, resulting from a cross with a single transgenic male, with 3 w^{1118} females, over three 3-day mating periods. The horizontal line indicates the mean number of offspring from the 3 mating periods, and error bars indicate standard deviation. To generate the statistic, a One-Way ANOVA, with a Dunnett's Multiple comparisons test to the w^{1118} control was used. (*=p<0.05, **=p<0.01, ***=p<0.001) ZnT = Zinc Transporter, Zip = Zrt-, Irt-like protein OE = overexpression, KD = RNAi knockdown.

4.3.2 Histological analysis of zinc transporter testicular overexpression and knockdown in flies

To examine the effect of altering zinc transport on testis histology, the *nos*-Gal4 and *tj*-Gal4 lines were combined with a *don juan (dj)-GFP* reporter transgene, which expressed a GFP-labelled protein, Don juan, which localises to the sperm tails. After dissection, the testes were fixed and stained with Phalloidin (red) which targets F-actin and DAPI (blue) which stains DNA. Histology was investigated in *Zip71B* OE, *Zip89B* OE, *Zip42C.1* KD and *foi* KD lines with the *tj-Gal4* driver (Figure 3 and 4) and *ZnT86D* OE with the *nos-Gal4* driver (Figures 5 and 6).

Both *Zip71B* over-expression and *foi* knockdown in the somatic cells of the testis resulted in a 'tiny testes' phenotype (Figures 3E-H and Q-T, respectively), where the testes are noticeably smaller than the w^{1118} control (Figures 3A-D). This phenotype has been previously described in (Yu et al., 2016). High magnification analysis of the seminal vesicles of these males revealed that none of the genotypes produced sperm (Figures 4E-H and Q-T). While the overexpression of *Zip89B* in the somatic cells revealed normal looking testes containing sperm (Figure 3I-L), the seminal vesicles of these males were empty of all sperm (Figures 4I-L).

When *Zip42C.1* was knocked down in the somatic cells of the testis, noticeably fewer sperm were observed at the proximal end of the testis (Figure 3M-P), and the seminal vesicle (Figures 4M-P) was distinctly smaller than the control line (w^{1118}). Over-expression of *ZnT86D* in the germline cells resulted in both a normal testis (Figures 5E-H) and normal seminal vesicle (Figures 6E-H) which were comparable in size to the control (Figures 3A-D and 4A-D)

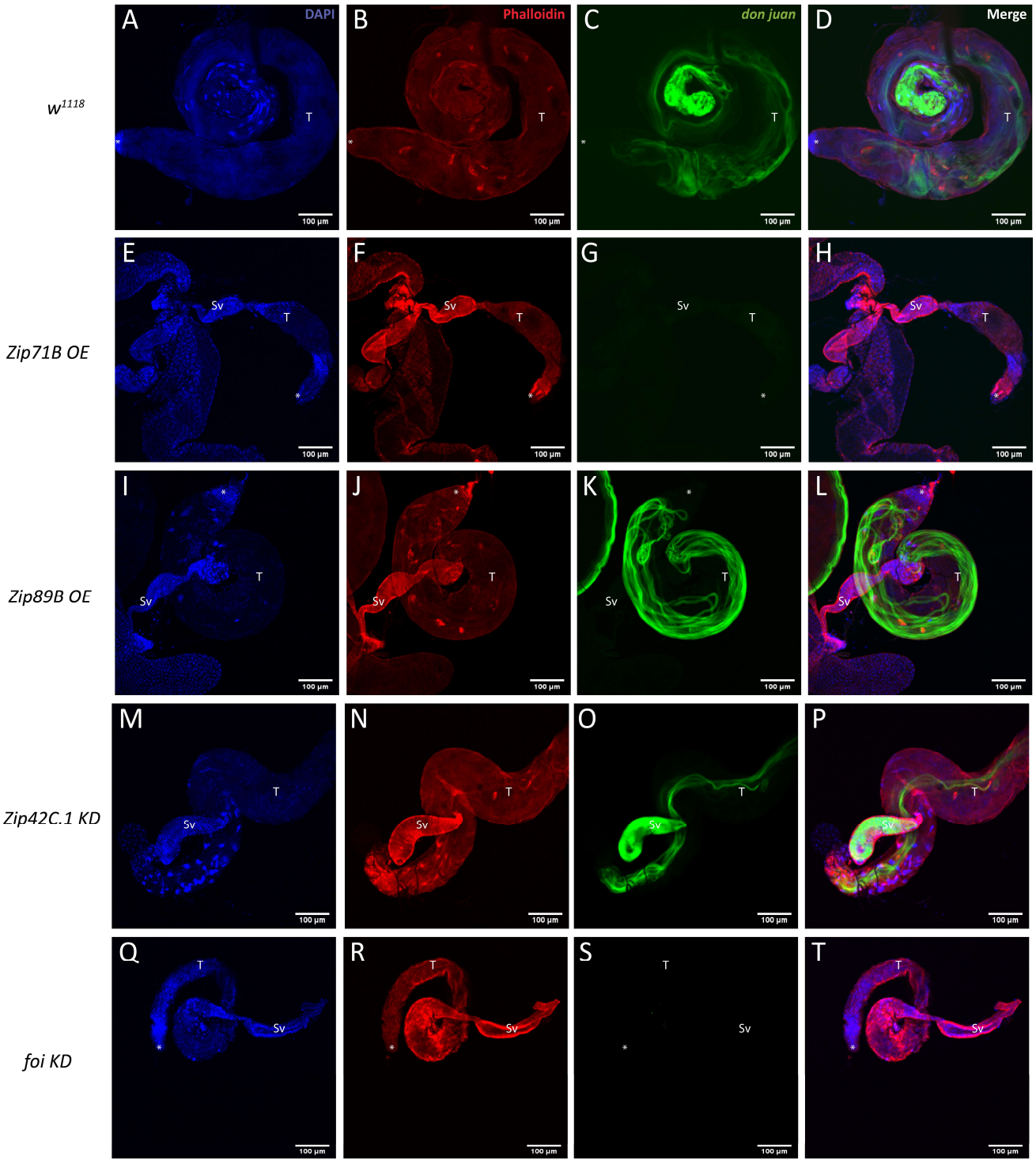

Figure 3: Histological analysis of the effects of zinc transporter knockdown or overexpression in the somatic cells of the testis. (A-D) *dj-GFP;tj-Gal4/w*^{1118}, **(E-H)** *dj-GFP;tj-Gal4/UAS-Zip71B-cDNA,* **(I-L)** *dj-GFP;tj-Gal4/UAS-Zip89B-cDNA*, **(M-P)** *dj-GFP;tj-Gal4/UAS-Zip42C.1-RNAi*, **(Q-T)** *dj-GFP;tj-Gal4/UAS-foi-RNAi.* RNAi caused knockdown; cDNA was used to induce over-expression. All samples were stained with DAPI (nuclei, blue) and Phalloidin (actin, red). The *dj (donjuan)-GFP* caused green fluorescence in the sperm tails. * = hub of the testis, Sv = seminal vesicle, T = testis.

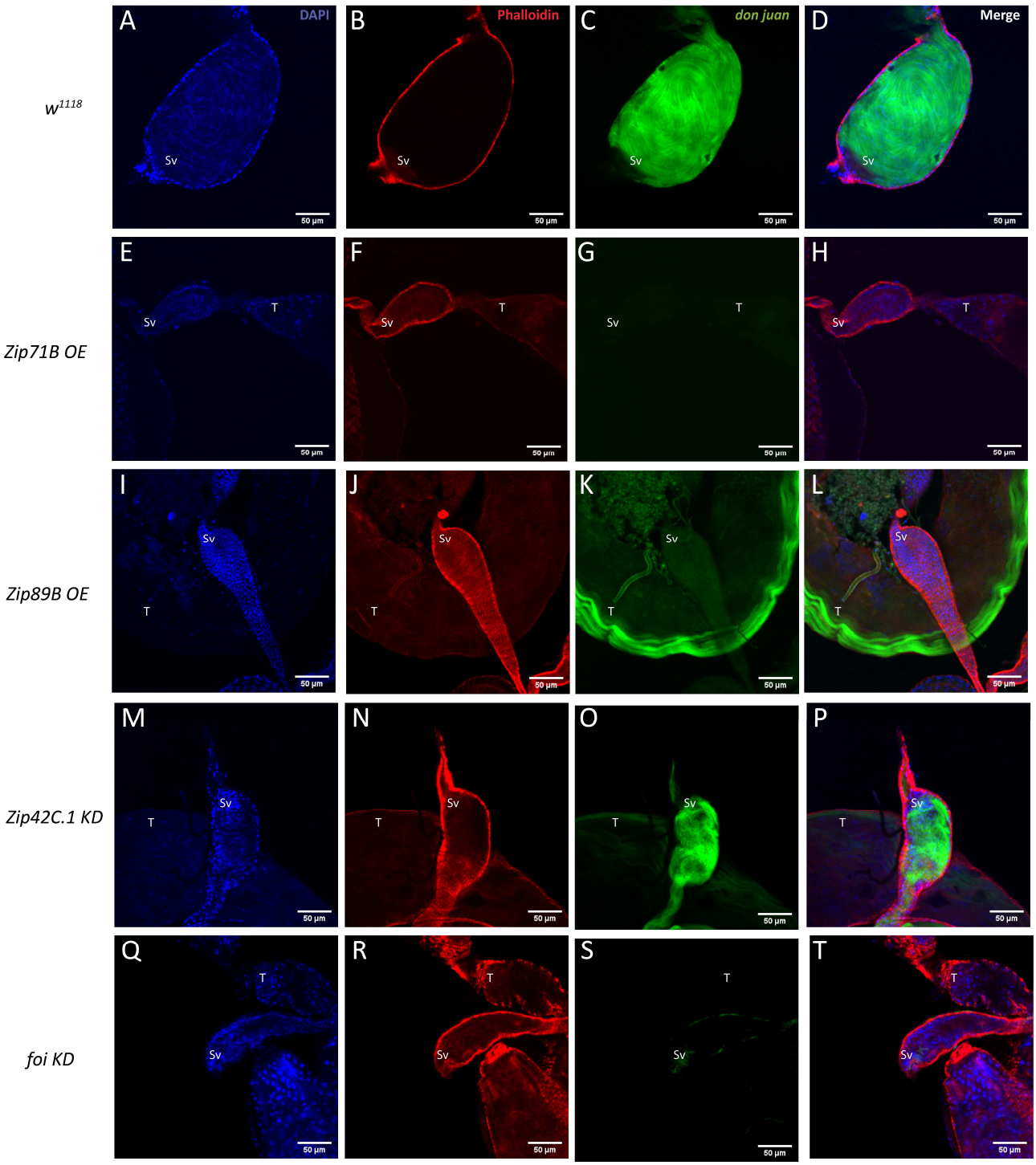

Figure 4: Histological analysis of the effects on the seminal vesicle of zinc transporter knockdown or overexpression in the somatic cells of the testis. (A-D) *dj-GFP;tj-Gal4/w-1118*, **(E-H)** *dj-GFP;tj-Gal4/UAS-Zip71B-cDNA,* **(I-L)** *dj-GFP;tj-Gal4/UAS-Zip89B-cDNA*, **(M-P)** *dj-GFP;tj-Gal4/UAS-Zip42C.1-RNAi*, **(Q-T)** *dj-GFP;tj-Gal4/UAS-foi-RNAi.* RNAi caused knock-down; cDNA was used to induce over-expression. All samples were stained with DAPI (nuclei, blue) and Phalloidin (actin, red). The *dj (donjuan)-GFP* caused green fluorescence in the sperm tails. * = hub of the testis, Sv = seminal vesicle, T = testis.

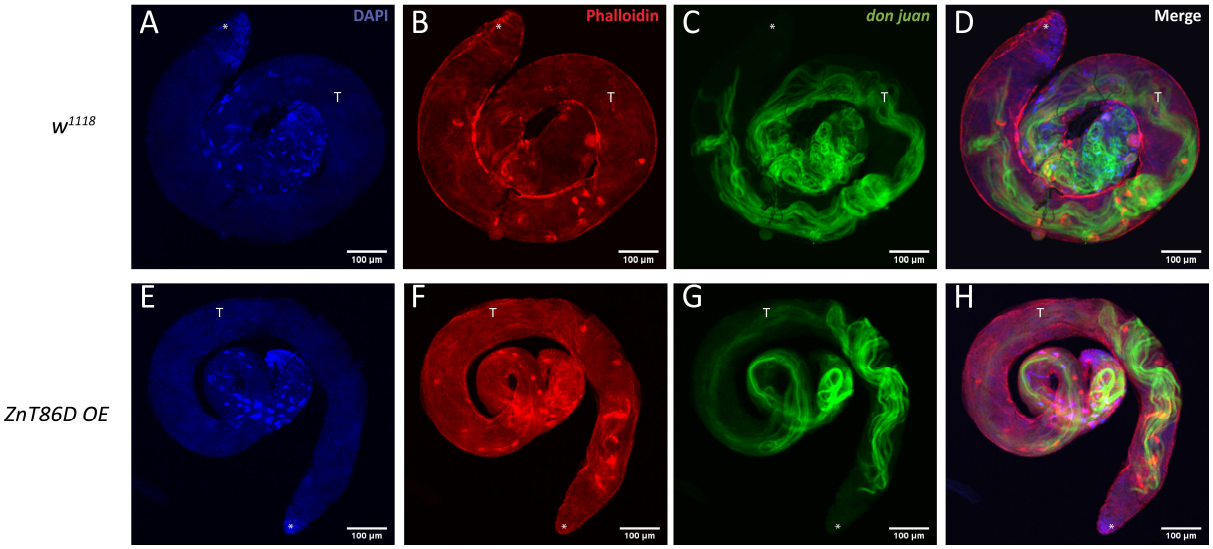

Figure 5: Histological analysis of the effects of zinc transporter knockdown or overexpression in the germline cells. (A-D) *dj-GFP;nos-Gal4/w*^{1118}, **(E-H)** *dj-GFP;nos-Gal4/UAS-ZnT86D-cDNA.* cDNA was used to induce over-expression. All samples were stained with DAPI (nuclei, blue) and Phalloidin (actin, red). The *dj (donjuan)-GFP* generated green fluorescence in the sperm tails. * = hub of the testis, T = testis.

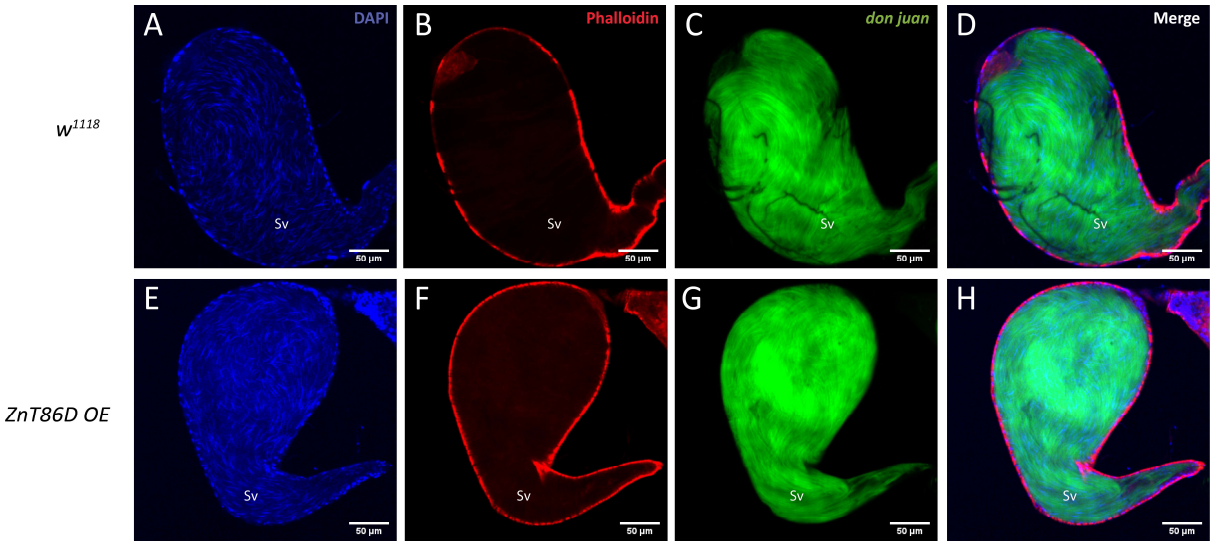

Figure 6: Histological analysis of the effects on the seminal vesicle of *ZnT86D* overexpression in germline cells. (A-D) *dj-GFP;nos-Gal4/w*^{1118}, **(E-H)** *dj-GFP;nos-Gal4/UAS-ZnT86D-cDNA.* cDNA was used to induce over-expression. All samples were stained with DAPI (nuclei, blue) and Phalloidin (actin, red). The *dj (donjuan)-GFP* caused green fluorescence in the sperm tails. Sv = seminal vesicle

Table 4: Summary of zinc transporter knockdown and overexpression phenotypes		
	Fertility	Histological description
Zip71B OE x tj	Sterile	Tiny testis, no sperm produced
Zip89B OE x tj	Sterile	Sperm in the testis, not in the seminal vesicle
Zip42C.1 KD x tj	Sterile	Sperm in testis and seminal vesicle, seminal vesicle is small
foi KD x tj	Sterile	Tiny testis, no sperm produced
ZnT86D x nos	Subfertile	Sperm in the testis and seminal vesicle

4.3.3 Expression analysis of zinc transporters in human testicular tissue

Functional characterisation of the *Drosophila* ZnTs and ZIPs demonstrated that several played an important role in fly fertility, in particular, *Zip42C.1, Zip89B, ZnT86D, foi, Zip71B, ZnT49B and ZnT86D*. In order to investigate whether the human orthologues of these genes played a similar functional role in male fertility, the human orthologues *ZIP1* and *ZIP3* (orthologous to *Zip42C.1* and *Zip89B)*, *ZIP5* (orthologous to *Zip71B*), *ZnT1* (orthologous to *ZnT63C* and *ZnT77C*) and *ZnT9* (orthologous to *ZnT49B*) were chosed for expression analysis (See Table 1 for the list of human zinc transporter families and their *Drosophila* family orthologues) based on the above functional characterization as well as previous published results.

RT-PCR primer pairs for *ZnT1, ZnT9, ZIP1, ZIP3* and *ZIP5* were used to analyse cDNA from the testes of patients with normal spermatogenesis (NSP) or a Sertoli-cell only (SCO) presentation. SCO patients were included, as the presence of mRNA in the NSP patient, but not in the SCO patients, would indicate that the gene is solely expressed in the germline, or in immature Sertoli cells. Each of the 5 genes were consistently expressed in both NSP and SCO samples (Figure 7) and are therefore present in both somatic and germline cell types.

To gain greater understanding into the cellular expression patterns of these zinc transporter genes, single cell (SC) RNA sequencing (RNA-seq) data obtained by the lab for human (Mahyari et al., 2021), mouse (Jung et al., 2019) and *Drosophila* (Witt et al., 2019) was analysed. Furthermore, *in* situ hybridisation probes for *ZIP1*, *ZIP5* and *ZnT9* were generated using PCR primers outlined in Table 3.

According to the SC RNA-seq data, *foi* was expressed primarily in early germ cells and spermatids, with little expression in cyst cells (Figure 8A). Conversely, the mammalian orthologues of *foi*, *Zip6* and *Zip10*, were also expressed thoughout spermatogenesis, including high expression of *Zip6* in Sertoli cells.

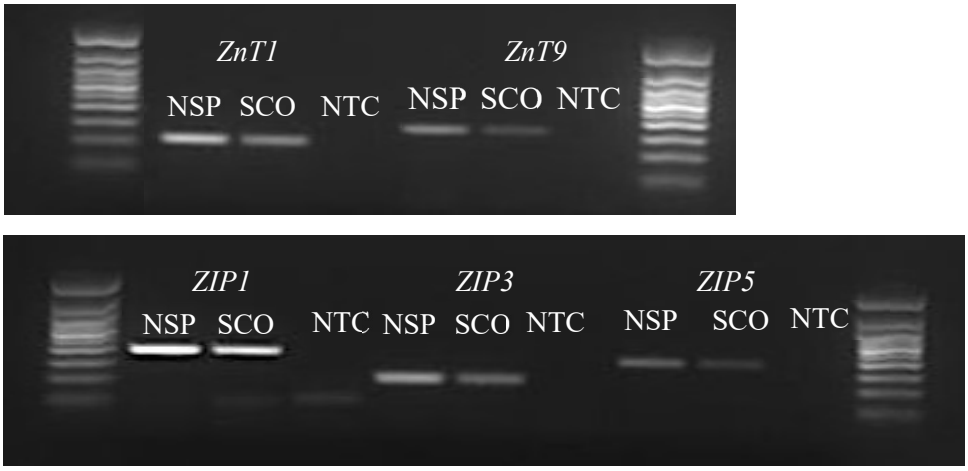

Figure 7: Qualitative RT-PCR using primers for ZnT1, ZnT9, ZIP1, ZIP3 and ZIP5 in cDNA isolated from testicular biopsies of men presenting with either normal spermatogenesis (NSP) or Sertoli-cell only (SCO). The PCR was run according to section 4.2.5. A minimum of N=5 patients of each of NSP and SCO samples were used for each primer pair. NTC indicates No Template Control

The *Drosophila* gene *ZnT86D* was most highly expressed in spermatogonia in the fly, and this was replicated in the mouse orthologues, *ZnT5, ZnT6* and *ZnT7* (Figure 8B). In the human however, the expression of this gene family was highest in the Sertoli cells.

Human and mouse *ZIP1* expression was primarily in spermatogonia (Figure 9A). However, the highly conserved *ZIP3,* was highly expressed throughout spermatogenesis, including Sertoli cells (Figure 9A). In the mouse, *Zip1* was expressed primarily in early germ cells and Sertoli cells, whereas *Zip3* was expressed in late spermatocytes. *Zip2* RNA-seq data was not available for the mouse.

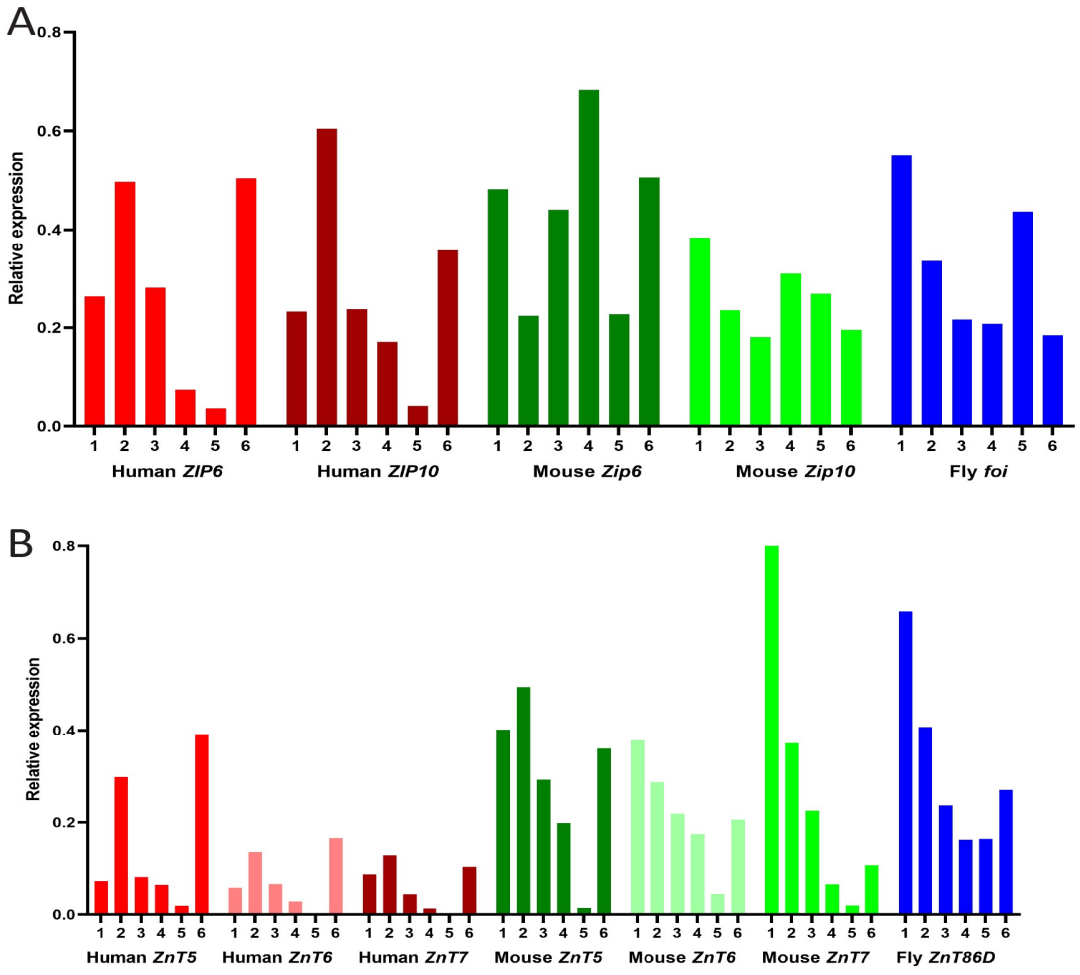

Figure 8: Expression in humans (red), mice (green) and flies (blue) of zinc transporters. A) Mammalian *ZIP6* and *ZIP10* with *Drosophila* orthologue *foi*, **B)** Mammalian *ZnT5, ZnT6 and ZnT7* with *Drosophila* orthologue *ZnT86D*. 1 = Undifferentiated/early spermatogonia, 2 = Differentiated/late spermatogonia, 3 = Diplotene/Zygotene/early spermatocytes, 4 = pachytene/late spermatocytes, 5 = round/early spermatids, 6 = Sertoli/cyst cells.

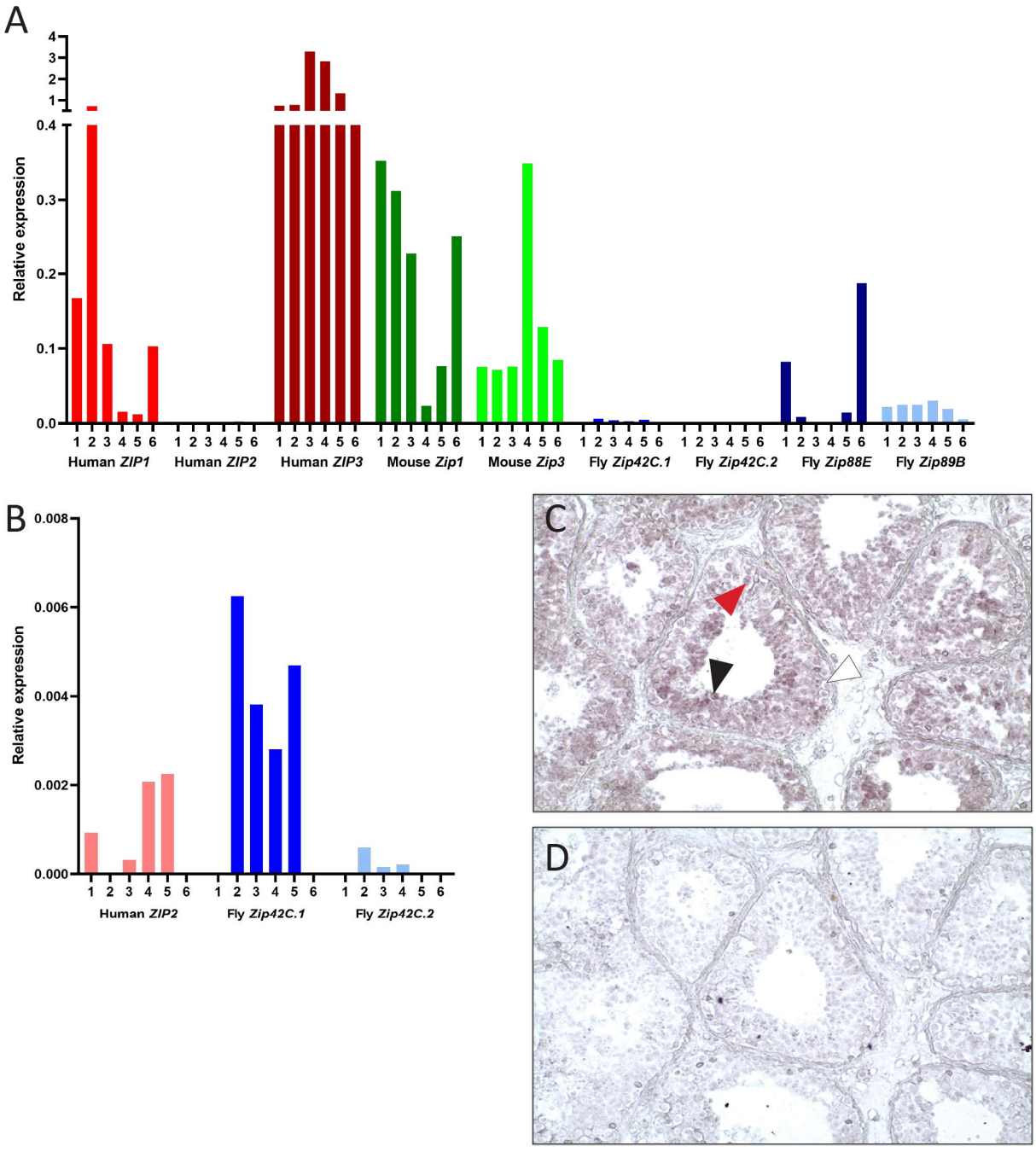

Figure 9: Expression of *ZIP1, ZIP2* and *ZIP3* in humans (red) and mice (green) and *Zip42C.1, Zip42C.2, Zip88E* and *Zip89B* in flies (blue). A) + B) 1 = Undifferentiated/early spermatogonia, 2 = Differentiated/late spermatogonia, 3 = Diplotene/Zygotene/early spermatocytes, 4 = pachytene/late spermatocytes, 5 = round/early spermatids, 6 = Sertoli/cyst cells. **C)** Sense and **D)** antisense for an in situ hybridization using on NSP testis with *ZIP1* probe with a Hybridization temperature of 44°C. Red arrowhead = spermatogonia, white arrowhead = stained Sertoli cell, black arrow = spermatid.

ZIP2 also showed very low expression in the human testis (Figure 9B). The most closely related *Drosophila* ZIPs all showed low expression in the fly testis (Figures 9A and B). Only *Zip88E* had high expression in early spermatogonia and in cyst cells (Figure 9A). RNA in situ hybridization showed that *ZIP1* was expressed in germ cells of NSP patients with potentially stronger staining in the spermatids, while Sertoli cells had minimal staining (Figure 9C).

ZIP5 was expressed early in spermatogenesis in undifferentiated spermatogonia, as well as later in spermatids, but had a low relative expression according to the data obtained from (Mahyari et al., 2021) (Figure 10A) and was not at all expressed in the human Sertoli cells. Conversely, the in situ hybridisation demonstrated *ZIP5* expression primarily in the human Sertoli cells (Figure 10B). Murine *Zip5* was primarily expressed in the Sertoli cells (Figure 10A). The single *Drosophila* orthologue, *Zip71B* was expressed most highly in the spermatogonia and cyst cells.

The last zinc transporter analysed was mammalian *ZnT9,* with the *Drosophila* orthologue, *ZnT49B.* In both the human and the fly, the expression of their respective genes was high in the somatic cells (Sertoli cells in the human, and cyst cells in the fly) (Figure 11A). All 3 orthologues however, were expressed throughout spermatogenesis. The in situ hybridization showed that *ZnT9* expression was highest in Sertoli cells (Figure 11B),which matches the RNA-seq data (Figure 11A)

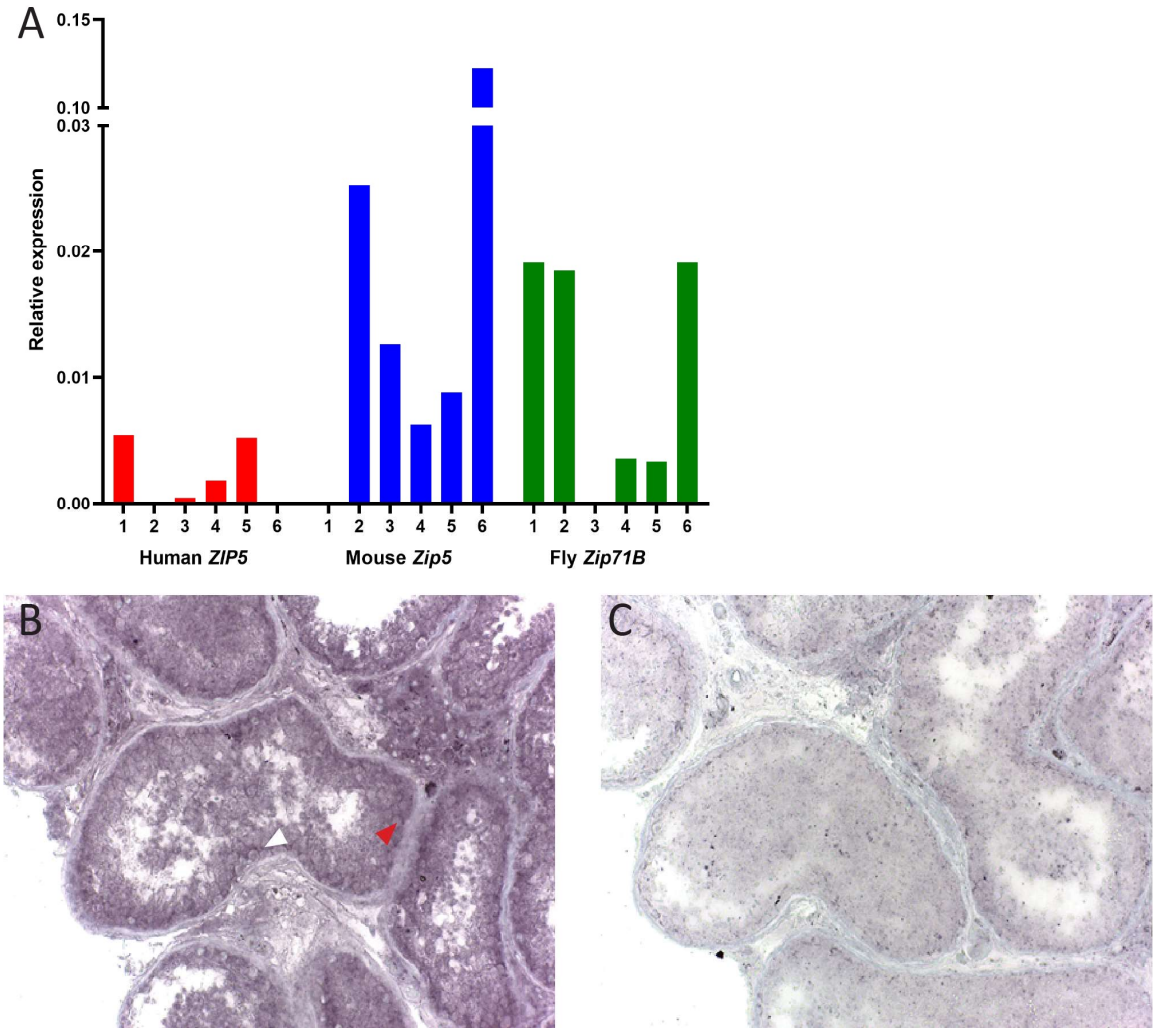

Figure 10: Expression of mammalian *ZIP5* in humans (red) and mice (green) and *Zip71B* in flies (blue). A) 1 = Undifferentiated/early spermatogonia, 2 = Differentiated/late spermatogonia, 3 = Diplotene/Zygotene/early spermatocytes, 4 = pachytene/late spermatocytes, 5 = round/early spermatids, 6 = Sertoli/cyst cells. **B)** Sense and **C)** antisense for an in situ hybridization using on NSP testis with *ZIP5* probe with a Hybridization temperature of 44°C. Red arrowhead = spermatogonia, white arrowhead = stained Sertoli cell

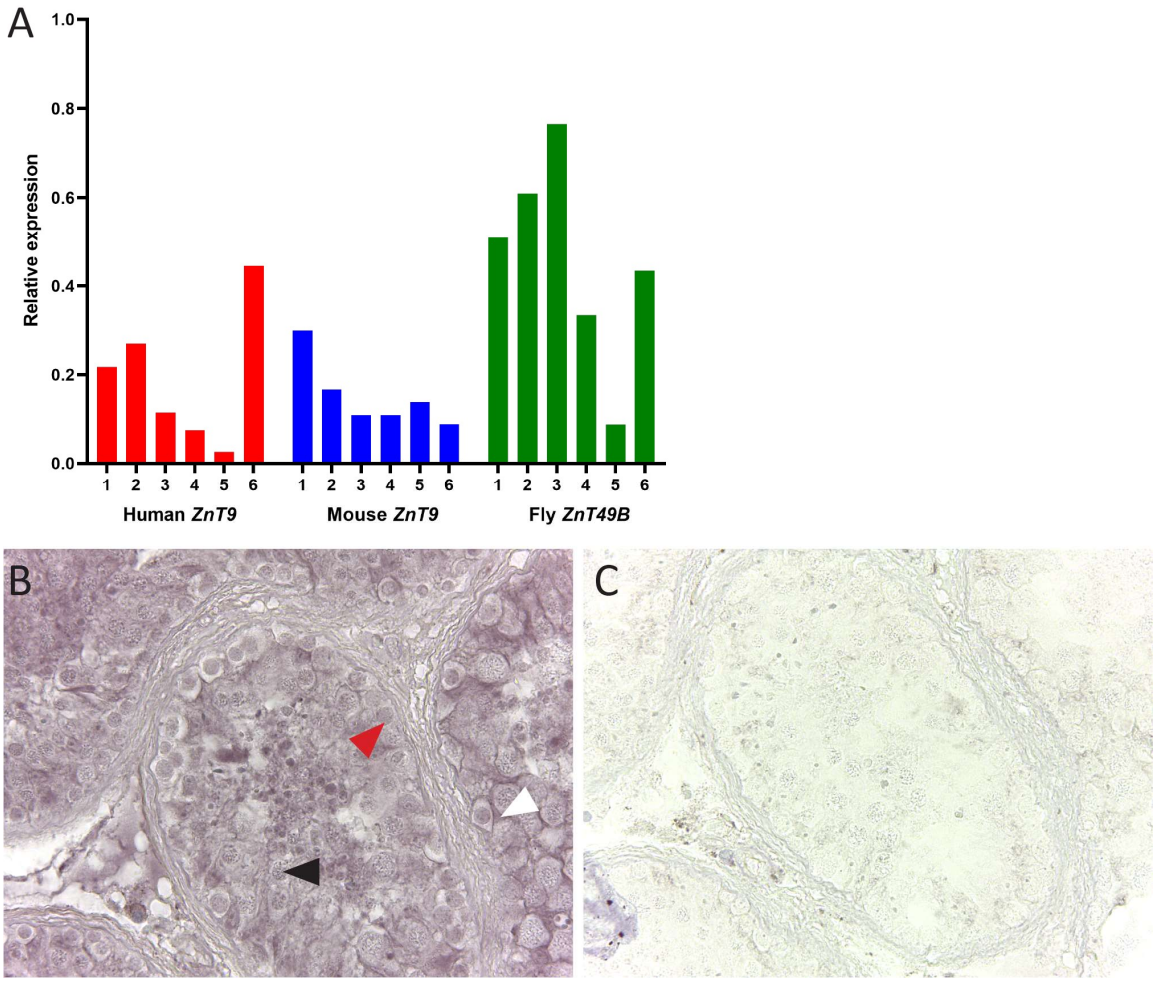

Figure 11: Expression of mammalian *ZnT9* in humans (red) and mice (green) and *ZnT49B* in flies (blue). A) 1 = Undifferentiated/early spermatogonia, 2 = Differentiated/late spermatogonia, 3 = Diplotene/Zygotene/early spermatocytes, 4 = pachytene/late spermatocytes, 5 = round/early spermatids, 6 = Sertoli/cyst cells. **B)** Sense and **C)** antisense for an in situ hybridization using on NSP testis with *ZnT9* probe with a Hybridization temperature of 44°C. Red arrowhead = spermatogonia, white arrowhead = stained Sertoli cell, black arrow = spermatocyte.

4.3.4 Removing copper or zinc from the adult diet had no effect on male fertility

In order to determine whether dietary zinc was critical for adult *Drosophila* male fertility, a sperm depletion assay was undertaken using a back-crossed population of wildtype Red Dahomey flies. Density controlled populations of Red Dahomey were raised to adulthood on normal SY diet, then males were transferred to a defined holidic media containing normal metal content (100N), no zinc (100N-Zn) and no copper (100N-Cu). Copper depletion was also tested, as copper uptake has previously been shown to be essential for *Drosophila* male fertility (Steiger et al., 2010, Ghaffari et al., 2019). All other metals and dietary components were retained as normal.

The Red Dahomey males were then assayed for fertility as described in section 4.2.10. While there was a noticeable reduction in fertility with increasing male age on all diets, the removal of either metal resulted in no difference in the proportion of females fertilised (Figure 12A) or the mean number of pupae produced from each mating (Figure 12B) compared to the control diet. Day 25 and 29 for the "100-Cu" were lost due to human error; the box for day 29 was mistakenly counted on day 25, and then discarded. This could not be repeated, as this was a large experiment, with months of preparation. Furthermore, these data points are present in the following sperm depletion assay.

In an attempt to completely deplete the sperm reserves in the seminal vesicle, and hence, test whether ongoing sperm production was adversely affected by zinc or copper depletion, the experiment was repeated under modified conditions; this time the males were not given 3 days to "recover" and were instead immediately given virgin females to mate. Again, there was also no difference in the proportion of females fertilised or the mean number of produced from each mating in this this second sperm depletion assay (Figure 13).

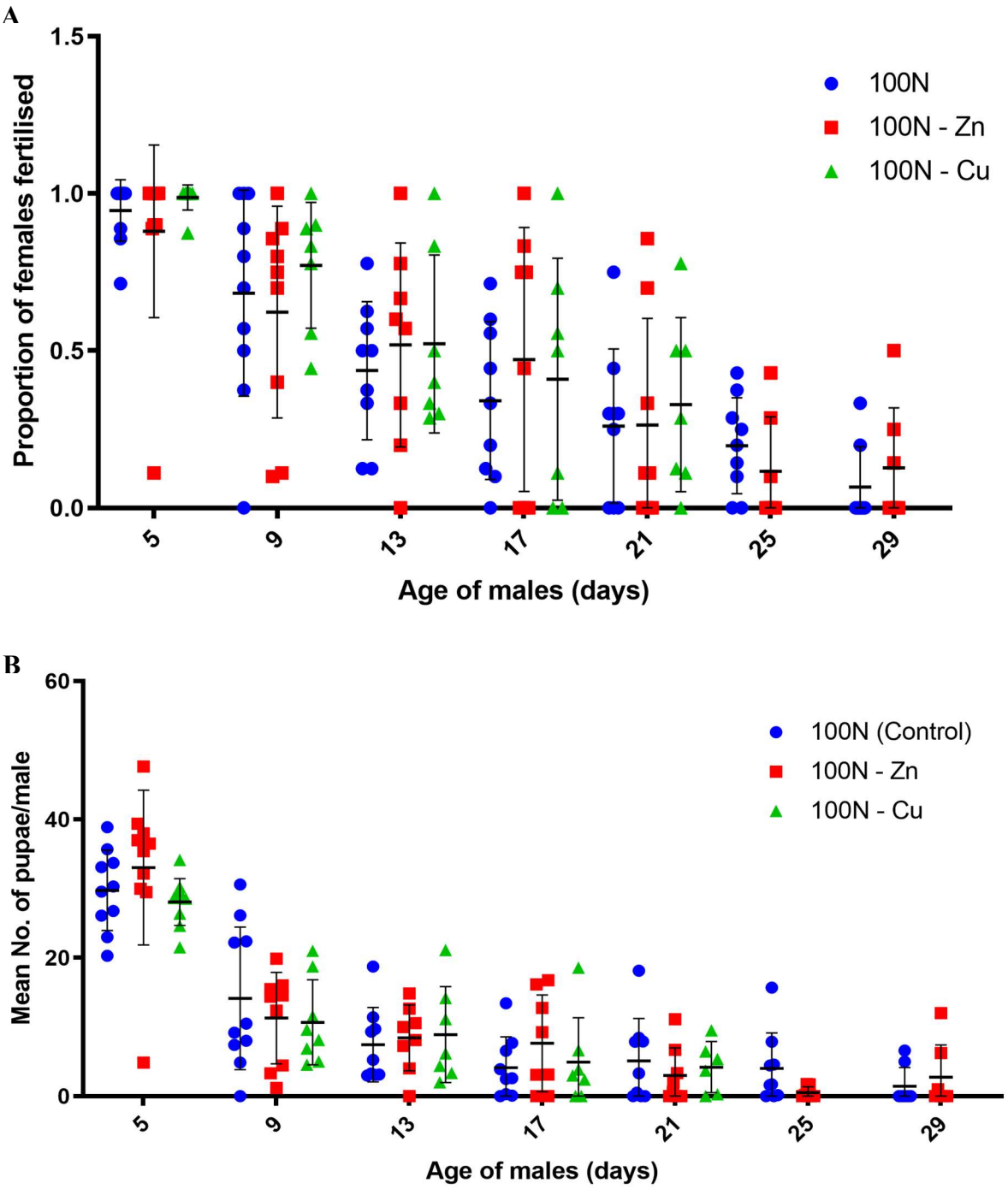

Figure 12: The effect on fertility of removing zinc and copper from the *Drosophila* diet. At each time point, single males on each of the three diets were placed in a vial with 10 virgin females and allowed to mate for 24 hours. The males were then placed onto the same diet for three days, after which 10 more virgin females were added. This was repeated 7 times for 100N and 100N-Zn, and 5 times for 100N-Cu. Each mated female was individually housed. **(A)** The number of fertilised females and **(B)** the mean number of pupae per male were recorded**.** The error bars indicate standard deviation for each time point. Day 25 and 29 for "100-Cu" were lost.

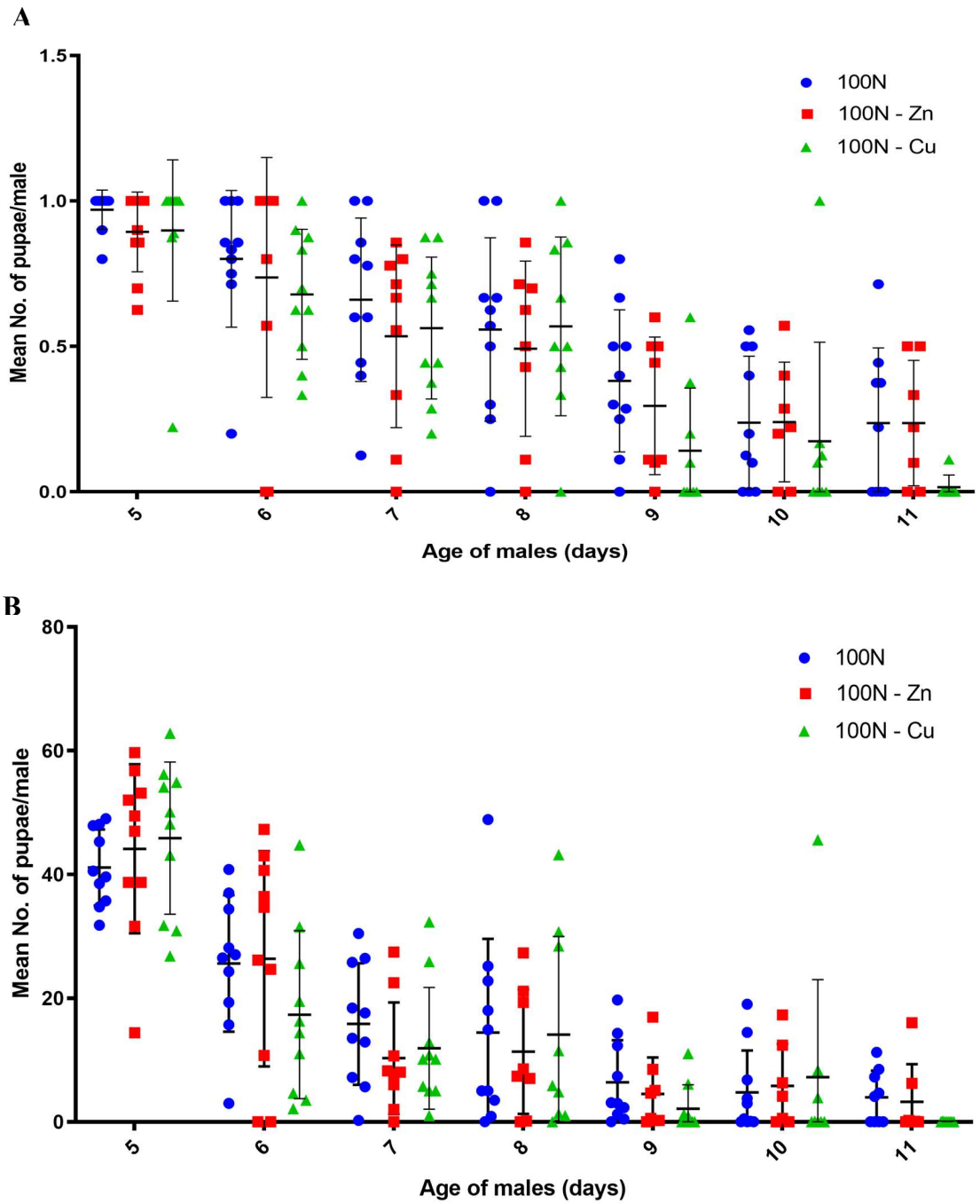

Figure 13: The effect on fertility of removing zinc and copper from the *Drosophila* diet. At each time point, single males on each of the three diets were placed in a vial with 10 virgin females and allowed to mate for 24 hours. The males were then placed onto the same diet, and immediately given 10 more virgin females. This was repeated 7 times for all diets. Each mated female was individually housed. The **(A)** number of fertilised females and **(B)** the mean number of pupae per male were recorded**.** The error bars indicate standard deviation for each time point.

4.4 Discussion

From chromatin stabilisation to sperm capacitation, zinc undoubtedly plays an important role in fertility (reviewed in Fallah et al. (2018)). However, little research has gone into understanding the potential role of zinc transporters in spermatogenesis. The two primary zinc transporter classes are the Zrt-, Irt-like protein family (ZIPs) which transport zinc into the cytosol, and the Zinc Transporter Family (ZnTs), which moves zinc out of the cytosol. It is important to determine whether these genes could be implicated in male fertility.

However, the genetic relationship between orthologues between species can sometimes be difficult to determine, as there is not always one-to-one orthology. For this reason, it can be difficult to directly correlate function between humans and flies. This is especially true when working with the ZnTs and ZIPs, where for example, one sub-family of three human genes (such as *ZIP1*, *ZIP2* and *ZIP3*) are orthologous to four members of the *Drosophila* sub-family (*Zip42C.1, Zip42C.2, Zip88E and Zip89B*).

This work has shown that by using *Drosophila*, a large number of genes can be screened rapidly and cheaply, resulting in a smaller number of genes to be followed up using more closely related animal models (such as mice) and precious human tissue. The breadth of data generated by the fly screen (Figures 1 and 2) demonstrate the validity of this, as the number of genes of interest was narrowed down from 24 potential mammalian ZIPs and ZnTs to five which were studied in more depth in the human. This was further verified, as all these genes were found expressed in the human testis (Figure 7).

4.4.1 *Drosophila foi*

Given that the *foi* had previously been shown to be important in gonad development (Carrasco-Rando et al., 2016), it was not surprising that its knockdown resulted in a sterile phenotype, and thus provided a reliable positive infertility control. The RNA sequencing data from Witt et al. (2019) demonstrated that *foi* was highly expressed in the spermatogonia (Figure 8A). Interestingly, the cyst cell knockdown of *foi* resulted in the "tiny testes" phenotype (Figures 3Q-T), previously defined in Yu et al. (2016). The stem cell niche appeared severely disrupted, with a large number of early germ cells migrating further along the testis (indicated by DAPI staining). This suggests that the cyst cells or spermatogonia are migrating along the testis, due to the lack of developing germ cells. The seminal vesicle was also completely empty, with a complete absence of sperm indicated by a lack of GFP which would have stained sperm tails (Figures 4Q-T). This phenotype is likely to be most akin to the human Sertoli-cell only phenotype, or arrest at the spermatogonial stage.

4.4.2 *Drosophila Zip71B* and human *ZIP5*

The overexpression of *Zip71B* in the somatic cells of the testis also resulted in a tiny testes phenotype (Figure 3E-H) and an absence of sperm in the seminal vesicles (Figures 4E-H). The RNA-seq data indicated that *Zip71B* was normally highly expressed in cyst cells and spermatogonia.

Zip71B overexpression has previously been studied in the *Drosophila*, where overexpression caused a severe eye phenotype (Dechen et al., 2015). In fact, it was the only ZIP which was able to cause a noticeable phenotype when expressed alone, whereas other ZIPs relied on knockdown of an opposing exporter to generate a zinc toxicity phenotype (Dechen et al., 2015). This suggests that *Zip71B* is a particularly potent ZIP and when overexpressed, it floods the cell with levels of zinc toxic to

potentially any tissue. As the infertility phenotype observed was so strong. For this reason, the human orthologue *ZIP5* was also investigated.

The expression of *ZIP5* in NSP testes was most prevalent in somatic cells (Figure 10B), with weaker expression in the germline cells. The expression in both somatic and germline cells was expected, as the infertility assay determined that *Zip71B* overexpresson caused infertility when expression was altered in both germline and somatic cells. This matches what was found in Foresta et al. (2014), where *ZIP5* was found to be expressed on murine germ cells all throughout spermatogenesis, as well as in Sertoli cells. This does however conflict with what was found in the human RNA-seq data (Figure 10A) which demonstrated no expression of *ZIP5* in the Sertoli cells. RNA-seq data from two other sources also validates that *ZIP5* is not expressed in Sertoli cells (Wang et al., 2018, Guo et al., 2018). Interestingly, the expression of mouse *Zip5* in the mouse RNA sequencing data extracted from (Jung et al., 2019) suggests that *Zip5* expression in Sertoli cells was very high compared to the other testicular cells. The strong contrasting evidence suggests that ZIP5 function has diverged between mice and humans.

Recent research has demonstrated that human *ZIP5* may play two distinct roles. The bulk of research currently in the field suggests that *ZIP5* plays a role in the development of oesophageal cancer. It was found that overexpression of *ZIP5* was detected in oesophageal cancer cells, and knockdown of *ZIP5* in these cells halted cell cycle progression in oesophageal cell carcinoma (Jin et al., 2015, Li et al., 2016). *ZIP5* downregulation was found to reduce the expression of COX2, a known tumour promoter (Li et al., 2016). Another paper has found that a loss-of-function mutation in *ZIP5* results in myopia, by studying a non-consanguineous family with autosomal dominant myopia (Guo et al., 2014a). The finding that the orthologue of *ZIP5*, *Zip71B* is involved in fertility is novel.

4.4.3 *Drosophila Zip89B* and *Zip42C.1* and human *ZIP1*

Zip89B over-expression in the somatic cells of the testis showed almost normal spermatogenesis in the testis, however the seminal vesicle was completely empty. This matches the sterility observed in Figure 2. It is clear that sperm with tails are produced in the testis, however something is preventing them from being transported to the seminal vesicles. This is most like the human arrest at spermatid stage pathology. A similar histological phenotype was observed in Yuan et al. (2019), with a mutation of the *Drosophila* gene *Pif1A,* the orthologue of human *CCDC517.* It was discovered that mutation of *Pif1A* was likely to be responsible for the individualisation of the sperm at the end of spermiogenesis. It is likely that this is a similar case here, as the actin cones (red, Figure 3J) do not appear to be associated with the DAPI-stained (blue, Figures 3I and 3L). This is the first time a zinc transporter has been associated with *Drosophila* sperm individualisation.

Knockdown of *Zip42C.1* in testis somatic cells resulted in sperm being produced, however the size of the seminal vesicle was noticeably reduced compared to control. This is most akin to human oligospermia, or a reduction in the number of sperm produced. Interestingly however, the fertility assay determined that these flies were sterile, thus suggesting that while there were sperm tails produced, these sperm were not capable of fertilising eggs.

Both *Zip42C.1* and *Zip89B* are a part of the ZIP subfamily analogous to human *ZIP1, ZIP2 and ZIP3.* The whole ZIP sub-family was analysed using SC RNA-seq data, and *ZIP1* was analysed using in situ hybridization in human testis tissue. Mammalian *ZIP1* expression was highest in spermatogonia (Figure 9C), which was confirmed by the SC RNA-seq data (Figures 9A and 9C). Other SC RNAseq data from Wang et al. (2018) and Guo et al. (2018) both suggest that *ZIP1* is expressed primarily in early spermatocytes, but also in Sertoli cells.

This contradicts the *Drosophila* data, where it was found that the *Drosophila* orthologues of *ZIP1* (*Zip42C.1*, *Zip42C.2* and *Zip89B*) caused infertility when expression was altered in the somatic cells, but not in the germline. This may be due to the fact that the decrease in fertility occurred in *Drosophila* when two of the genes (*Zip42C.2* and *Zip89B*) were overexpressed rather than knocked down. This is especially interesting when accounting for the *Drosophila* RNA-seq data (Figure 9A and B) which showed very low expression of *Zip42C.1, Zip42C.2* and *Zip89B* in the normal *Drosophila* testis. When these genes were overexpressed, the cells were importing zinc from transporters not usually expressed so highly, potentially flooding the cell with toxic amounts of zinc.

This suggests that altered expression of this ZIP family is more sensitive in *Drosophila* than it would be in the human. Foresta et al. (2014) found that *ZIP1* was expressed spermatids and spermatozoa. This corroborates what is seen in the in situ hybridization (Figure 9C) but does not particularly corroborate the single cell RNA sequencing data (Figure 9A).

ZIP1 is one of the better studied genes of the ZIP family and has previously been found to have a potential role in some cancers, including prostate cancer. It was found that ZIP1 was downregulated and zinc was depleted in adenocarcinomatous glands, which when linked with the fact that decreased intracellular zinc increases malignancy in prostate cancer, demonstrates that ZIP1 downregulation may play a key role in prostate cancer development (Makhov et al., 2009, Franklin et al., 2005). More recent studies have found that decreased expression of *ZIP1* may play a role in the development of a wide variety of mucinous cancers (Desouki et al., 2015). Therefore, the discovery that the ZIP1 sub-family may also play a role in sperm development is novel, especially as a previous doubkle knockout of *ZIP1* and *ZIP3* was shown to be fertile (Dufner-Beattie et al., 2006).

4.4.4 *Drosophila ZnT49B* and human *ZnT9*

ZnT9 was also analysed in human tissue, as the *Drosophila* orthologue, *ZnT49B* knockdown in somatic cells of the testis caused a severe reduction in fertility. To our knowledge there has been no reported function for *ZnT49B*, hence the discovery that its knockdown in the somatic cells of the testis causes such a severe subfertility phenotype is novel, and worthy of further investigation. The expression of *ZnT9* in the human testis was localised primarily to Sertoli cells (Figure 11B). The human single cell RNA-seq data supported this finding (Figure 11A). Interestingly, the mouse *ZnT9* RNA sequencing data suggests that ZnT9 has relatively low expression in the testis (Figure 11A).

Previous research on *ZnT9* has found that is associated with the Wnt signalling pathway (Chen et al., 2007) This pathway is a regulator of many developmental processes such as cell growth, and disruption has been shown to cause cancer (Polakis, 2000). Chen et al. (2007) proposed that *ZnT9* cooperates with β-catenin to activate the Wnt pathway.

Interestingly, the Wnt pathway has been previously associated with disrupted spermatogenesis in the mouse. One particular paper found that disruption of Wnt signalling in the Sertoli cell had no effect on spermatogenesis, whereas in germ cells, loss of Wnt signalling caused disrupted spermatogenesis in an age dependant manner (Chen et al., 2016).

4.4.5 Summary of ZnTs and ZIP experiments

It is important to outline some of the caveats of using *Drosophila* as a model organism, especially when attempting to relate results back to a human gene and phenotype. While the use of RNAi is widespread in *Drosophila* genetics, it is not a perfect knockout as it only results in a knockdown of the target gene, rather than the complete knockout which would be achieved using a method such as

CRISPR/Cas9. As the purpose of the experiment was to screen a large number of genes, RNAi was more than sufficient. Furthermore, the overexpression phenotypes do not give us any specific information on the endogenous role of the gene itself, and it would therefore be difficult to translate these results directly to the human. This phenotype in itself is not useless however, as it does provide an explanation into how zinc transport is regulated. The phenotype observed with the overexpression of *Zip42C.2* and *Zip89B* is a prime example of this, as it demonstrated the effect of inappropriate zinc influx. As these genes had such low expression in the testis, it was therefore unsurprising that this resulted in toxicity.

As previously mentioned, the distinction between gene families, rather than direct one-to-one comparison makes it even more difficult to examine the function of these mutations solely in *Drosophila* and again exemplifies the need for further analysis of the candidates elucidated in this thesis in a higher model.

4.4.6 Dietary zinc and fertility

The latter part of this chapter involved analysing the effect of removing copper or zinc from the adult fly diet. Neither the original sperm depletion assay, where the males were given 3 days to recover between matings (Figure 11) nor the more intense sperm depletion assay (Figure 12) suggested that removal of zinc or copper from the adult's diet affected fertility. This lack of reduction does not necessarily mean that neither zinc nor copper are important for male fertility. A chemically defined diet was used as it provided a simple experiment to examine the effects of removing zinc from the diet. However, as this diet is optimised for adult nutritional requirement, it is not sufficient for the larval stages of the developing fly. Therefore, both during the larval stages, and for a short time after eclosion from the pupal case, the males consumed the standard SY diet. As this diet contains yeast,

both during development and shortly after reaching adulthood, the flies consumed a diet that contained zinc and copper. For this reason, it is expected that the residual zinc and copper consumed and stored during these early stages of development was sufficient to ensure that fertility did not decrease significantly when these metals were removed from the diet. In future, it would be beneficial to undertake an Inductively coupled plasma mass spectrometry (ICP-MS) assay, previously used in worms (Jenkins et al., 2020) to quantify metal ion levels in flies raised on control and metal-dropout diets.

There is clear evidence that zinc plays a role in fertility, yet there has been very little research undertaken into the roles of the major zinc transporters in spermatogenesis. The research in this chapter presents the idea that ZnTs and ZIPs may play a much bigger role in spermatogenesis. The discovery of even one zinc transporter as a candidate fertility gene could pave the way for many others. Future research should continue to use the *Drosophila* model, including using CRISPR/Cas9 to completely knockout the expression of these genes. In addition, mouse models, to further examine both the human zinc transporters studied here, as well as the ones which have not been covered. Finally, more detailed in situ hybridization analysis of human testis tissue should be undertaken in order to better characterise the human expression of these genes.

4.5 References

BERGMANN, M. & KLIESCH, S. 2010. Testicular Biopsy and Histology. *In:* NIESCHLAG, E., BEHRE, H. M. & NIESCHLAG, S. (eds.) *Andrology: Male Reproductive Health and Dysfunction.* Berlin: Springer.

CARRASCO-RANDO, M., ATIENZA-MANUEL, A., MARTIN, P., BURKE, R. & RUIZ-GOMEZ, M. 2016. Fear-of-intimacy-mediated zinc transport controls the function of zinc-finger transcription factors involved in myogenesis. *Development,* 143**,** 1948-57.

CHEN, S. R., TANG, J. X., CHENG, J. M., HAO, X. X., WANG, Y. Q., WANG, X. X. & LIU, Y. X. 2016. Does murine spermatogenesis require WNT signalling? A lesson from Gpr177 conditional knockout mouse models. *Cell Death Dis,* 7**,** e2281.

CHEN, Y. H., YANG, C. K., XIA, M., OU, C. Y. & STALLCUP, M. R. 2007. Role of GAC63 in transcriptional activation mediated by beta-catenin. *Nucleic Acids Res,* 35**,** 2084-92.

CROXFORD, T. P., MCCORMICK, N. H. & KELLEHER, S. L. 2011. Moderate zinc deficiency reduces testicular Zip6 and Zip10 abundance and impairs spermatogenesis in mice. *J Nutr,* 141**,** 359-65.

DECHEN, K., RICHARDS, C. D., LYE, J. C., HWANG, J. E. & BURKE, R. 2015. Compartmentalized zinc deficiency and toxicities caused by ZnT and Zip gene over expression result in specific phenotypes in Drosophila. *Int J Biochem Cell Biol,* 60**,** 23-33.

DESOUKI, M. M., FRANKLIN, R. B., COSTELLO, L. C. & FADARE, O. 2015. Persistent low expression of hZip1 in mucinous carcinomas of the ovary, colon, stomach and lung. *J Ovarian Res,* 8**,** 40.

DUFNER-BEATTIE, J., HUANG, Z. L., GEISER, J., XU, W. & ANDREWS, G. K. 2006. Mouse ZIP1 and ZIP3 genes together are essential for adaptation to dietary zinc deficiency during pregnancy. *Genesis,* 44**,** 239-51.

FALLAH, A., MOHAMMAD-HASANI, A. & COLAGAR, A. 2018. Zinc is an Essential Element for Male Fertility: A Review of Zn Roles in Men's Health, Germination, Sperm Quality, and Fertilization. *J Reprod Infertil,* 19**,** 69-81.

FIETZ, D., BERGMANN, M. & HARTMANN, K. 2016. In Situ Hybridization of Estrogen Receptors alpha and beta and GPER in the Human Testis. *Methods Mol Biol,* 1366**,** 189-205.

FORESTA, C., GAROLLA, A., COSCI, I., MENEGAZZO, M., FERIGO, M., GANDIN, V. & DE TONI, L. 2014. Role of zinc trafficking in male fertility: from germ to sperm. *Human Reproduction,* 29**,** 1134-1145.

FRANKLIN, R. B., FENG, P., MILON, B., DESOUKI, M. M., SINGH, K. K., KAJDACSY-BALLA, A., BAGASRA, O. & COSTELLO, L. C. 2005. hZIP1 zinc uptake transporter down regulation and zinc depletion in prostate cancer. *Mol Cancer,* 4**,** 32.

GHAFFARI, R., DI BONA, K. R., RILEY, C. L. & RICHBURG, J. H. 2019. Copper transporter 1 (CTR1) expression by mouse testicular germ cells, but not Sertoli cells, is essential for functional spermatogenesis. *PLoS One,* 14**,** e0215522.

GUO, H., JIN, X., ZHU, T., WANG, T., TONG, P., TIAN, L., PENG, Y., SUN, L., WAN, A., CHEN, J., LIU, Y., LI, Y., TIAN, Q., XIA, L., ZHANG, L., PAN, Y., LU, L., LIU, Q., SHEN, L., LI, Y., XIONG, W., LI, J., TANG, B., FENG, Y., ZHANG, X., ZHANG, Z., PAN, Q., HU, Z. & XIA, K. 2014. SLC39A5 mutations interfering with the BMP/TGF-beta pathway in non-syndromic high myopia. *J Med Genet,* 51**,** 518-25.

GUO, J., GROW, E. J., MLCOCHOVA, H., MAHER, G. J., LINDSKOG, C., NIE, X., GUO, Y., TAKEI, Y., YUN, J., CAI, L., KIM, R., CARRELL, D. T., GORIELY, A., HOTALING, J. M. & CAIRNS, B. R. 2018. The adult human testis transcriptional cell atlas. *Cell Res,* 28**,** 1141-1157.

JIN, J., LI, Z., LIU, J., WU, Y., GAO, X. & HE, Y. 2015. Knockdown of zinc transporter ZIP5 (SLC39A5) expression significantly inhibits human esophageal cancer progression. *Oncol Rep,* 34**,** 1431-9.

JENKINS, N. L., JAMES, S. A., SALIM, A., SUMARDY, F., SPEED, T. P., CONRAD, M., RICHARDSON, D. R., BUSH, A. I & McCOLL, G. 2020. Changes in ferrous iron and glutathione promote ferrotopsis and frailty in aging *Caenorhabditis elegans*. *eLife*, 9: e56580.

JUNG, M., WELLS, D., RUSCH, J., AHMAD, S., MARCHINI, J., MYERS, S. R. & CONRAD, D. F. 2019. Unified single-cell analysis of testis gene regulation and pathology in five mouse strains. *Elife,* 8.

KERNS, K., ZIGO, M. & SUTOVSKY, P. 2018. Zinc: A Necessary Ion for Mammalian Sperm Fertilization Competency. *International Journal of Molecular Sciences,* 19.

LEVAOT, N. & HERSHFINKEL, M. 2018. How cellular Zn(2+) signaling drives physiological functions. *Cell Calcium,* 75**,** 53-63.

LI, Q., JIN, J., LIU, J., WANG, L. & HE, Y. 2016. Knockdown of Zinc Transporter ZIP5 by RNA Interference Inhibits Esophageal Cancer Growth In Vivo. *Oncol Res,* 24**,** 205-14.

LICHTEN, L. A. & COUSINS, R. J. 2009. Mammalian zinc transporters: nutritional and physiologic regulation. *Annu Rev Nutr,* 29**,** 153-76.

MAHYARI, E., GUO, J., LIMA, A. C., LEWINSOHN, D. P., STENDAHL, A. M., VIGH-CONRAD, K. A., NIE, X., NAGIRNAJA, L., ROCKWEILER, N. B., CARRELL, D. T., HOTALING, J. M., ASTON, K. I. & CONRAD, D. F. 2021. Comparative single-cell analysis of biopsies clarifies pathogenic mechanisms in Klinefelter syndrome. *Am J Hum Genet,* 108**,** 1924-1945.

MAIR, W., PIPER, M. D. & PARTRIDGE, L. 2005. Calories do not explain extension of life span by dietary restriction in Drosophila. *PLoS Biol,* 3**,** e223.

MAKHOV, P., GOLOVINE, K., UZZO, R. G., WUESTEFELD, T., SCOLL, B. J. & KOLENKO, V. M. 2009. Transcriptional regulation of the major zinc uptake protein hZip1 in prostate cancer cells. *Gene,* 431**,** 39-46.

MERKER, H. J. & GÜNTHER, T. 1997. Testis Damage Induced by Zinc Deficiency in Rats. *Journal of Trace Elements in Medicine and Biology,* 11**,** 19-22.

PIPER, M., BLANC, E., LEITAO-GONCALVES, R., YANG, M., HE, X., LINFORD, N., HODDINOTT, M., HOPFEN, C., SOULTOUKIS, G., NIEMEYER, C., KERR, F., PLETCHER, S., RIBEIRO, C. & PARTRIDGE, L. 2014. A holidic medium for Drosophila melanogaster. *Nature Methods,* 11**,** 100-5.

PLEUGER, C., FIETZ, D., HARTMANN, K., SCHUPPE, H. C., WEIDNER, W., KLIESCH, S., BAKER, M., O'BRYAN, M. K. & BERGMANN, M. 2017. Expression of ciliated bronchial epithelium 1 during human spermatogenesis. *Fertil Steril,* 108**,** 47-54.

POLAKIS, P. 2000. Wnt signaling and cancer. *Genes Dev.,* 14**,** 1837-51.

QIN, Q., WANG, X. & ZHOU, B. 2013. Functional studies of Drosophila zinc transporters reveal the mechanism for dietary zinc absorption and regulation. *BMC Biology,* 11**,** 101-16.

RICHARDS, C. D., WARR, C. G. & BURKE, R. 2015. A role for dZIP89B in Drosophila dietary zinc uptake reveals additional complexity in the zinc absorption process. *Int J Biochem Cell Biol,* 69**,** 11-9.

ROHMER, C., DAVID, J. R., MORETEAU, B. & JOLY, D. 2004. Heat induced male sterility in Drosophila melanogaster: adaptive genetic variations among geographic populations and role of the Y chromosome. *J Exp Biol,* 207**,** 2735-43.

SIDDALL, N. A. & HIME, G. R. 2017. A Drosophila toolkit for defining gene function in spermatogenesis. *Reproduction,* 153**,** R121-R132.

STEIGER, D., FETCHKO, M., VARDANYAN, A., ATANESYAN, L., STEINER, K., TURSKI, M. L., THIELE, D. J., GEORGIEV, O. & SCHAFFNER, W. 2010. The Drosophila copper transporter Ctr1C functions in male fertility. *J Biol Chem,* 285**,** 17089-97.

VAN DOREN, M., MATHEWS, W. R., SAMUELS, M., MOORE, L. A., BROIHIER, H. T. & LEHMANN, R. 2003. fear of intimacy encodes a novel transmembrane protein required for gonad morphogenesis in Drosophila. *Development,* 130**,** 2355-64.

WANG, M., LIU, X., CHANG, G., CHEN, Y., AN, G., YAN, L., GAO, S., XU, Y., CUI, Y., DONG, J., CHEN, Y., FAN, X., HU, Y., SONG, K., ZHU, X., GAO, Y., YAO, Z., BIAN, S., HOU, Y., LU, J., WANG, R., FAN,

Y., LIAN, Y., TANG, W., WANG, Y., LIU, J., ZHAO, L., WANG, L., LIU, Z., YUAN, R., SHI, Y., HU, B., REN, X., TANG, F., ZHAO, X. Y. & QIAO, J. 2018. Single-Cell RNA Sequencing Analysis Reveals Sequential Cell Fate Transition during Human Spermatogenesis. *Cell Stem Cell,* 23**,** 599-614 e4.

WANG, X., WU, Y. & ZHOU, B. 2009. Dietary zinc absorption is mediated by ZnT1 in Drosophila melanogaster. *FASEB J,* 23**,** 2650-61.

WITT, E., BENJAMIN, S., SVETEC, N. & ZHAO, L. 2019. Testis single-cell RNA-seq reveals the dynamics of de novo gene transcription and germline mutational bias in Drosophila. *Elife,* 8.

WONG, W., FLIK, G., GROENEN, P., SWINKELS, D., THOMAS, C., COPIUS-PEEREBOOM, J., MERKUS, H. & STEEGERS-THEUNISSEN, R. 2001. The impact of calcium, magnesium, zinc, and copper in blood and seminal plasma on semen parameters in men. *Reprod Toxicol,* 15**,** 131-6.

YANG, J., ZHANG, Y., CUI, X., YAO, W., YU, X., CEN, P., HODGES, S. E., FISHER, W. E., BRUNICARDI, F. C., CHEN, C., YAO, Q. & LI, M. 2013. Gene Profile Identifies Zinc Transporters Differentially Expressed in Normal Human Organs and Human Pancreatic Cancer. *Curr Mol Med,* 13**,** 401-9.

YIN, S., QIN, Q. & ZHOU, B. 2017. Functional studies of Drosophila zinc transporters reveal the mechanism for zinc excretion in Malpighian tubules. *BMC Biol,* 15**,** 12.

YU, J., LAN, X., CHEN, X., YU, C., XU, Y., LIU, Y., XU, L., FAN, H. Y. & TONG, C. 2016. Protein synthesis and degradation are essential to regulate germline stem cell homeostasis in Drosophila testes. *Development,* 143**,** 2930-45.

YUAN, X., ZHENG, H., SU, Y., GUO, P., ZHANG, X., ZHAO, Q., GE, W., LI, C., XI, Y. & YANG, X. 2019. Drosophila Pif1A is essential for spermatogenesis and is the homolog of human CCDC157, a gene associated with idiopathic NOA. *Cell Death Dis,* 10**,** 125.

ZHAO, J., DONG, X., HU, X., LONG, Z., WANG, L., LIU, Q., SUN, B., WANG, Q., WU, Q. & LI, L. 2016. Zinc levels in seminal plasma and their correlation with male infertility: A systematic review and meta-analysis. *Sci Rep,* 6**,** 22386.

4.6 Supplementary Figures

Supp Table 1: Cordonbleu medium recipe for 15 L of food	
Water (Hot)	1062 mL
Potassium tartrate	108 g
Calcium Chloride	6.75 g
Agar	72 g
Yeast	162 g
Dextrose	720 g
Sugar (raw)	360 g
Bring to boil	
Water (cold)	2700 mL
Semolina	900 g
Bring to boil	
Water	1800 mL
Cool to ~60°C	
Nipagen	108 mL
Propionic Acid	54 mL
Makes ~18 trays of food	

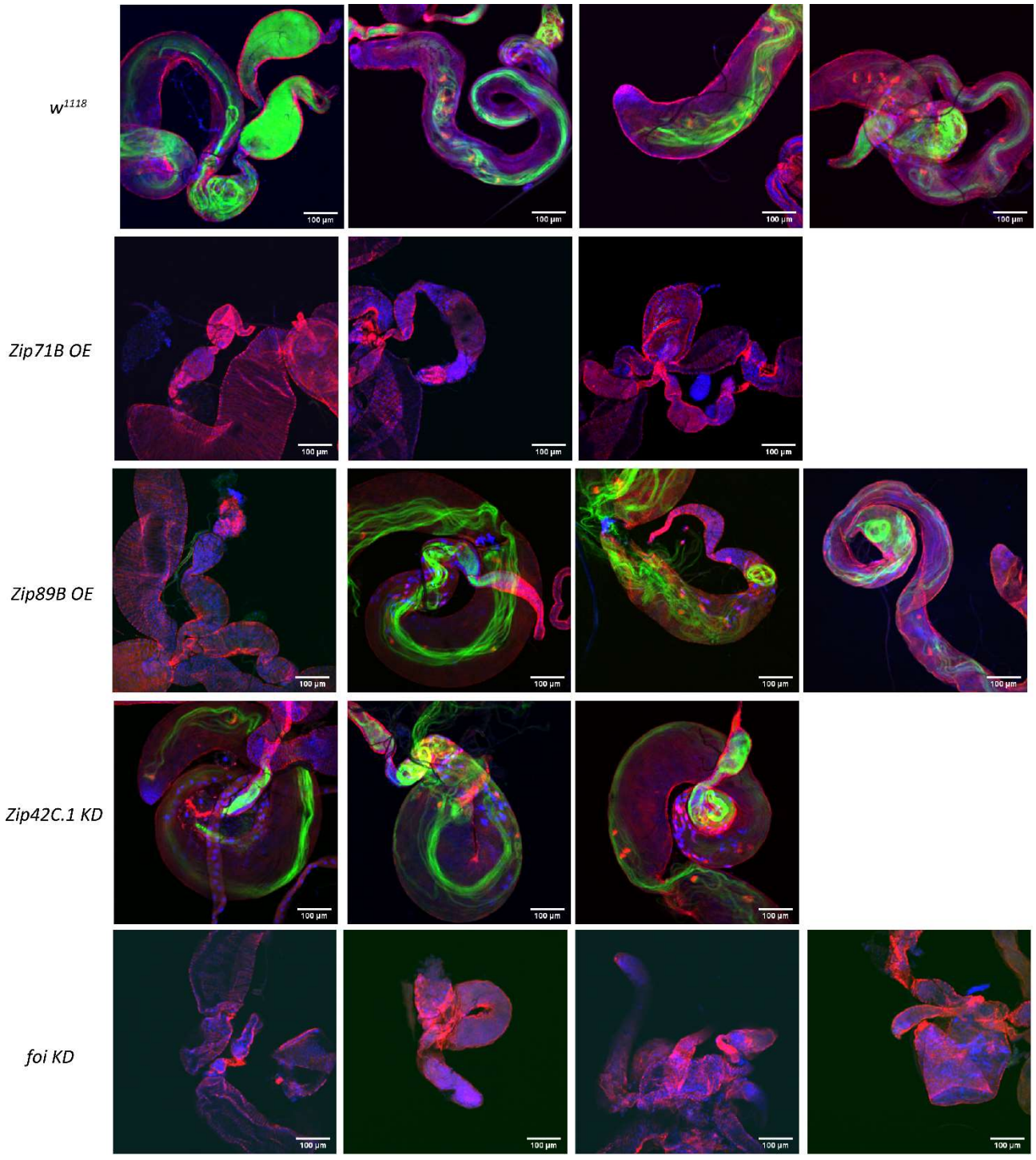

Supp Figure 1: Extra histology images for the *Drosophila* mis-expression of zinc

Final conclusions

Male reproduction is a particularly complex disorder. Although it affects an estimated 7% of men, in the vast majority of cases, the disease aetiology is unknown (Tournaye et al., 2017). Part of this complexity lies in the fact that infertility can be caused by both environmental factors and genetics, or in many cases a combination of both. Also, the large number of genes that display testis-only or testis enriched expression dramatically increases the number of potential targets for infertility causing mutations. Infertility by its very nature is unlikely to be passed on to future generations, however an increase in the use of assisted reproductive technologies has allowed infertile men to father children (de Mouzon et al., 2020), which can inadvertently lead to potential infertility mutations being passed on to future generations.

While male infertility is clinically relevant on a population scale, the incidence of each individual infertility-causing mutation is expected to be relatively low. In short, these mutations are high in number, but low in incidence. For this reason, extremely large cohort studies are needed to validate mutations across or within cohorts, making it a costly and time-consuming feat to study these genes in the human population. In contrast, model organisms such as *Drosophila* and mouse can be used to relatively cheaply screen and eventually validate genes identified through mutations in even a single infertile male. As described in the introduction to this thesis, the process of spermatogenesis is highly conserved in these models (reviewed in White-Cooper and Bausek (2010) and Bonilla and Xu (2008)) making them prime candidates for screening candidate infertility mutations.

The aim of this research was to use model organisms to expand our knowledge of the genes required for male reproduction. The first objective was to undertake a comparative analysis of mammalian and *Drosophila* spermatogenesis (Chapter 1), in order to determine which aspects are strongly conserved and which elements are more dissimilar. This provided a deeper understanding as to which processes

in spermatogenesis can be most accurately studied using *Drosophila* (Chapter 1). The second objective was to screen candidate fertility genes previously outlined by whole exome sequencing of infertile men, using animal models and human tissue (Chapter 2 and 3). The third objective was to specifically study the role of zinc and zinc transport in fertility (Chapter 4).

5.1 Spermatogenesis is well conserved between *Drosophila* and human

The first chapter of the thesis was a literature review and comparative analysis of spermatogenesis in *Drosophila* and mammals which is the first of its kind. While there have been numerous papers comparing individual processes within spermatogenesis, there has yet to be any publication which has analysed these differences more broadly. This chapter provides a solid introduction to anyone looking to start using *Drosophila* to study fertility genes, as it provides a basic description of spermatogenesis in both invertebrates and mammals, and succinctly describes some of the main differences.

One of the key differences which can lead to confusion is the structure and nomenclature of the male reproductive system in each organism. For example, in mammals the sperm are stored in the epididymis for post-testicular modification and the seminal vesicle produces part of the semen content. In *Drosophila* however, the sperm are stored in the organ named the “seminal vesicle”, and do not undergo post-testicular modifications. While the main role of the somatic cells in both organisms is to protect the developing germ cells, the Sertoli cells in mammals are mostly fixed after development, whereas the cyst cells in *Drosophila* develop synchronously with the developing germ cells. Another important difference is that there is no recombination in the *Drosophila* male germline during meiosis, due to the absence of chiasmata.

The spermiogenic processes naturally have some slight differences, but much of the development of key structures are analogous between flies and humans. Sperm from both species have acrosomes that are derived from the Golgi, however the mammalian acrosome is also derived from the endocytic pathway. There are some significant differences between the axonemes of each species, most notably the differences in the relative lengths of the cytosolic and compartmentalised axonemes. As the process of chromatin condensation is essential, this is highly conserved. Finally, as the structure of the testicular somatic cells is distinctly different between the organisms, it comes as no surprise that the spermiation processes are quite diverse.

In summary, this review shows that there is significant similarity between flies and mammals in spermatogenesis. Flies have a much shorter generation time, making them much more efficient for studying genetic mutations, particularly ones, such as fertility mutations, that are rare in the human population. This review provided the foundation for the research in the following chapters, where both reverse and forward genetics approaches were used in order to discover novel infertility mutations.

5.2 *Drosophila Zn72D* and *DCAF12* knockdown causes male infertility

The second chapter involved primarily a reverse genetic approach of gene discovery, where candidate infertility mutations found in the exomes of infertile men, were then analysed in model organisms. The International Male Infertility Genomics Consortium is the type of collaboration needed to study fertility genes, bringing clinicians and researchers together from all over the world. Of the list of 35 genes sent by our collaborator Don Conrad (Oregon Health and Science University, USA), only 10 had *Drosophila* orthologues with sufficient homology to undertake further analysis. This is considerably lower than the widely accepted estimate that 70% of human disease genes that have

Drosophila orthologues (Pandey and Nichols, 2011) and is likely to be due to the unusual rapidity with which reproductive genes evolve (Clark et al., 2006).

Knockdown of *Zn72D* (with the human orthologue *ZFR2*) in both the somatic and germline cells resulted in complete sterility, and knockdown of *DCAF12* (with the human orthologue *DCAF12L1*) resulted in subfertility when knocked down in the germline. *ZFR2* and *DCAF12L1* and *DCAF12* were all found to be expressed in human testes, and RNA sequencing data extracted from Mahyari et al. (2021) demonstrated that *ZFR2* was expressed primarily in human meiotic and pre-meiotic germline cells. Due to the severity of fertility reduction in the *Zn72D* mutant, it was decided that a knockout mouse model would be made for the mammalian *Zfr2* gene. This model provided the basis for the second results chapter of this thesis.

The *ZFR2* variant found in the infertile man was a premature stop mutation, leading to a truncated protein, and likely inducing nonsense-mediated decay. Given that *ZFR2* contains three C_2H_2 domains, it was originally thought to be a transcription factor and predicted to play a role in DNA and RNA-binding. The meiotic and premeiotic *ZFR2/Zf2* expression found in the single cell RNA sequencing data supports such a role, as post-meiosis, much of the DNA is bound to histones and ZFR2 would therefore be unable to bind as easily to its usual target sequences. *ZFR2* antibody staining of human testes also supported a predominantly pre-meiotic expression pattern of *ZFR2*, as staining began to decrease in the pachytene spermatocytes, and was not seen in the A_{dark} spermatogonia. Both somatic and germline *Zn72D* knockdowns clearly showed a decrease in the amount of sperm present in the fly testis, and a complete absence of sperm in the seminal vesicle. These findings added to the belief that *ZFR2* was playing a key role in human male fertility.

5.3 *Zfr2* is not absolutely required for fertility in the male mouse

The third chapter involved the investigation of the role of *Zfr2* in a mouse model, through analysis of a *Zfr2*$^{-/-}$ knockout mouse line. This involved the excision of exon 2 of *Zfr2,* which resulted in a truncated protein (likely subject to nonsense-mediated decay) similar to that seen in the infertile man. The *Zfr2*$^{-/-}$ mouse was generally healthy, and none of the assessed fertility parameters, including number of offspring, sperm motility, and histological analysis all were statistically different from the wildtype control. qPCR data clearly demonstrated that *Zfr2* was absent or severely reduced in the mouse, and there was no compensatory upregulation of the homologue *Zfr*.

The fertility of the *Zfr2* knockout mouse was unexpected. The results from the fertility screen in the second chapter clearly demonstrated that *Zn72D* was necessary for fertility and the human patient with the *ZFR2* mutation presented with azoospermia. Analysis of *ZFR2* in human testes clearly showed expression in germ cells and somatic testicular cells. However, the *Zfr2*$^{-/-}$ knockout mouse did not show any significant reduction in fertility, suggesting that *Zfr2* is not crucial for fertility. Therefore, there was a disconnect between the results seen in Chapter 2, where *ZFR2* and *Zn72D* were thought to play a critical role in fertility, and in the third chapter, which indicated that *Zfr2* was not critical for murine fertility. As mentioned throughout this thesis, the difficulty in understanding the specific mechanisms behind infertility stems from the fact that it can be caused by numerous genetic and/or environmental factors.

Our initial hypothesis was that compensation may have been occurring in the *Zfr2* knockout mouse through the upregulation of *Zfr*, as *Zn72D* in *Drosophila* is the only orthologue of both *Zfr* and *Zfr2* in mammals. Therefore, the sterility observed in the fly model may have been due to effectively removing both *Zfr* and *Zfr2* in the same organism. However, further analysis determined that this was

unlikely. Firstly, the human patient had only the *ZFR2* mutation and was infertile. Furthermore, the qPCR results clearly determined that there was no significant change to the expression of *Zfr* in the absence of *Zfr2*. However, it is also possible that upregulation of *Zfr* was not necessary to compensate for loss of *Zfr2*, and that the similarity between *Zfr2* and *Zfr* means there is a potential for functional redundancy. RNA sequencing data (Guo et al., 2018) suggests that both *ZFR* and *ZFR2* are expressed primarily in spermatocytes, which further validates the theory that there may be some redundancy. There is also a small possibility that the presence of additional, compounding genetic variants may be affecting spermatogenesis in the infertile man.

A *Zfr* knockout mouse has previously been shown to result in embryonic lethality (Meagher and Braun, 2001), so to examine the requirement for both *Zfr* and *Zfr2* in spermatogenesis would require the generation of a testis-specific conditional double-knockout. While we currently do not have access to the original *ZFR2* mutant sample, it would be beneficial to sequence the entire genomic region of *ZFR* in this sample to determine if there is an additional mutation in its regulatory sequence. The whole-exome sequencing methods used to identify the original infertility mutation would not detect mutations affecting non-coding gene regions.

While redundancy remains a formal possibility, perhaps a more likely hypothesis stems from our understanding that infertility can be caused by a combination of factors. Lab-generated knockout mice are raised in optimal conditions, with a healthy diet, ambient temperature, a lack of environmental pollutants and minimal risk of infection. Humans, in contrast, are not subject to such perfect conditions. Therefore, it is possible that *ZFR2* mutation may cause infertility in conjunction with an environmental or lifestyle stressor. As the mice are not exposed to these stressors, it is possible that they are not stressed enough to require *Zfr2* for fertility. As we only have a single patient with

this mutation, we do not have the ability to look at different lifestyle factors or environmental conditions to determine whether they are influencing the requirement for *Zfr2*. This could, however, be analysed in future studies with the *Zfr2* knockout mouse, by changing the environmental or lifestyle conditions to determine if *Zfr2* is in fact needed under these stressed conditions, however this is beyond the scope of this thesis.

Work by Haque et al. (2018) showed that *ZFR* modulates alternate splicing in macrophages. In the absence of *ZFR,* genes important in the type I interferon immune response are incorrectly spliced, and leading to increased type I interferon response, which in turn, increases innate immune response. However, a more recent paper provided strong evidence that *Zn72D*/*Zfr* is also playing a key role in Adenosine-to-inosine (A-to-I) RNA editing, through catalysis of adenosine deaminase acting on RNA (ADAR) proteins (Sapiro et al., 2020).

Sapiro et al. (2020) found *Zn72D* to be critical for neuronal A-to-I RNA editing at hundreds of sites. *Zn72D* binds ADAR in an RNA-dependent manner, and its neuronal knockdown resulted in lower ADAR protein levels, disrupting neuromuscular junction architecture. However, the effects of *Zn72D* loss were distinct from those of lowered ADAR levels, indicating that *Zn72D* plays another role than solely ADAR binding. Knockdown of *Zfr* in the murine primary neurons similarly resulted in the subsequent reduction in murine *Adar2* expression. *Zfr2* was unfortunately not examined in this study. Both *Adar* and *Adarb1* are expressed in murine Sertoli cells and germ cells, and a global knockout of *Adarb1* resulted in complete loss of A-to-I RNA editing. However these mice were both viable and fully fertile, indicating that while ADARs do in fact mediate A-to-I RNA editing in the testis, these editing events are not explicitly required for fertility in optimal laboratory conditions (Snyder et al., 2017).

Human *ADAR1* has previously been implicated in viral restriction, particularly for paramyxoviruses (such as Measles) and orthomyxoviruses (Ward et al., 2011). Therefore, Snyder et al. (2017) proposed that the ADARs act as a protective mechanism against viral infection. It was proposed that viral infection increases ADAR expression, thereby negatively affecting spermatogenesis. If this is the case, mice raised in an optimal lab environment would not require the ADAR family, and would not be negatively impacted by ADAR expression.

In this thesis it was found that *ZFR2* mutation was likely to be causing infertility in a human patient, but not in mice raised in an optimal environment. If ADARs were only required when viral infection is present and *Zfr* has been shown to interact with ADARs, then logically, *Zfr*/*Zfr2* may also only be required under these stressed conditions. Therefore, we are seeing this effect in the male patient (who may have been exposed to these viral infections) and not in the mouse (which was raised in the optimal environment). Under this scenario, the patient's infertility may have been contributed to by an infection, which upregulated *ADAR/ZFR2* expression, thereby potentially impairing spermatogenesis.

Future experiments are needed to test this hypothesis. Infection of *Zfr2* knockout mice with a paramyxovirus would virally stress the mouse, upregulate the ADAR/*Zfr2* mechanism, and potentially cause infertility. It would also be interesting to assess RNA editing in the *Zfr2* knockout mice. This could be done through similar mechanisms to Sapiro et al. (2020), where RNA sequencing can be used to determine editing levels in the *Zfr2* knockout mouse compared to the wildtype.

The fly model could also be further exploited to examine *ZFR2* function. The Gal4/UAS system used in chapter 2 and 4 of this thesis can also be used to express mammalian orthologues of *Drosophila*

genes. This would allow the combination of the *Zn72D* knockdown with the expression of the mammalian *ZFR* or *ZFR2* gene in the same tissue. This would determine whether expression of either human orthologue was able to rescue the knockdown caused by the *Zn72D* RNAi. This would provide insight into whether the human orthologue is playing a similar functional role to the fly orthologue. This method can also be used to introduce the patient mutation in the *Zn72D* knockdown fly, to determine if this mutation also causes infertility in the fly.

In summary, *ZFR2* was discovered as a candidate fertility gene in exome sequencing of infertile men. The knockdown of the *Drosophila* orthologue, *Zn72D*, also resulted in infertility. However, *Zfr2* was found to not be absolutely required for male fertility in the mouse raised in optimal lab conditions.

5.4 How to effectively use *Drosophila* to study human disease genes

It is important to discuss the overall efficacy of using *Drosophila* as a model organism for validating human fertility genes. Here, only 2 of the studied 10 genes (20%) studied in *Drosophila* were hits for causing male infertility when knocked down. Previous work by Yu et al. (2015) discovered 7 genes out of 22 *Drosophila* orthologues studied (32.8%), a similar hit rate.

There are many reasons why this may be the case. One potential reason is that this mutation alone in a particular gene may not be sufficient to cause infertility in the human patient. This could be because there were modifying mutations which can be contributing to infertility in the patient, or that only under certain environmental conditions can these mutations result in male infertility. There is also the possibility that RNAi line was simply not effective enough at reducing the RNA expression. This can however be solved by using multiple RNAi lines for these genes, which was done in this thesis.

In this study, both hits from the initial *Drosophila* screen failed to translate to a mammalian model – the orthologue knockouts of *Dcaf12l1* and *Zfr2* were both fully fertile. Given the time and cost involved in generating and analysing knockout mouse strains, we need to consider ways to improve the selection process. In both cases studied here, a single fly gene, essential for fertility had two or three close mouse orthologues, raising the inherent possibility of redundancy. Future studies might benefit from prioritising genes with only a single mouse orthologue for knockout studies.

Alternatively, an intermediate or surrogate strategy would be to perform a gene rescue/replacement experiment in the fly. This involves the endogenous gene knockdown in *Drosophila*, and supplementation with a wildtype copy of the human gene, in order to determine if its function was similar enough to that of it's fly orthologue to rescue the fertility defect. Furthermore, if the patient mutation is known, this gene variant could also be inserted into the fly genome to determine if this mutation can also cause infertility in the fly. This would also assist in compensating for the redundancy observed when there is a one *Drosophila* gene to many human genes orthology. If the patient mutation also caused infertility in the fly, this would further validate this gene as a necessary gene in male fertility. This would make this mutation a better candidate for translation to a mouse model, which would be required to provide more functional validation of this gene.

This does not however mean that the screen used in this thesis is not a valid assay to study human fertility genes. There is a certain amount of serendipity involved. Previous screens in our lab have had similar hit rate studying the *Drosophila* orthologues of human candidate genes (17%). To date, no genes have yet been transferred from initial human patient mutation, to fly knockdown, and then to a mouse knockout with consistent infertility. However, this is largely due to a strategy where the best candidate genes have been taken directly to a mouse model. With the large number of genes

required for male fertility, and the high rate of infertility in humans, *Drosophila* is still a useful model to initially screen these genes. Further analysis, such as the experiments suggested above, could be undertaken in order to increase the chances of this mutation being translated to infertility in a mouse model.

5.5 Altering zinc transport in the *Drosophila* testis can cause infertility

The primary aim of the fourth chapter was to use a forwards genetics approach in order to examine the role of zinc, and zinc transport in fertility. As an important and easily manipulable dietary nutrient, zinc is an excellent candidate for potential fertility-boosting interventions. A recent meta-analysis determined that zinc levels were significantly lower in the semen of infertile men, and that sub-fertile men who took zinc supplements had increased semen volume, and improved sperm motility and morphology (Zhao et al., 2016a). This chapter exploited the experimental advantages of the fly to carry out two main experiments. The first examined the effect of mutating (by either knockdown (KD) or over-expression (OE)) all known ZnT and ZIP zinc transport proteins in the *Drosophila* testis, while the other involved the removal of zinc (as well as copper) from the *Drosophila* diet, to determine the effect on fertility.

Thirty-five zinc transporter RNAi or cDNA lines were expressed in the somatic or germline cells of the testis. Only one line (*ZnT86D* KD) resulted in complete sterility of the male when expressed in the germline cells of the testis. However, when expressed in the somatic cells *Zip42C.1* KD, *Zip89B* OE and *fear-of-intimacy* KD were able to cause sterility, and *Zip42C.2* OE, *Zip71B* OE and *ZnT49B* KD caused a significant reduction in fertility.

A number of these gene manipulations were analysed at the histological level using a *don juan-GFP* reporter gene which indicates the presence of sperm tails, therefore allowing analysis of the point at which point spermatogenesis was being halted under each gene manipulation. Interestingly when zinc transport was altered, many different phenotypes or spermatogenic arrests were observed.

For example, when *Zip71B* or *foi* expression was altered, the fly had the "tiny testis" phenotype, where no sperm at all were present. Furthermore, the seminal vesicle was completely empty. When *Zip89B* was over expressed, spermatogenesis in the testis appeared relatively normal. However, the seminal vesicle was clearly empty, indicating that there is an issue in the transport of the sperm from the testis to the seminal vesicle. Finally, while the *Zip42C.1* knockdown resulted in sperm being produced, the seminal vesicle was noticeably smaller than the control.

These results are interesting as they demonstrate that, like in the human, different mutations can have variable penetrance with respect to spermatogenesis. For example, the phenotype caused by *Zip89B* over-expression would be most akin to a defect in sperm motility in humans. Similarly, the reduction of sperm in the seminal vesicle seen in the *foi* knockdown is most akin to the human Sertoli-cell only phenotype, or at the very least, maturation arrest before the spermiogenesis. Finally, the *Zip42C.1* knockdown mimics human oligospermia, where the number of sperm in the semen is reduced.

Interestingly, a *Zip5* knockout mouse has already been created, and lead to a severe reduction in liver, pancreas and intestine zinc accumulation (Geiser et al., 2013), and it was suggested that ZIP5 is primarily responsible for protecting against zinc toxicity. These global *Zip5* knockout mice did not show a reduction in fertility. *Zip71B* overexpression caused the reduction of fertility observed in the

original screen, so it likely that in this case, the cells were flooded with toxic levels of zinc, resulting in cell death.

This demonstrates one of the challenges of interpreting overexpression phenotypes. In the above case, *Zip71B* may be being expressed in the cells of the testis where it is not usually expressed, or at considerably higher levels than normal. For this reason, the *ZIP*/*ZnT* knockdown phenotypes are much more informative when trying to identify the functional requirement for each zinc transporter, but overexpression is nonetheless useful in examining the potentially pathogenic consequences of mis-expressed zinc transport.

A *ZnT9* mutant mouse has not yet been reported. Previous studies in humans suggest that *ZnT9* mutation plays a role in a cerebro-renal syndrome, as it was shown that mutation in *ZnT9* resulted in a decrease in cytosolic zinc levels (Perez et al., 2017). Previous cell-based experiments suggest a role of ZnT9 in the activation of Wnt signalling (Chen et al., 2007). As the *ZnT49B* knockdown caused such a severe reduction in fertility, and *ZnT49B* is a one-to-one orthologue with *ZnT9*, a knockout mouse model would be useful in order to validate *ZnT9* as a potential candidate gene important for fertility.

There are naturally some limitations with using RNAi in *Drosophila* as a screening system for potential human fertility genes. The primary limitation when working with ZnTs and ZIPs is the limited one-to-one, or one-to-many orthology between fly and mammalian zinc transporters. In particular, the human *ZIP1-3* show higher homology to each other than to any of the four closely related fly Zips, *Zip42C.1*, *Zip42C.2*, *Zip89B* and *Zip88E*, complicating attempts to align fly functional data with mouse and human expression data. There are, however, a number of *Drosophila*

ZnTs and ZIPs that do have a clear one-to-one (e.g., *Zip71B to ZIP5*) or one-to-many (e.g., *ZnT86D to ZnT5/6/7)* orthology relationship with mammalian transporters. With these transporter genes, direct comparisons between the phenotypes observed in the fly and human can be made with greater confidence.

RNAi is an imperfect method for gene knockdown, with efficacy levels varying widely from gene to gene, and even between independent RNAi fly lines of a single gene. Targeted, tissue specific CRISPR/Cas9 is currently showing great promise as a more effective method of gene ablation in *Drosophila*. As CRISPR/Cas9 in flies is currently expensive, when many genes are being investigated, the benefit of using *Drosophila* (with the cheap and reliable Gal4/UAS system) is lost. However, once the screen is complete, using CRISPR/Cas9 in the fly, before generating a mouse model is an attractive option. In future, this technique will start to rival, and even surpass RNAi as genome-wide libraries of transgenic sgRNA fly strains become available.

5.6 Omitting zinc from the *Drosophila* adult diet did not cause a reduction in fertility

As it had previously been shown that zinc supplementation had a positive effect on human fertility, the requirement for dietary zinc was tested in *Drosophila* through the complete removal of zinc from the adult diet. This was undertaken using holidic media (Piper et al., 2014), a synthetic diet, where zinc (and separately copper) were individually omitted. This approach was thought to be more effective than the more traditional method of adding metal chelators to the diet, to reduce metal availability, since chelators are notoriously non-specific. Initially, the males were given a three-day break to recover and replenish their sperm stocks, between each 24-hour mating period. However, neither the zinc- nor the copper-dropout diet resulted in a reduction in the number of females

fertilised, nor the mean number of pupae produced per male. For this reason, a more intense sperm depletion assay was attempted, where the males were not given a three-day recovery period, but were instead immediately given fresh females to mate with. This also did not result in a significant difference in any of the tested diets.

The observed lack of reduction in fertility does not necessarily mean that zinc and copper are not important in fertility; this result may be due to a flaw in the assay. The holidic synthetic diet has been optimised for adult fly survival and fertility, but unfortunately is less effective for supporting larval and pupal development. For this reason, during development and in very early adulthood, the tested flies consumed a standard diet containing zinc and copper, before being shifted to the metal dropout diets at early adult stages. It is quite feasible that zinc and copper accumulated by the animals during development were sufficient maintain normal fertility over the periods tested.

One way to potentially remedy this issue would be to ensure that at least the adult males were not exposed to any zinc during their adulthood, even though the larvae require the SY food for survival. This can be facilitated by hatching the eggs on the SY diet and transferring the pupal cases to the experimental diet. This was not done, as it was expected that the few hours on the SY diet would not have been sufficient to prevent the reduction in fertility. If this experiment were to be repeated, it would be worth dissecting the males at the end of the experiment and staining their testes and seminal vesicles to determine whether the lack of zinc caused any noticeable change in the histology of the testis. Alternatively, a zinc chelator such as TPEN could be added to the SY media to reduce dietary zinc availability during the flies' developmental stages.

The results from chapter four demonstrate that zinc, through several key zinc transporters (specifically *Zip42C.1, foi, ZnT49B* and *ZnT86D*), play a critical role in male fertility in the fly. All of the studied zinc transporters have mammalian orthologues and expression data from the human testis supports roles in spermatogenesis for all of these orthologues. This is unsurprising, given the significant amount of data suggesting that zinc plays a role in male fertility (Zhao et al., 2016a). However, it must be stressed that each *Drosophila* zinc transporter family member often has two or three human orthologues. Therefore, while mutating one of *Drosophila* genes may cause infertility in the fly, it could be expected that in mammals, redundancy between highly conserved paralogues could allow the loss of one zinc transporter to be compensated for by another family member. For instance, a mouse double knockout of *Zip1* and *Zip3* is fertile (Dufner-Beattie et al., 2006). This suggests that *Zip2* may be sufficient to support normal spermatogenesis in the absence of its two closest homologues.

This is the first study to comprehensively analyse all the predicted *Drosophila* zinc transporters in male fertility. *Zip71B*, with the sole human orthologue of *ZIP5*, is likely to be the best candidate for a fertility gene which arose from this study. In the human testis, *ZIP5* appeared to be expressed primarily in the somatic cells, but also showed weak expression in the germ cells. This matched what we saw the *Drosophila* overexpression of *Zip71B*, where sterility and sub-fertility were found in the germline and somatic cells, respectively. Previous research on *ZIP5* has focussed on oesophageal cancer (Li et al., 2016) and myopia (Guo et al., 2014a). *ZIP1*, with the *Drosophila* orthologues *Zip88E, Zip42C.1, Zip42C.2* and *Zip89B*, is one of the better studied ZIPs and has been found to potentially play a role in prostate cancer (Makhov et al., 2009).

5.7 Final conclusions

In summary, the aim of this thesis was to use model organisms to further understand genes important in fertility. It is clear that male infertility is a complex and burgeoning issue, that requires further investigation. This work demonstrates how model organisms can be used to this end. In using the *Drosophila* model, over 25 individual genes were investigated including several cases where both knockdown and overexpression were examined. Through this, a number of genes of interest were able to be sorted into a high priority group for future detailed investigation in a mammalian model or human tissue. This is the way in which male fertility genes can be most successfully analysed. While both the knockout mouse models resulted in mice that were fertile, this only enhances the need for more research into the mechanisms of male reproduction. Future research should aim to further investigate the complex environmental/genetic interaction, as well as continuing to use model organisms to investigate candidate infertility mutations of interest.

5.8 References

BONILLA, E. & XU, E. Y. 2008. Identification and characterization of novel mammalian spermatogenic genes conserved from fly to human. *Mol Hum Reprod,* 14**,** 137-42.

CHEN, Y. H., YANG, C. K., XIA, M., OU, C. Y. & STALLCUP, M. R. 2007. Role of GAC63 in transcriptional activation mediated by beta-catenin. *Nucleic Acids Res,* 35**,** 2084-92.

CLARK, N. L., AAGAARD, J. E. & SWANSON, W. J. 2006. Evolution of reproductive proteins from animals and plants. *Reproduction,* 131**,** 11-22.

DE MOUZON, J., CHAMBERS, G. M., ZEGERS-HOCHSCHILD, F., MANSOUR, R., ISHIHARA, O., BANKER, M., DYER, S., KUPKA, M. & ADAMSON, G. D. 2020. International Committee for Monitoring Assisted Reproductive Technologies world report: assisted reproductive technology 2012dagger. *Hum Reprod,* 35**,** 1900-1913.

DUFNER-BEATTIE, J., HUANG, Z. L., GEISER, J., XU, W. & ANDREWS, G. K. 2006. Mouse ZIP1 and ZIP3 genes together are essential for adaptation to dietary zinc deficiency during pregnancy. *Genesis,* 44**,** 239-51.

GEISER, J., DE LISLE, R. C. & ANDREWS, G. K. 2013. The zinc transporter Zip5 (Slc39a5) regulates intestinal zinc excretion and protects the pancreas against zinc toxicity. *PLoS One,* 8**,** e82149.

GUO, H., JIN, X., ZHU, T., WANG, T., TONG, P., TIAN, L., PENG, Y., SUN, L., WAN, A., CHEN, J., LIU, Y., LI, Y., TIAN, Q., XIA, L., ZHANG, L., PAN, Y., LU, L., LIU, Q., SHEN, L., LI, Y., XIONG, W., LI, J.,

TANG, B., FENG, Y., ZHANG, X., ZHANG, Z., PAN, Q., HU, Z. & XIA, K. 2014. SLC39A5 mutations interfering with the BMP/TGF-beta pathway in non-syndromic high myopia. *J Med Genet,* 51**,** 518-25.

GUO, J., GROW, E. J., MLCOCHOVA, H., MAHER, G. J., LINDSKOG, C., NIE, X., GUO, Y., TAKEI, Y., YUN, J., CAI, L., KIM, R., CARRELL, D. T., GORIELY, A., HOTALING, J. M. & CAIRNS, B. R. 2018. The adult human testis transcriptional cell atlas. *Cell Res,* 28**,** 1141-1157.

HAQUE, N., OUDA, R., CHEN, C., OZATO, K. & HOGG, J. R. 2018. ZFR coordinates crosstalk between RNA decay and transcription in innate immunity. *Nat Commun,* 9**,** 1145.

LI, Q., JIN, J., LIU, J., WANG, L. & HE, Y. 2016. Knockdown of Zinc Transporter ZIP5 by RNA Interference Inhibits Esophageal Cancer Growth In Vivo. *Oncol Res,* 24**,** 205-14.

MAHYARI, E., GUO, J., LIMA, A. C., LEWINSOHN, D. P., STENDAHL, A. M., VIGH-CONRAD, K. A., NIE, X., NAGIRNAJA, L., ROCKWEILER, N. B., CARRELL, D. T., HOTALING, J. M., ASTON, K. I. & CONRAD, D. F. 2021. Comparative single-cell analysis of biopsies clarifies pathogenic mechanisms in Klinefelter syndrome. *Am J Hum Genet,* 108**,** 1924-1945.

MAKHOV, P., GOLOVINE, K., UZZO, R. G., WUESTEFELD, T., SCOLL, B. J. & KOLENKO, V. M. 2009. Transcriptional regulation of the major zinc uptake protein hZip1 in prostate cancer cells. *Gene,* 431**,** 39-46.

MEAGHER, M. J. & BRAUN, R. E. 2001. Requirement for the murine zinc finger protein ZFR in perigastrulation growth and survival. *Mol Cell Biol,* 21**,** 2880-90.

PANDEY, U. B. & NICHOLS, C. D. 2011. Human disease models in Drosophila melanogaster and the role of the fly in therapeutic drug discovery. *Pharmacol Rev,* 63**,** 411-36.

PEREZ, Y., SHORER, Z., LIANI-LEIBSON, K., CHABOSSEAU, P., KADIR, R., VOLODARSKY, M., HALPERIN, D., BARBER-ZUCKER, S., SHALEV, H., SCHREIBER, R., GRADSTEIN, L., GUREVICH, E., ZARIVACH, R., RUTTER, G. A., LANDAU, D. & BIRK, O. S. 2017. SLC30A9 mutation affecting intracellular zinc homeostasis causes a novel cerebro-renal syndrome. *Brain,* 140**,** 928-939.

PIPER, M., BLANC, E., LEITAO-GONCALVES, R., YANG, M., HE, X., LINFORD, N., HODDINOTT, M., HOPFEN, C., SOULTOUKIS, G., NIEMEYER, C., KERR, F., PLETCHER, S., RIBEIRO, C. & PARTRIDGE, L. 2014. A holidic medium for Drosophila melanogaster. *Nature Methods,* 11**,** 100-5.

SAPIRO, A. L., FREUND, E. C., RESTREPO, L., QIAO, H. H., BHATE, A., LI, Q., NI, J. Q., MOSCA, T. J. & LI, J. B. 2020. Zinc Finger RNA-Binding Protein Zn72D Regulates ADAR-Mediated RNA Editing in Neurons. *Cell Rep,* 31**,** 107654.

SNYDER, E. M., LICHT, K. & BRAUN, R. E. 2017. Testicular adenosine to inosine RNA editing in the mouse is mediated by ADARB1. *Biol Reprod,* 96**,** 244-253.

TOURNAYE, H., KRAUSZ, C. & OATES, R. D. 2017. Novel concepts in the aetiology of male reproductive impairment. *The Lancet Diabetes & Endocrinology,* 5**,** 544-553.

WARD, S. V., GEORGE, C. X., WELCH, M. J., LIOU, L. Y., HAHM, B., LEWICKI, H., DE LA TORRE, J. C., SAMUEL, C. E. & OLDSTONE, M. B. 2011. RNA editing enzyme adenosine deaminase is a restriction factor for controlling measles virus replication that also is required for embryogenesis. *Proc Natl Acad Sci U S A,* 108**,** 331-6.

WHITE-COOPER, H. & BAUSEK, N. 2010. Evolution and spermatogenesis. *Philos Trans R Soc Lond B Biol Sci,* 365**,** 1465-80.

YU, J., WU, H., WEN, Y., LIU, Y., ZHOU, T., NI, B., LIN, Y., DONG, J., ZHOU, Z., HU, Z., GUO, X., SHA, J. & TONG, C. 2015. Identification of seven genes essential for male fertility through a genome-

wide association study of non-obstructive azoospermia and RNA interference-mediated large-scale functional screening in Drosophila. *Hum Mol Genet,* 24**,** 1493-503.

ZHAO, J., DONG, X., HU, X., LONG, Z., WANG, L., LIU, Q., SUN, B., WANG, Q., WU, Q. & LI, L. 2016. Zinc levels in seminal plasma and their correlation with male infertility: A systematic review and meta-analysis. *Sci Rep,* 6**,** 22386.